

Bangor University

DOCTOR OF PHILOSOPHY

High-resolution three-dimensional ecosystem mapping of temperate reef systems

Jackson-Bue, Tim

Award date:
2022

Awarding institution:
Bangor University

[Link to publication](#)

General rights

Copyright and moral rights for the publications made accessible in the public portal are retained by the authors and/or other copyright owners and it is a condition of accessing publications that users recognise and abide by the legal requirements associated with these rights.

- Users may download and print one copy of any publication from the public portal for the purpose of private study or research.
- You may not further distribute the material or use it for any profit-making activity or commercial gain
- You may freely distribute the URL identifying the publication in the public portal ?

Take down policy

If you believe that this document breaches copyright please contact us providing details, and we will remove access to the work immediately and investigate your claim.

Download date: 09. Apr. 2024

High-resolution three-dimensional ecosystem mapping of temperate reef systems



Tim Jackson-Bué

School of Ocean Sciences

Bangor University

2022

Thesis submitted for the degree of *Doctor of Philosophy*

Abstract

Organism-environment interactions take place through a multitude of processes that generate patterns across scales in space and time, but our understanding of pattern and processes is traditionally constrained by observational limitations. Contemporary technological advances in remote sensing, explored in this thesis, are extending the power and capability of ecological investigation. Three-dimensional (3D) ecosystem structure can now be analysed across scales from millimetres to kilometres and from minutes to decades, providing insight into scale-dependent patterns and their driving processes in complex and dynamic systems like temperate reefs.

Remote sensing technologies are available for 3D mapping and recent years have seen a rapid expansion in their use in field ecology. In chapter 2, I reviewed the current state of the art in high-resolution 3D ecosystem mapping technologies and their applications, highlighting the emerging era of 3D spatial ecology and identifying potential barriers to widespread uptake. I addressed a paucity of information on the accuracy and practicality of emerging optical remote sensing tools in ecological contexts by testing structure-from-motion photogrammetry and terrestrial laser scanning, in three coastal habitats, over three spatial scales. The accuracy of structure-from-motion photogrammetry, compared to terrestrial laser scanning models, was greatest at fine spatial scales (25 m², < 1 cm resolution) on more stable substrates like rock, with mean \pm sd absolute difference of 4 mm \pm 14 mm. Accuracy decreased with increasing spatial scale and in less stable vegetated scenes, with a maximum difference of 56 mm \pm 111 mm in saltmarsh at a scale of 2500 m² extent and <2 cm resolution. Structure-from-motion photogrammetry was more portable, faster, flexible and lower-cost than terrestrial laser scanning, but was more vulnerable to error propagation.

Capturing sufficient ecologically relevant spatial and temporal variation in 3D structure is challenging in complex, dynamic habitats like intertidal temperate reefs. In chapter 3 I used the tools tested in chapter 2 to investigate spatial and temporal patterns in the structure of biogenic *Sabellaria alveolata* reef across scales. At a habitat scale (~35,000 m² extent, 10 cm horizontal resolution) most of the variation in reef structural change was explained by a combination of systematic trends with shore height and positive spatial

autocorrelation up to the scale of colonies (1.5 m) or patches (4 m). Plot-scale mapping (2500 m² extent, 10 cm horizontal resolution) over five years (2014-2019, 6-month intervals) revealed previously undocumented temporal patterns in reef accretion and erosion. The system was highly dynamic at small spatial and temporal scales (<4 m, 6 months), but reef accretion and erosion compensated each other, resulting in stable habitat structure over larger scales (>130 m, 5 years). This scale-dependent variability would have been impossible to capture with conventional methods like quadrat, transect or point-based survey using GPS or theodolite, demonstrating the value of modern 3D mapping technologies to enhance our understanding of ecosystem dynamics across scales.

Subtidal temperate reefs hosting diverse communities are often found in high-energy waters, but these are understudied compared to lower energy seas, and knowledge of reef distribution is lacking. In chapter 4 I used multiscale 3D seafloor data and hydrodynamic information to predict the spatial distribution of geogenic reef and biogenic *Sabellaria spinulosa* reef habitats in a high tidal energy region. Random Forest models for reef substrate and *S. spinulosa* reef had balanced accuracy mean \pm 95% CI of 80.7% \pm 0.8% and 77% \pm 1% respectively. Mean bed shear stress was the most important variable in both models, highlighting the importance of including measures of hydrodynamic energy in predictive mapping of high-energy temperate reef habitats.

My research demonstrates the increased power and insight that can be gained with contemporary 3D mapping and monitoring tools in field ecology. I showed that habitat structure in complex systems can be simultaneously highly dynamic and remarkably stable depending on the scale of observation, and that multiscale structural metrics are central to cost-effective mapping of subtidal temperate reef ecosystems. The collective works highlight the need for multiscale and multidisciplinary analysis and the value of embracing technological solutions for ecology in the age of big data. The emerging field of 3D ecosystem mapping and high-resolution remote sensing will have far-reaching implications for research, management and public engagement.

Table of Contents

Abstract.....	i
List of figures and tables	vii
Acknowledgements.....	xiii
Author's declaration	xv
1 General introduction.....	1
1.1 Remote sensing in ecology	1
1.2 Three-dimensional ecosystem structure in marine systems	2
1.2.1 Recording and measuring ecosystem structure.....	2
1.3 Temperate reef systems.....	3
1.3.1 Structure in reef systems.....	4
1.4 Thesis aims and structure	6
2 Three-dimensional digital mapping of ecosystems: a new era in spatial ecology	9
2.1 Abstract	9
2.2 Introduction.....	11
2.3 Remote sensing in ecology	12
2.4 High-resolution remote sensing tools for spatial ecology	15
2.4.1 Terrestrial laser scanning.....	16
2.4.2 Structure-from-motion photogrammetry.....	17
2.4.3 Georeferencing	18
2.5 Accuracy of structure-from-motion models in ecological settings	19
2.5.1 Methods.....	19
2.5.2 Results and discussion	25
2.6 A case for increased adoption of 3D mapping techniques in ecology	28
2.6.1 Understanding relationships between organisms and habitat structure	28

2.6.2 Measuring and monitoring small, slow and complicated variation in 3D form	29
2.6.3 Virtual sampling, digital archiving and addressing problems of scale in ecology	30
2.6.4 Value to managers, policy makers and the public.....	31
2.7 Barriers to wider uptake in ecology	32
2.8 Conclusion.....	35
3 Three-dimensional mapping reveals scale-dependent dynamics in biogenic reef habitat structure.....	37
3.1 Abstract.....	37
3.2 Introduction	39
3.3 Methods	41
3.3.1 Data collection	41
3.3.2 Data analysis.....	43
3.4 Results	53
3.4.1 Habitat-scale (~35,000 m ²) spatial patterns in <i>S. alveolata</i> reef emergence, accretion rate and erosion rate.....	53
3.4.2 Plot-scale (2,500 m ²) temporal patterns in reef structure.....	59
3.5 Discussion	64
3.5.1 Spatial patterns in biogenic reef structure	64
3.5.2 Temporal patterns in biogenic reef structure	66
3.5.3 Conclusion	68
4 Mapping temperate reef habitats in high energy waters.....	70
4.1 Abstract.....	70
4.2 Introduction	72
4.3 Method	76
4.3.1 Study site.....	76

4.3.2	Habitat observations.....	77
4.3.3	Environmental predictor variables.....	80
4.3.4	Classification model and predictive mapping.....	85
4.4	Results.....	88
4.4.1	Reef substrate.....	88
4.4.2	Potential <i>Sabellaria spinulosa</i> biogenic reef.....	90
4.4.3	The influence of backscatter.....	93
4.5	Discussion.....	96
5	General discussion.....	101
5.1	Overview.....	101
5.2	New insight from 3D mapping of ecosystems.....	102
5.2.1	Recording and analysing 3D structure.....	103
5.2.2	Scale-dependence in ecological patterns and processes.....	105
5.3	Limitations.....	107
5.3.1	Limitations of technologies used.....	108
5.3.2	Study limitations and extensions.....	111
5.4	Future research priorities, opportunities, and challenges.....	114
6	References.....	119

List of figures and tables

Figure 2.1 An overview of high-resolution three-dimensional ecosystem mapping tools, data formats and scales. Tools include terrestrial laser scanning and structure-from-motion photogrammetry. Point cloud data can be processed into mesh formats by interpolating between points, and raster formats to produce digital elevation models (DEMs) by averaging point elevations in a regular 2D grid. 3D information can be analysed at multiple spatial scales from organism to ecosystem. These tools enable investigation at spatial scales (resolution and extent) that are understudied in ecology. Plot shading (adapted from [Estes et al., 2018]) indicates number of ecological studies at specific scales, dashed areas represent the approximate sampling scales for terrestrial laser scanning and structure-from-motion (using drone-mounted and handheld cameras). Grey areas have no data in the original study.14

Figure 2.2 Major steps for capturing data with terrestrial laser scanning and structure-from-motion using handheld and drone-mounted cameras. A) Identify features of interest and estimate scanning positions or camera angles. B) Set out reference targets for terrestrial laser scanning, or ground control points, check points and scaling objects for structure-from-motion. For laser scanning, targets are used to align data from different stations, although scene geometry can sometimes be used for alignment instead of, or in addition to targets. For structure-from-motion, reference points are used for aligning images and constraining the modelling process, and for accuracy assessment and scaling. C) Terrestrial laser scanning collects data from a number of discrete stations, to be combined during processing. For structure-from-motion, many overlapping photographs are taken, from which a 3D model is generated during processing. D) Georeferencing, typically using a commercial grade Global Navigation Satellite System, is required to position the resulting 3D models in real-world space, and for scaling in large structure-from-motion models.15

Figure 2.3 Survey methods for comparison of terrestrial laser scanner and structure-from-motion photogrammetry 3D ecosystem mapping data at three scales. Shared targets were used to align data from the two techniques without introducing georeferencing error. Scaling objects were used to scale fine-scale structure-from-motion models. Reference objects enabled comparison of shape reconstruction by the two techniques.....21

Figure 2.4 Accuracy of a structure-from-motion point cloud quantified as the point-by-point distance to a reference terrestrial laser scanning point cloud in three habitats (rocky shore, biogenic reef and saltmarsh) and at three scales (fine: 25 m² with < 1 cm resolution, medium: 2,500 m² with < 2 cm resolution and broad: 2,500 m² with 5 cm resolution). Distances were measured at 100,000 points and plotted as density curves, with the area under each curve being equal. Curve tails beyond 0 ± 0.1 m are not shown. Mean absolute error (MAE) ± 1 standard deviation (m) distance is reported.26

Figure 2.5 Differences in 3D point cloud models generated by terrestrial laser scanning (TLS, black points) and structure-from-motion photogrammetry (SfM, red points) at three spatial scales and three habitats.

Models agree closely at fine scales (25 m² extent, <1 cm resolution) in areas of solid substrate or short vegetation. In tall and dense vegetation the models differ, with points captured from further into the feature by terrestrial laser scanning. At medium-scales (2500 m² extent, <2 cm resolution) on solid substrate average difference in models is low, but fine details are generalised by structure-from-motion. Terrestrial laser scanning data have gaps due to some areas being out of line-of-sight from any scanning position. At broad-scales (2500 m² extent, 5 cm resolution), SfM models the general form of the scene well but detailed topographic morphology is more accurate in terrestrial laser scanner data. As scale increases detailed features become smoothed by structure-from-motion, as demonstrated by models of reference objects with known shape and size.....27

Figure 2.6 Examples in ecology and environmental management with existing or potential applications for 3D ecosystem mapping. 1) Multiscale experimental design with high-resolution 3D mapping across large extents. 2) Mapping fine-scale variation in topography across tidal flats and wetlands. 3) Automated species identification and biometric measurement in forests. 4) Comparing topographic variation in natural and artificial hard coastal substrates. 5) Digital archiving of 3D habitat structure in inaccessible ecosystems. 6) Monitoring variation in reef topography in space and time. 7) Modelling growth in complex 3D organisms like mangrove trees. 8) Mapping 3D structure in habitats with canopy cover and overhangs.....32

Figure 3.1 A) *Sabellaria alveolata* biogenic reef habitat comprises aggregations of sediment tubes in colonies that emerge above a hard, non-reef substrate. B) Close-up image of a prograding colony surface showing dense tube openings of ~5 mm diameter. C) Cross section of 3D terrestrial laser scan point cloud data from 3 years, demonstrating the detailed information about spatial and temporal dynamics in habitat structure that can be captured using modern 3D mapping technology. Reef colonies accrete upwards and outwards from the non-reef substrate in characteristic mushroom-like hummocks that coalesce into platforms. Erosion of reef colonies is often rapid and catastrophic.....41

Figure 3.2 Interpreting spatial patterns in processes that generate spatial variables using variography. Variograms visualise spatial self-similarity, or autocorrelation, in a variable by plotting semivariance (γ) against lag, the distance between two samples. As lag increases samples become less similar (higher γ) until a plateau (sill) is reached at a distance (range), beyond which sample values are not autocorrelated. Here we show three simulated examples of a variable generated with different processes, and their respective variograms. Top: a fine-scale process generates a variable that is autocorrelated only over short distances, so the range (point and dashed line) is small. Bottom: a broad-scale process generates a variable that is autocorrelated over longer distances, producing a variogram with a larger range. Middle: the fine- and broad- scale processes have been added together, producing a variable with both short- and long-distance autocorrelation, generating a nested variogram with two ranges.45

Figure 3.3 Data processing method used to classify habitat-scale digital surface models (DSMs) as reef or non-reef substrate. We generated 0.1 m XY resolution DSMs using drone aerial imagery and structure-from-motion photogrammetry. From the DSM we generated a digital elevation model (DEM) representing the ground level at the same resolution by interpolating between the lowest point in each square of a 2 m grid.

We calculated emergence by subtracting the DEM from the DSM elevation. Finally, within the known reef area (Figure 3.5A) we used a binary classification of reef (≥ 0.15 m emergence) and non-reef substrate (< 0.15 m emergence).....48

Figure 3.4 Data processing method used to sample reef emergence through time at independent reef locations within a 50 x 50 m plot mapped using terrestrial laser scanning at 6-month intervals over 5 years (Appendix B2). 1) Example section of 3D point cloud data. 2) We used a cloth simulation filter to generate a digital elevation model (DEM) for each time point and retained only points ≥ 0.2 m above the DEM. 3) We generated a digital surface model (DSM, 0.1 m XY resolution) of mean point elevation, then used the DSM to generate a mask that removed low point density pixels, isolated pixels, and colony edges. 4) We combined the masks from all time points. 5) We used a 2 m grid to generate spatially stratified random points (5 points per strata). 6) We randomly selected one point per strata with a minimum spacing of 1.5 m to generate our sample point locations. 7) At each sample location we calculated a timeseries of emergence by subtracting the elevation of a common digital elevation model representing the ground level from the DSM for each time point (Figure 3.7).....51

Figure 3.5 A) The foreshore at Llanddulas, Wales, UK. Habitat-scale 3D structure data were analysed within a $\sim 35,000$ m² reef area polygon digitised from an aerial imagery orthomosaic. Presence of emergent reef is shown at 1 m XY resolution. B) Maximum reef colony emergence increases lower down the shore. The reef colonies that we analysed had a minimum emergence of 0.15 m. C) Reef colony emergence was spatially autocorrelated over short distances (1.5 m) both along the shore (purple) and down the shore (orange), ranges indicated by left-most vertical lines and arrows. There was a secondary autocorrelation structure that had a longer range (110 m) in the along shore direction compared to down the shore (20 m), ranges shown by right-most vertical lines and arrows.54

Figure 3.6 Spatial variation in *S. alveolata* reef elevation changes from April 2018 to April 2019 within the reef area (Figure 3.5A). A) Both positive and negative elevation changes increased towards the lower shore. Samples showing positive changes (blue) were greater in number than those with negative change (red), but the larger average magnitude of negative changes resulted in little change in overall elevation, shown by the boxplot of all samples crossing 0. Grey points represent samples with changes within the alignment uncertainty estimate of ± 0.03 m. B) Variogram showing spatial autocorrelation scales of positive elevation changes (accretion) after accounting for trend (Table 3.2). The majority of spatial autocorrelation is explained by a short range (0.75 – 1.05 m) structure (left-most vertical lines and arrows), with a secondary structure showing a longer range (130 m) in the alongshore orientation compared to down the shore (30 m). C) Variogram showing spatial scales of negative elevation changes (erosion) after accounting for trend (Table 3.2). Spatial autocorrelation only occurs up to a short range (2.9 – 3.84 m, vertical lines and arrows).57

Figure 3.7 Colony-scale variation balances out to produce plot-scale stability in *S. alveolata* reef habitat structure over several years. Emergence was measured at 454 stratified random, spatially independent sample locations in a 2,500 m² plot in autumn and spring each year from September 2014 (month 0) to

October 2019 (month 61). Thin blue lines show individual sample timeseries. Bold blue line and dashed lines show the mean \pm 1 sd emergence of all samples. Six example sample timeseries' are highlighted to show the diversity of fine-scale dynamics in reef accretion and loss over time, clustered into two groups: fast colonies with rapid accretion and short persistence (orange) and slow colonies with slower accretion and longer persistence (red).60

Figure 3.8 2,500 m² plot showing 0.01 m² pixels containing *S. alveolata* reef in at least one of 11 surveys over 5 years (grey) and stratified random, spatially independent samples (crosses). Cluster analysis identified two groups of colonies based on patterns of topographic change through time. *Fast* colonies (blue) have rapid accretion and short persistence at their maximum emergence above the non-reef substrate, and are more prevalent towards the lower shore. *Slow* colonies (red) have slower accretion and longer persistence at their maximum emergence, and are distributed evenly throughout the plot.61

Figure 3.9 Boxplot of emergence within the 2,500 m² plot surveyed using terrestrial laser scanning at approximately 6 month intervals over 5 years, with median (bar) and mean (open circles) displayed. We used the data shown to test for effects of year, season and their interaction on emergence using permutational analysis of variance (Table 3.4). The data are balanced samples (n=45) of independent reef locations within the plot, with no missing data and no repeat sampling. To maintain a balanced design, we did not include data from autumn 2014 in this analysis.61

Figure 4.1 A & B) Location of the study site in north west Wales, UK. C) Bathymetry of the study area showing point and transect drop-down video sampling locations, extent of backscatter data and the leased area boundary (white). D) Modelled tidally induced mean bed shear stress across the study site.76

Figure 4.2 Correlation matrix of variables included in the full extent predictive models.82

Figure 4.3 Our hydrodynamic model validates well against Holyhead tidal gauge harmonic data in A) amplitude, B) phase and C) elevation. Tidal elevation was processed in Python using *ttide_py* (https://github.com/moflaher/ttide_py) for tidal analysis and numpy to calculate r-squared values.84

Figure 4.4 A) Predicted reef substrate map with visually identified misclassified areas masked out. B) Confidence map for substrate, calculated by multiplying the frequency of the most commonly predicted class with the average probability of the most common class. C) Predicted *Sabellaria spinulosa* presence and potential reef with D) associated confidence map.87

Figure 4.6 A) Relative importance of predictor variables in the reef substrate model. B) Partial dependence plots for the three variables with highest importance. The plots visualise the response of the model to an individual variable. The plots visualise the influence of each variable on the likelihood that an observation is predicted to be each of four classes. For example, observations with low mean bed shear stress are less likely to be classified as bedrock reef and more likely to be classified as sediment or stony reef (low resemblance).90

Figure 4.7 A) Relative importance of predictor variables in the potential <i>S. spinulosa</i> reef model. B) Partial dependence plots for mean bed shear stress, the variable with highest importance.....	92
Figure 4.8 Variable importance plots for models of reef substrate and <i>Sabellaria spinulosa</i> presence and potential reef, with and without backscatter derivatives (<u>underlined</u>) included.....	94
Table 2.1 Characteristics of point cloud datasets derived from terrestrial laser scanning (TLS) and structure-from-motion photogrammetry (SfM) analysed at multiple scales and habitats. Raw point counts are after cropping to the study area. Processed point counts are after cleaning and subsampling. Median and interquartile range (IQR) point density are of the processed point clouds.....	24
Table 3.1 Spatial structure parameters of reef and non-reef substrate emergence within the ~35,000 m ² reef area, derived from variography.	55
Table 3.2 Spatial structure parameters of reef accretion (positive elevation change) and erosion (negative elevation change) within the ~35,000 m ² reef area over one year, derived from variography.....	58
Table 3.3 Average accretion and erosion metrics for two groups of reef colonies identified within the 2,500 m ² plot.....	60
Table 3.4 Results of permutational analysis of variance, testing for the effects of year, season and their interaction on emergence within the 2,500 m ² plot. Number of permutations = 9999. Significant results ($P < 0.05$) are highlighted in bold	62
Table 4.1 Classification system for video samples. Each 30 second section of video was assigned a class for reef substrate and potential biogenic reef. Distance between laser points = 50 mm	79
Table 4.2 Bathymetric and backscatter derivatives used as predictor variables following removal of colinear variables. Scale mostly indicates the edge length of a square observation window. For BPI, scale indicates the diameter of a focal circle. Derivatives are calculated by operations on matrix or raster format data, for details see references in the methods column.....	81
Table 4.3 Error matrix of a model to predict reef substrates. Cross validation of each bootstrap model run ($n = 25$) was used to generate an error matrix normalised by the number of test observations in each class. The normalised values from all error matrices are summarised here as mean \pm 95% confidence interval. True positives are highlighted in grey.....	89
Table 4.4 Performance metrics for the reef substrate model. Values calculated from the error matrices from each bootstrap model run cross validation are summarised here as mean \pm 95% confidence interval.	89

Table 4.5 Error matrix of the potential *S. spinulosa* reef model. Cross validation of each bootstrap model run (n = 25) was used to generate an error matrix normalised by the number of test observations in each class. The normalised values are summarised here as mean ± 95% confidence interval..... 91

Table 4.6 Performance metrics for the potential *S. spinulosa* reef model. Values calculated from the error matrices from each bootstrap model run cross validation are summarised here as mean ± 95% confidence interval. 92

Table 4.7 Results of Mann-Whitney U tests comparing performance metrics of predictive models that excluded (BS -) and included backscatter derivatives (BS +). Significant differences are indicated in **bold**. 95

Acknowledgements

This thesis would not have been possible without the support of many people. First, I would like to thank my supervisors. Andy Davies for having faith in me from the start, being a mentor since before my PhD journey and continuing to provide support and expert insight throughout. Gareth Williams for taking a risk on an adopted student, having enthusiasm for my work even while we were all still trying to work out what my topic actually was, and transforming my understanding of how to produce good science. Jon King as both supervisor and manager for supporting my efforts to pursue a PhD alongside my employment. All the chapters of this thesis are collaborative efforts, and I thank my co-authors for all their hard work. I thank my colleagues on the SEACAMS and SEACAMS2 projects, in the Centre for Applied Marine Sciences and in the School of Ocean Sciences at Bangor University for their friendship, guidance and contributions, and for making the department a friendly and productive working community. I thank the administrative and technical staff in the department and the crew of the RV Prince Madog for their hard work and expertise, without whom little of this work would have been possible. Finally, a big thank you to my friends and family for their support and encouragement, especially Mathilde for pushing me on throughout and reminding me of the bigger picture.

The research within this thesis was conducted as part of the SEACAMS and SEACAMS2 projects, part funded by the European Regional Development Fund (ERDF) through the West Wales and the Valleys programmes 2007–2013 and 2014–2020.

The SEACAMS (Sustainable Expansion of the Applied Coastal and Marine Sector) project aimed to facilitate growth in coastal and marine businesses in Wales through collaborative research with Welsh universities. The SEACAMS2 project followed with a focus on the marine renewable energy sector. The collaborative research within these the projects was part-funded by the ERDF with match funding from the universities involved, and in-kind contributions from industry partners that included access to resources, data and staff time. Collaborating partners are listed at the start of each chapter.

Author's declaration

I hereby declare that this thesis is the results of my own investigations, except where otherwise stated. All other sources are acknowledged by bibliographic references. This work has not previously been accepted in substance for any degree and is not being concurrently submitted in candidature for any degree unless, as agreed by the University, for approved dual awards.

Yr wyf drwy hyn yn datgan mai canlyniad fy ymchwil fy hun yw'r thesis hwn, ac eithrio lle nodir yn wahanol. Caiff ffynonellau eraill eu cydnabod gan droednodiadau yn rhoi cyfeiriadau eglur. Nid yw sylwedd y gwaith hwn wedi cael ei dderbyn o'r blaen ar gyfer unrhyw radd, ac nid yw'n cael ei gyflwyno ar yr un pryd mewn ymgeisiaeth am unrhyw radd oni bai ei fod, fel y cytunwyd gan y Brifysgol, am gymwysterau deuol cymeradwy.

1 General introduction

1.1 Remote sensing in ecology

Observing patterns in nature is central to developing and testing ecological theory (Weiner, 1995). Observations must be made across scales for a comprehensive understanding, but the possible scales of observation are constrained by the capabilities of available technology, maintaining a divide between theory and testable questions (Levin, 1992). Throughout the history of ecology, advances in observational technologies like telemetry, molecular techniques and remote sensing have been accompanied by step-changes in our understanding of ecology and ecosystem functioning (Sagarin and Pauchard, 2010). Since the 1970s remote sensing data from satellites like Landsat have enabled advances in understanding patterns and processes in ecosystems through analysis of spatially continuous environmental information spanning regional and global extents (Cohen and Goward, 2004), and several decades (Pasquarella et al., 2016). With remote sensing, ecological theory could be tested in inaccessible ecosystems and at new spatial and temporal scales, providing evidence to support new and updated concepts, and to contextualise plot-scale observations (Kerr and Ostrovsky, 2003; Platt et al., 2003; Vierling et al., 2008). Remote sensing data from satellite, space shuttle and (crewed) aircraft platforms provides a suite of information about terrestrial systems, but for the remaining 70% of the globe covered by water, observational data at comparable resolution are sparse (Mayer et al., 2018). The interface between land and sea provides challenges for remote sensing, being too shallow for vessel-based surveys and periodically obscured from air- or space borne sensors with the tidal cycle, resulting in under-sampling of intertidal zones without expensive, dedicated satellite passes or aircraft flights (Leon et al., 2013; Westhead et al., 2015). In the subtidal marine realm, optical remote sensing from air or space is not possible beyond very shallow, clear waters. Here, acoustic remote sensing of the seabed with swath bathymetry technologies has been applied in similar ways to optical remote sensing in terrestrial systems to advance ecological understanding about species distribution, ecosystem pattern and organism-environment interactions (Brown et al., 2011).

1.2 Three-dimensional ecosystem structure in marine systems

Ecosystems are three-dimensional (3D) spaces but have traditionally been mapped, modelled and analysed as two-dimensional (2D) patch-mosaics or gradient models (Lepczyk et al., 2021). 2D models are easier to conceptualise and visualise, are less computationally demanding to analyse, and at spatial scales of kilometres or more are appropriate representations of the environment. However, when considering organism-environment interactions and processes that operate over finer spatial scales, it becomes increasingly important to capture the three-dimensional nature of ecosystems to understand patterns and processes (Vierling et al., 2008). For instance, broad-scale depth gradients, substrate and oceanographic conditions mapped in 2D may predict species distribution and benthic community variation across regional or global extents (Davies and Guinotte, 2011), but across local extents with resolution of metres or less, 3D structural complexity plays a critical role in controlling organism distribution and behaviour (Lecours et al., 2015; Pittman and Brown, 2011; Wedding et al., 2019).

1.2.1 Recording and measuring ecosystem structure

Structural information at global scales is freely available for terrestrial ecosystems in products including Shuttle Radar Topography Mission (SRTM) and Advanced Spaceborne Thermal Emission and Reflection Radiometer Global Digital Elevation Model (ASTER GDEM), but with pixel resolution of tens of metres, these large extent products are mismatched from the finer scale of many ecological processes. Airborne light detection and ranging (LiDAR) data offer 3D information at decimetre resolution, sufficient to resolve larger structural units like trees, buildings and geological features. LiDAR data are valuable for many ecological investigations (Vierling et al., 2008) and are becoming increasingly available for free, but coverage is limited and LiDAR data are costly to collect for new sites. For many ecological processes and interactions, structural information on the scale of centimetres or finer is important, so high-resolution 3D data collection tools are needed (Anderson and Gaston, 2013). In recent years, tools capable of high-resolution 3D mapping have been developed that offer the capability of analysing 3D ecosystem structure at scales relevant to many organisms and ecological processes (Lepczyk et al., 2021).

1.3 Temperate reef systems

For many the term “reef” conjures up images of tropical seascapes dominated by stony corals forming habitats hosting diverse fish, invertebrates and megafauna. But the definition of a reef, originally referring to a navigational hazard, also encompasses shallow or intertidal features that may be comprised of rock as well as material built by corals and other organisms, in any region of the globe. Temperate reefs can be defined as hard substrate marine habitats between the tropics and the poles (Bennett et al., 2016). These habitats include rocky shores, subtidal rocky or stony habitats, and habitats with hard substrate built by reef-building organisms from several phyla including corals, annelids and molluscs, that may be intertidal or subtidal. The term “habitat” can be generally defined as a physical space with set of environmental variables that support a given community (Whittaker et al., 1973), but several definitions have been used in the literature in different contexts. In this thesis we define marine benthic habitats as areas of seabed that are distinct from each other in terms of their visual, physical and environmental characteristics, such that they are assumed to support distinct communities. This definition aligns with the benthic habitat mapping and marine environmental management literature (Brown et al., 2011; Lecours et al., 2015; MESH project, 2008).

Temperate reefs can support rich and diverse communities of sessile epibiota and mobile reef-associated species, representing hotspots of biodiversity, especially when surrounded by sedimentary habitats (Dubois et al., 2002). The habitats also provide valuable ecosystem services to humans, supporting commercial fisheries, tourism and shoreline protection (Bennett et al., 2016; Borsje et al., 2011). By building biogenic reefs, reef-building organisms modify resource availability for other organisms, making them ecosystem engineers (Jones et al., 1994). The resources that are modulated are diverse, and include those provided directly by the reef substrate, like spaces for refuge from predation and settlement space for propagules, as well indirect effects, like particulate food supply and water chemistry changing as boundary layer flows respond to substrate roughness (Fréchette et al., 1989).

1.3.1 Structure in reef systems

Organisms may interact directly with the physical structure of an ecosystem, for example, by using it as substrate on which to grow or using crevices as refuge from larger predators, or indirectly through the influence of structure on a range of environmental conditions. Physical ecosystem structure has long been known to influence biodiversity (MacArthur and MacArthur, 1961) and is the ultimate driver of many environmental and biological stress gradients in marine habitats, influencing ecological processes across scales (Denny et al., 2004). In rocky shores, wave exposure, desiccation and thermal stress are controlled by shore aspect and gradient at broad scales of kilometres or more (Denny et al., 2004), while topographic heterogeneity over metres or less produces microrefugia from such stressors (Carington Bell and Denny, 1994; Guichard and Bourget, 1998; Helmuth and Denny, 2003; Meager et al., 2011). Settlement patterns of invertebrates are controlled both by regional transport influenced by bathymetry and hydrodynamics, as well as local topography (Chiba and Noda, 2000; Robins et al., 2013; Whitman and Reidenbach, 2012). Habitat structure has a strong influence on biodiversity and behaviour across reef systems including tropical reefs and rocky shores (Beck, 2000; Graham and Nash, 2013; Gratwicke and Speight, 2005; Kovalenko et al., 2012). In biogenic reefs, structure can provide information about the engineering species' life history, productivity, health and resilience (Jones et al., 2018; Plicanti et al., 2016; Rodriguez et al., 2014). Structural metrics can be useful to direct conservation and management resources. For example, member states are required to designate Natura 2000 sites to protect habitats listed in Annex 1 of the EC Habitats Directive, recognised for their ecological importance. Reefs are listed as Annex 1 habitats and are defined by their structure as areas of hard substrate that are "topographically distinct from the surrounding seafloor" (European Commission, 2013). Thresholds of structural metrics including relative elevation have been proposed to improve quantification and consistency in the definition of Annex 1 reef, aiding efficiency in environmental management with limited resources (Hendrick and Foster-Smith, 2006; Irving, 2009).

Ecosystems are dynamic across temporal scales. From organism behaviour over seconds to geological processes over millennia, the biological, chemical and physical structure of habitats and ecosystems are constantly changing and interacting. In temperate reefs, stochastic disturbance and changes in environmental conditions interact with biological

processes like competition and recruitment to maintain continuous variation in resource availability and biological and physical habitat structure (Connell and Sousa, 2015; Levin and Paine, 1974; Paine and Levin, 1981; Sousa, 1984). On rocky reefs, sedimentation can lead to changes in the physical structure of a habitat on hourly time scales, causing disturbance to biological communities through smothering and abrasion (Schiel et al., 2006). In biogenic reefs, dynamics in physical structure mediated by reef-building organisms can result from combinations of physical, chemical and biological processes. For example temporal variation in reef-building by polychaetes can result from increased anthropogenic nutrient input (Jaubet et al., 2013), and interaction between hydrodynamic regime and engineering species reproduction patterns (Ayata et al., 2009; Bush et al., 2015; Dubois et al., 2007).

As in other systems, technological and logistical limitations have traditionally hindered our ability to understand the influence of structure in reef systems (Helmuth and Denny, 2003). Transects using theodolite or more recently, global navigation satellite systems (GNSS) provide 2D information about gradient and complexity across intertidal reefs over extents of tens of metres to kilometres, and profile gauges may be used for fine-scale transects of centimetres to metres (Frost et al., 2005). Methods have been developed to capture similar 2D information within the more challenging working environment of subtidal reefs (Dustan et al., 2013; McCormick, 1994). Commonly, 2D transects are used to estimate habitat complexity using the chain-and-tape method, where complexity is quantified as the ratio of the length of a flexible chain draped across a surface to the linear distance between the two chain ends (Risk, 1972). Variability in 2D transects can be high, resulting in limited repeatability and a need for many replicate samples. Critically, conventional approaches for measuring complexity in reefs are not generally scalable, requiring integration with other methods, technologies or data sources to examine scaling in ecological processes (Denny et al., 2004; Marvin et al., 2016). This thesis focuses on the use of contemporary remote sensing tools and analysis approaches to enable collection of detailed 3D ecosystem structural information across scales, and examine scale dependent patterns in marine ecology.

1.4 Thesis aims and structure

In this thesis, I explore the state-of-the-art in 3D mapping tools and analysis in ecology, with a focus on temperate reef systems. The aims and objectives were:

Aim 1:

Assess the performance and potential applications of contemporary and emerging tools for investigating 3D ecosystem structure to advance understanding of patterns and processes in marine and coastal ecology.

Objectives:

- Review the 3D mapping technologies of structure-from-motion photogrammetry and terrestrial laser scanning and their applications in marine and coastal ecology.
- Identify barriers to entry for the use of these technologies in marine and coastal ecology.
- Test the accuracy of 3D models generated by structure-from-motion photogrammetry compared to terrestrial laser scanning in environments and at scales relevant to marine and coastal ecology.

Aim 2:

Characterise patterns of spatial and temporal variation in the 3D structure of temperate intertidal biogenic reef built by *Sabellaria alveolata*.

Objectives:

- Quantify temporal patterns in *Sabellaria alveolata* reef accretion and erosion by mapping the 3D structure of reef at sub-metre resolution over several years.
- Quantify characteristic spatial scales of variation in reef structure and structural dynamics by mapping the 3D reef structure at a habitat-scale extent and sub-metre resolution.

Aim 3:

Predict the spatial distribution of temperate reef habitats in a high energy marine area, using information about 3D ecosystem structure.

Objectives:

- Characterise the range of reef habitats in a high energy marine site.
- Integrate observation data with high resolution bathymetry mapping and simulated hydrodynamic information to predict the distribution of geogenic and biogenic reef habitats in the area.

In chapter 2, published in *Proceedings of the Royal Society B* in 2020, I review the field of 3D mapping in ecology and provide an accessible introduction to two of the most accessible and powerful tools for fine-scale 3D mapping in field ecology. I identify barriers to widespread adoption of these tools, given that their uptake in ecology has lagged behind other fields. I then address a key barrier to entry identified by testing the accuracy and practicality of the tools in a range of contexts, in three habitats and at three scales. In chapter 3, published in *Remote Sensing in Ecology and Conservation* in 2021, I apply the tools tested in chapter 2 to examine spatial and temporal dynamics in the structure of an ecologically important but understudied intertidal biogenic reef habitat. The state-of-the-art remote sensing tools enabled observation at unprecedented scales. My findings revealed scale-dependent and previously undocumented patterns in structural dynamics in the habitat, providing insight into ecological processes and having implications for ecosystem management. In chapter 4, at the time of writing in review with *Estuarine, Coastal and Shelf Science*, I examine structural patterns in subtidal temperate reef habitats using acoustic rather than optical remote sensing. I use 3D bathymetry mapping to predict the spatial distribution of biogenic and temperate reef habitats in a challenging, high-energy environment. I use a machine learning approach and incorporate simulated hydrodynamic energy as predictor in the model, revealing this as a key variable for mapping reef habitat distribution in this context.

The chapters of this thesis comprise studies that are each collaborative pieces of work with several co-authors. I am the lead author of all chapters having conceptualised, designed, implemented, and written each study. Contributions from co-authors mostly comprised facilitation of the studies including providing access to resources and existing data, assistance with data collection, comments on writing and framing of the work to publication standards, and general support and guidance. Co-author contributions are listed at the start of each chapter.

2 Three-dimensional digital mapping of ecosystems: a new era in spatial ecology

2.1 Abstract

Ecological processes occur over multiple spatial, temporal and thematic scales in three-dimensional ecosystems. Characterising and monitoring change in 3D structure at multiple scales is challenging within the practical constraints of conventional ecological tools. Remote sensing from satellites and crewed aircraft has revolutionised broad-scale spatial ecology, but fine-scale patterns and processes operating at sub-metre resolution have remained understudied over continuous extents. We introduce two high-resolution remote sensing tools for rapid and accurate 3D mapping in ecology – terrestrial laser scanning and structure-from-motion photogrammetry. These technologies are likely to become standard sampling tools for mapping and monitoring 3D ecosystem structure across currently under-sampled scales. We present practical guidance in the use of the tools and address barriers to widespread adoption, including testing the accuracy of structure-from-motion models for ecologists. We aim to highlight a new era in spatial ecology that uses high-resolution remote sensing to interrogate 3D digital ecosystems.

This chapter has been published as a peer-reviewed article:

D'Urban Jackson, T.*, Williams, G.J., Walker-Springett, G. and Davies, A.J., 2020. Three-dimensional digital mapping of ecosystems: a new era in spatial ecology. *Proceedings of the Royal Society B*, 287(1920), p.20192383. <https://doi.org/10.1098/rspb.2019.2383>

* T. Jackson-Bué previously known as T. D'Urban Jackson

This chapter was based on a collaborative research project between SEACAMS2, Bangor University and Tidal Lagoon Power Ltd

Co-author contributions:

G.J. Williams and A.J. Davies assisted with conceptualisation, framing and commenting on drafts.

G. Walker-Springett assisted with data collection

2.2 Introduction

Understanding how ecosystems vary in space and time underpins land- and seascape management, but to be effective, accurate and comprehensive information must be captured across multiple scales. Our knowledge of ecosystems represents decades of observations by ecologists using field equipment like quadrats, to capture biological information, and theodolites or satellite positioning systems (e.g. GPS) to record habitat topography. Direct observation field techniques capture detailed habitat information but are labour and resource intensive, resulting in trade-offs between three types of scale: spatial, temporal and thematic, and their components of resolution and extent (Lecours et al., 2015; Rhodes et al., 2015). For example, an abundance survey of all macro-organisms to species level (high thematic resolution and extent) with sampling at 1 m intervals (high spatial resolution) cannot feasibly cover an extent of 1 km² (limited spatial extent) or if it does, would take a very long time (limited temporal resolution). The impracticality of conventional methods for spatially or temporally continuous sampling has led to an average difference of 5.6 orders of magnitude between the extent represented and extent actually sampled in ecological studies, necessitating interpolation or extrapolation with the risk of over-leveraging data (Estes et al., 2018).

Remote sensing technologies to rapidly record detailed, spatially-referenced biological and physical information are now accessible to the field ecologist. These techniques overcome some of the logistical challenges and trade-offs of direct observation field sampling and extend the scales of remote sensing capability. This review considers tools able to capture three-dimensional (3D) ecosystem data at finer scales than can be achieved with remote sensing from satellites or crewed aircraft. We present an introduction to two of the most accessible high-resolution 3D mapping techniques, which hold enormous potential for the rapid collection of ecologically relevant, spatially continuous data at multiple scales: terrestrial laser scanning and structure-from-motion photogrammetry (Figure 2.1). Uptake of these new technologies varies widely across disciplines and user groups, and there is a strong case for their increased adoption in ecology. Our primary audiences are ecologists, environmental managers and other interested parties who have limited or no experience with these high-resolution remote sensing tools. We direct more experienced users to our analysis of the accuracy of structure-from-motion photogrammetry models at scales and contexts relevant to

ecological studies, addressing a key barrier to uptake (Section 2.5). Our aim is to shed light on powerful and increasingly user-friendly tools, encourage innovative and novel analytical approaches, and highlight the new era of 3D digital spatial ecology.

2.3 Remote sensing in ecology

Remote sensing from satellite and crewed aircraft has revolutionised spatial ecology with diverse applications that continue to grow as technology advances in capability, accessibility and familiarity. Passive earth observation from satellites has enabled global-scale mapping and monitoring of land cover, ecosystem function and climatic variables (Kerr and Ostrovsky, 2003), and now offers metre and sub-metre resolution daily imagery of anywhere on the globe, presenting new opportunities for ecology, conservation and management (Asner et al., 2017). Active spaceborne sensors have facilitated the study of broad-scale (km to global) ecosystem structure (Turner et al., 2003), enabling estimation of global ocean bathymetry (Smith and Sandwell, 1997) and continuous global topography (Farr et al., 2007). The ICESat-2 laser altimetry mission has ecosystem characterisation applications through mapping heights of ice, vegetation canopy and freshwater bodies (Seidleck, 2018), as well as unanticipated potential for nearshore bathymetric mapping (Parrish et al., 2019).

Remote sensing from crewed aircraft provides similar data products to satellite sources at higher resolution over smaller extents. Airborne laser scanning has become a widely used tool for characterising 3D habitat structural complexity and exploring organism-habitat relationships (Davies and Asner, 2014; Wedding et al., 2008). Remote sensing at higher temporal and spatial resolutions can provide information about ecosystems at scales relevant to mobile organism behaviour over days, months and years, and resulting ecological connectivity (Marvin et al., 2016; Pimm et al., 2015). In addition, technologies like laser scanning can provide structural information in 3D, rather than “2.5D”. In raster format 2.5D data, appropriate for mapping at broad spatial scales, each XY position on a regular grid has a single Z value. In 3D data formats, usually point clouds, data points each have an XYZ position, better representing 3D features (Figure 2.1). This increased density of information is valuable for examining multi-layered ecosystems but comes with additional processing and analysis challenges and so 3D information are often translated to 2.5D for analysis and visualisation (Figure 2.1). Bespoke or repeat airborne laser scanning surveys are uncommon in academic research due to high operating costs of

crewed aircraft, and compatibility issues pose challenges for the analysis of existing available data (Eitel et al., 2016).

Satellite and crewed aircraft remote sensing is irreplaceable for continuous mapping at spatial resolutions of several metres at up to global extent. However, the technique becomes logistically inappropriate when detailed information is required across smaller spatial extents (metres to hectares) or shorter time periods (hours to weeks) due to limits of data resolution, accuracy or cost. For 3D mapping at these scales, recent technological advances have led to the emergence of high-resolution (millimetre to centimetre), rapidly deployable remote sensing tools that include terrestrial laser scanning and structure-from-motion photogrammetry (Figure 2.1) (Anderson and Gaston, 2013; Danson et al., 2018; Kalacska et al., 2017). Advancement in sampling technology drives an ever-expanding range of questions we can ask about the natural world, and the ability to accurately map ecosystems in three or more dimensions is changing the way we study their ecology and management (Davies and Asner, 2014; Eitel et al., 2016; Vierling et al., 2008).

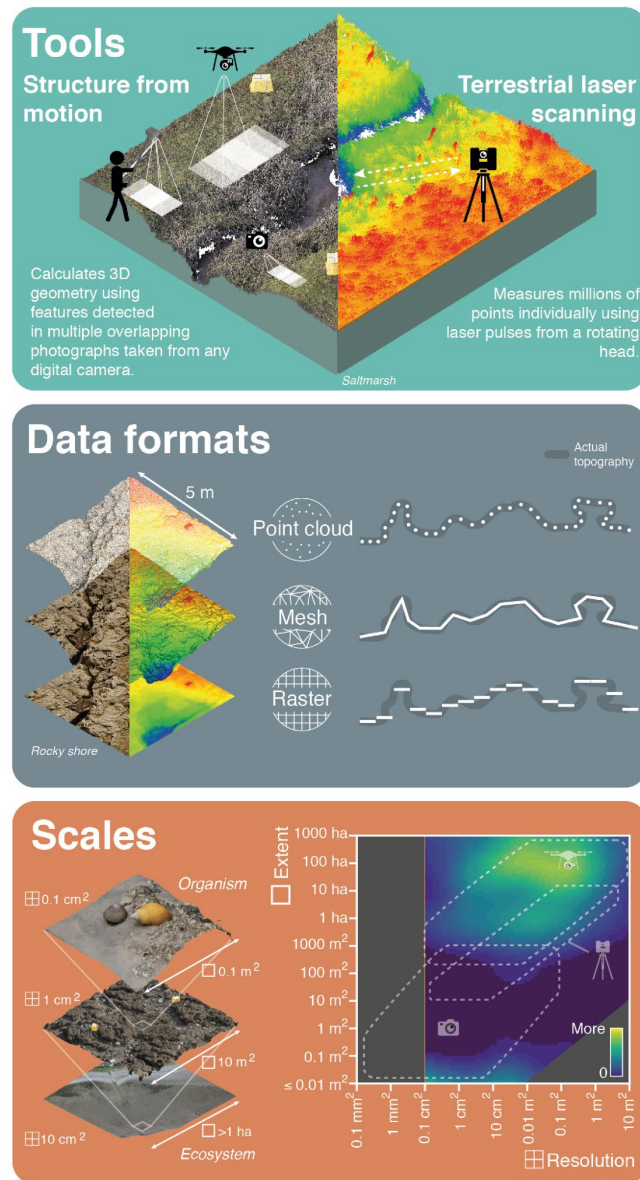


Figure 2.1 An overview of high-resolution three-dimensional ecosystem mapping tools, data formats and scales. Tools include terrestrial laser scanning and structure-from-motion photogrammetry. Point cloud data can be processed into mesh formats by interpolating between points, and raster formats to produce digital elevation models (DEMs) by averaging point elevations in a regular 2D grid. 3D information can be analysed at multiple spatial scales from organism to ecosystem. These tools enable investigation at spatial scales (resolution and extent) that are understudied in ecology. Plot shading (adapted from [Estes et al., 2018]) indicates number of ecological studies at specific scales, dashed areas represent the approximate sampling scales for terrestrial laser scanning and structure-from-motion (using drone-mounted and handheld cameras). Grey areas have no data in the original study.

2.4 High-resolution remote sensing tools for spatial ecology

Terrestrial laser scanning and structure-from-motion photogrammetry both generate accurate, high-resolution digital 3D models of the environment in the form of a point cloud (Figure 2.1). A point cloud is simply a collection of individual points with X, Y and Z coordinates describing their 3D position. Additional attributes can be added to each point to provide information such as colour or other local statistic. From point clouds, other topographic data products like mesh models and rasters can be generated for additional analyses (Figure 2.1). Although their outputs appear similar, terrestrial laser scanning and structure-from-motion photogrammetry generate point clouds in different ways, resulting in differences in the point cloud characteristics. For an overview of data collection steps using these two techniques see Figure 2.2.

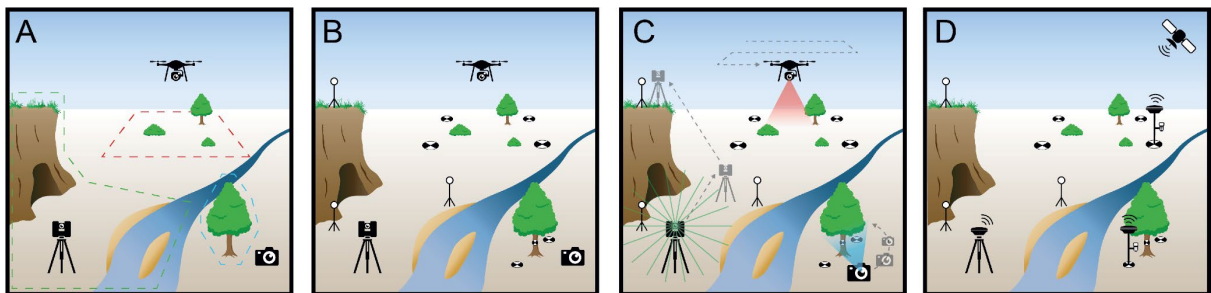


Figure 2.2 Major steps for capturing data with terrestrial laser scanning and structure-from-motion using handheld and drone-mounted cameras. A) Identify features of interest and estimate scanning positions or camera angles. B) Set out reference targets for terrestrial laser scanning, or ground control points, check points and scaling objects for structure-from-motion. For laser scanning, targets are used to align data from different stations, although scene geometry can sometimes be used for alignment instead of, or in addition to targets. For structure-from-motion, reference points are used for aligning images and constraining the modelling process, and for accuracy assessment and scaling. C) Terrestrial laser scanning collects data from a number of discrete stations, to be combined during processing. For structure-from-motion, many overlapping photographs are taken, from which a 3D model is generated during processing. D) Georeferencing, typically using a commercial grade Global Navigation Satellite System, is required to position the resulting 3D models in real-world space, and for scaling in large structure-from-motion models.

2.4.1 Terrestrial laser scanning

Using the same principles as airborne laser scanning, terrestrial laser scanning is a high-precision ground-based survey technique used extensively in civil engineering. It is an active remote sensing approach that builds an accurate model of the surroundings by emitting millions of laser pulses in different directions and analysing the reflected signals (Heritage and Large, 2009). Data collected using calibrated laser scanning equipment have intrinsic precision and real-world scale.

Terrestrial laser scanning is conducted from a set of discrete stations using a tripod-mounted instrument, collecting data radially from a low elevation (generally < 2 m). This results in a reduction in both point density and angle of incidence to the ground with increasing distance from the scanner, and sectors of missing data behind obstructions like trees. Regions with low point density are filled by merging data from multiple scanning stations (Figure 2.2), introducing a low level of quantifiable error. Data extent, resolution and coverage must be balanced with the survey time needed, especially in complex ecosystems like forests where many stations are required for comprehensive coverage of a large extent. Terrestrial laser scanning typically penetrates through fine-scale features like vegetation to record points on internal surfaces (e.g. branches) and the ground, as the independent laser pulses can travel through small gaps. Compared to crewed airborne systems, terrestrial laser scanning offers higher resolution, more accurate data from a near-ground perspective, with lower operating costs and responsive deployment capability, but across a more limited survey extent.

Falling costs and improved portability have increased the accessibility of terrestrial laser scanning to a wide variety of users (Danson et al., 2018; Heritage and Large, 2009). Custom built versions have lowered costs even further (Eitel et al., 2013), although the equipment and software required is still expensive compared to structure-from-motion photogrammetry, and may be prohibitively so for some users. Early adoption of terrestrial laser scanning for natural sciences was concentrated in the fields of geography and geoscience (Buckley et al., 2008; Heritage and Large, 2009). More recently it has seen application in ecology (Eitel et al., 2016), particularly in forest ecology where the below-canopy perspective complements airborne data collection. Applications include quantifying biomass, growth and 3D structure of forest vegetation (Danson et al., 2018; Dassot et al., 2011; Maas et al., 2008; Orwig et al., 2018; Watt and Donoghue, 2005), non-

destructive estimation of above ground grass and mangrove biomass (Cooper et al., 2017; Feliciano et al., 2014), assessing vegetation water content (Elsherif et al., 2018), studying cave-dwelling bat and bird colonies (Azmy et al., 2012; McFarlane et al., 2015), mapping freshwater habitats (Milan et al., 2010) and exploring the relationships between organisms and fine-scale topography (Hannam and Moskal, 2015; Hollenbeck et al., 2014).

2.4.2 Structure-from-motion photogrammetry

Structure-from-motion photogrammetry is a low-cost machine vision technique that enables the reconstruction of a detailed 3D model from a set of overlapping two-dimensional digital photographs (Westoby et al., 2012). The camera may be handheld or pole-mounted for small scenes, while drone-mounted cameras are commonly used to capture larger extents (Cunliffe et al., 2016). Commercial adoption of structure-from-motion is increasing as a low-cost, flexible survey tool, but questions remain over best practices for producing repeatable and high-quality outputs.

With structure-from-motion photogrammetry, the geometry of a scene is reconstructed from the relative positions of thousands of common features detected in multiple photographs taken from different vantages. Structure-from-motion is a passive remote sensing technique because photographs capture reflected light from an external source like the sun. While a basic model can be generated entirely automatically, manual input into the processing stage is required for accurate outputs. Structure-from-motion models have no inherent real-world scale, so known coordinates or distances must be incorporated to generate scale. There is greater opportunity for error introduction with structure-from-motion compared to terrestrial laser scanning, and uncertainty in data outputs varies widely and unpredictably within (James et al., 2017b) and among studies (Eltner et al., 2016). For example, error can be introduced through camera lens distortion, poorly focused images, movement of features in the scene, and imprecision in manual processing stages. Care must be taken to minimise the propagation of error through the model construction pipeline (Eltner et al., 2016). Structure-from-motion generates more homogenous and comprehensive data coverage compared to terrestrial laser scanning in less time, because the camera is moved around the scene, often using an aerial platform. However, multiple images of a point on a feature are needed to calculate a position, so internal surfaces of complex features (e.g. branches of a dense bush or coral), shaded

surfaces and moving features (e.g. blades of grass in the wind) are less likely to be captured or positioned accurately. Structure-from-motion tends to return a generalised outer surface of such features, lacking finer details.

The algorithms used for structure-from-motion are computationally demanding but falling costs of computer processing power and affordable, user-friendly software are making this technique increasingly accessible (see (Eltner et al., 2016) for popular software options). As with terrestrial laser scanning, structure-from-motion saw early adoption in geography and geoscience (Westoby et al., 2012). Ecological applications include modelling forest and vegetation structure and biomass (Cooper et al., 2017; Cunliffe et al., 2016; Iglhaut et al., 2019; Wallace et al., 2016), and quantifying fine-scale habitat topography and structure (Kalacska et al., 2018, 2017; Olsoy et al., 2018; Woodget et al., 2015). Recently there has been particular interest in underwater structure-from-motion for measuring and mapping 3D habitat complexity in coral reef systems (Bayley et al., 2019; Leon et al., 2015; Storlazzi et al., 2016).

2.4.3 Georeferencing

Georeferencing is required to position 3D data generated using terrestrial laser scanning and structure-from-motion in real-world space. Positions of equipment (e.g. laser scanner, drone) or identifiable features (e.g. targets) are typically recorded using a survey grade Global Navigation Satellite System (GNSS) with an accuracy of 1-3 cm. This stage can represent one of the largest sources of error in the 3D modelling processing pipeline. The influence of georeferencing error on terrestrial laser scanning and small-extent structure-from-motion data (e.g. $< 100 \text{ m}^2$) can be minimised by incorporating it at a late stage in processing, and with low weighting. However, with large scenes modelled with structure-from-motion using drones, georeferencing using well-distributed ground control points must be incorporated into the process at an earlier stage to provide scale, and prevent warping of geometry (Nex and Remondino, 2014). With sub-centimetre-resolution 3D data, georeferencing error can be a limiting factor for detection of fine-scale change in topography through time (Hannam and Moskal, 2015), and for estimating the accuracy of survey techniques (Mancini et al., 2013), demanding positioning technology with sub-centimetre accuracy (e.g. Total Station).

2.5 Accuracy of structure-from-motion models in ecological settings

Structure-from-motion photogrammetry can achieve impressive accuracy, but the flexibility of the technique makes it vulnerable to the introduction of error that is method and context specific. Most assessments of accuracy in natural settings have been in the field of geoscience, with measurement error varying from < 1 mm to over 3 m and somewhat dependent on the distance between camera and surface (Eltner et al., 2016). The appropriate scale of ecological study is driven by the research question, and the scale of patterns and processes relevant to that question. The spatial scales of ecological patterns often include the very fine (< 10 cm), so an estimate of the realistic achievable accuracy of structure-from-motion photogrammetry at this order of magnitude of scale is crucial to assess its usefulness to ecologists and environmental managers.

2.5.1 Methods

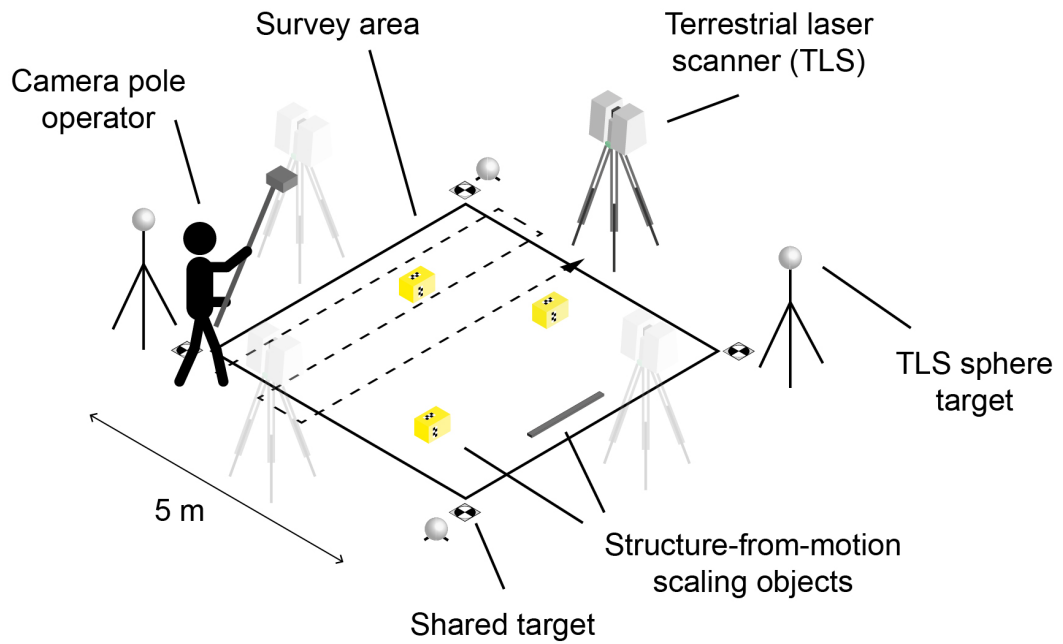
We tested error in structure-from-motion photogrammetry models against terrestrial laser scanner baseline data in three common and ecologically important habitats (rocky shore, honeycomb worm (*Sabellaria alveolata*) biogenic reef and saltmarsh) that together cover approximately 72% of UK intertidal land (Rowland et al., 2017). Rocky shores are a classic model for investigating relationships between biodiversity and habitat structural complexity (Kovalenko et al., 2012). Saltmarshes are vegetated habitats with both terrestrial and marine features where fine-scale variation in topography can result in substantial biological and physical responses (Langlois et al., 2003). Honeycomb worm (*Sabellaria alveolata*) reef is a habitat of conservation importance listed in national and international environmental legislation, making up the most significant intertidal bioconstructions in Europe (Desroy et al., 2011). Study sites were located along the North Wales coast (UK) with fieldwork conducted on spring low tides during summer and autumn 2017.

We conducted terrestrial laser scanning and structure-from-motion surveys for each plot simultaneously for direct comparison of outputs. Weather conditions were optimal for both survey techniques, with data collected on days with sunshine, low wind speed and no precipitation. We conducted tests at three spatial scales to maximise the relevance of results to a wide range of ecological study designs: three 25

m² quadrats per habitat with a target spatial resolution of < 1 cm (fine-scale), a single 2500 m² area per habitat with < 2 cm resolution (medium-scale) and the same 2500 m² area with 5 cm resolution (broad-scale). Fine-scale plots represented quadrat scale field sampling, medium-scale plots tested the level of detail and accuracy achievable at a habitat scale and broad-scale sampling was based on a typical design for a large extent drone survey that could be used for ecosystem scale studies.

We used the same tripod-mounted terrestrial laser scanning equipment (Leica Geosystems ScanStation C10) at all scales. We used terrestrial laser scanning as the baseline because it is a commercially recognised technique with known standards and precision (6 mm at 50 m range for the model we used), and the most accurate 3D mapping technique available to us at the time. For all surveys we used full field-of-view (360° horizontal, 270° vertical), medium resolution scans (point spacing of 10 cm at 100 m range) with no photographs due to tidal time constraints. For fine-scale plots we used four scanning stations whereas for medium- and broad-scale plots we used 7–8 stations (Figure 2.3). 3D mapping using structure-from-motion simply requires a set of overlapping photographs of a scene as input. We took photographs for structure-from-motion using a pole mounted camera (18 MP Canon EOS M with 22mm prime lens) for fine scale plots, and a quadcopter drone (DJI Phantom 3 Pro with 12 MP camera) for medium- and broad-scale plots, flying at 25 m and 90 m altitude respectively to simulate typical survey designs and achieve the desired ground sampling distances, the real-world size of each image pixel (Figure 2.3). The drone was flown on an automated parallel track flight path by a professional drone pilot (OcuAir Ltd.). We used shared reference targets (flat, black and white quadrant targets) were used for terrestrial laser scanning and structure-from-motion so that data from the two techniques could be aligned without introducing GNSS georeferencing error (Figure 2.3). Fine-scale plots included scaling objects that provided scale reference along X, Y and Z axes. Medium- and broad-scale plots included reference objects of known size and shape for comparison of results.

Fine scale



Medium / Broad scale

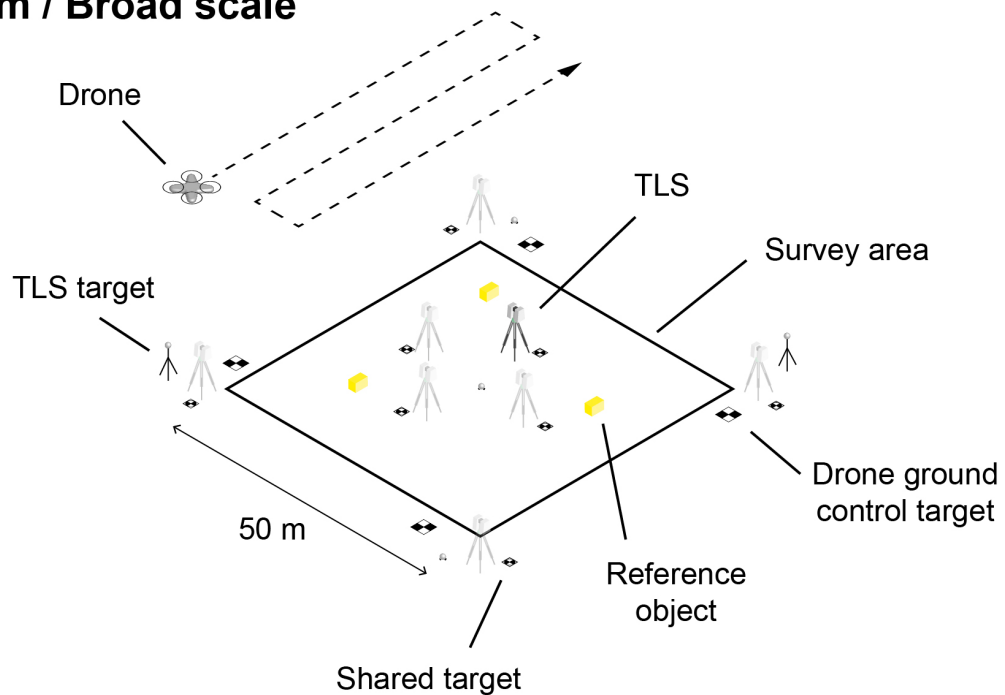


Figure 2.3 Survey methods for comparison of terrestrial laser scanner and structure-from-motion photogrammetry 3D ecosystem mapping data at three scales. Shared targets were used to align data from the two techniques without introducing georeferencing error. Scaling objects were used to scale fine-scale structure-from-motion models. Reference objects enabled comparison of shape reconstruction by the two techniques.

After data collection, both terrestrial laser scanning and structure-from-motion require a series of data processing steps to ensure high quality outputs. With calibrated equipment, data from each terrestrial laser scanning station are correctly scaled, levelled, and have known precision (6 mm individual measurement precision at a range of 50 m for the equipment we used). We conducted data processing using Leica Geosystems Cyclone software, which involved aligning data from multiple stations using reference target positions or regions of overlapping geometry. We combined individual station data to produce a single complete dataset per plot with maximum 3D errors in target positions between individual stations of 6 mm. We manually cleaned each complete point cloud dataset of unwanted objects (e.g. people), artefacts (e.g. reflections in water surfaces) and noise (erroneous points).

We conducted data processing for structure-from-motion using the popular software Agisoft Photoscan Professional, chosen because it provides a good balance between quality of outputs, control over settings, user-friendliness and cost (Eltner et al., 2016). The workflow for processing structure-from-motion data using Photoscan is similar to other software options. First, we checked images for sharpness and exposure, discarded blurred images and corrected exposure where necessary. We masked background and moving features like shadows from images. We automatically aligned images using “High” accuracy and 40,000 tie points to generate a sparse point cloud. We manually placed markers at the centre of each reference target in each image. For fine-scale image sets, we placed 15-19 pairs of scale markers at various separations from 1 cm to 1 m. For shared reference markers we assigned coordinates from the relevant terrestrial laser scanning dataset. Image alignment was iteratively optimised after marker placement using the gradual selection tool to delete low quality tie points using a workflow adapted from USGS (2017). We then generated a dense cloud using “High” quality setting and “Mild” depth filtering to retain fine topographic features while removing noise. We exported the resulting point cloud for analysis.

We cropped pairs of aligned terrestrial laser scanning and structure-from-motion point cloud models to common extents, subsampled to similar point densities (Table 2.1) and further cleaned point clouds using the statistical outlier removal tool in the open-source software CloudCompare. We generated broad-scale terrestrial laser scanning data by

subsampling medium-scale data to a density similar to broad-scale drone data (5 cm point spacing)(Table 2.1).

We measured the distance between each pair of models at 100,000 random positions using the multiscale model-to-model cloud comparison algorithm (M3C2), a robust method developed specifically for comparison of point cloud data from natural environments that contain multiscale complexity, implemented in CloudCompare (Lague et al., 2013). In brief, the algorithm calculates the distance between point clouds along the direction of the local surface orientation, known as the normal, at each measured point. This is an improvement over nearest neighbour methods or measuring distance along a single axis, typically vertically (Lague et al., 2013).

We used the mean of absolute distances between point clouds to quantify the accuracy of the structure-from-motion model relative to the terrestrial laser scanning model, as mean absolute error (MAE) (Figure 2.4). While another metric, root mean square error (RMSE) is commonly used for model comparisons, this can be heavily influenced by a small number of large errors which were likely to be present in our data due to some noise remaining after data cleaning. By comparing point cloud data we avoided the introduction of error by the more common approach of interpolating and averaging data to a raster format digital elevation model (DEM) (Mancini et al., 2013). We visually analysed point cloud models and cross sections to assess the key differences between outputs from two different techniques (Figure 2.5).

Table 2.1 Characteristics of point cloud datasets derived from terrestrial laser scanning (TLS) and structure-from-motion photogrammetry (SfM) analysed at multiple scales and habitats. Raw point counts are after cropping to the study area. Processed point counts are after cleaning and subsampling. Median and interquartile range (IQR) point density are of the processed point clouds.

	Habitat	Quadrat	Technique	Raw point count (M)	Processed point count (M)	Median point density (n m ⁻²)	IQR of point density (n m ⁻²)
Fine scale	Rocky shore	1	TLS	2.49	0.88	29,200	10,000
			SfM	24.34	0.75	24,000	4,400
		2	TLS	28.25	0.93	23,200	5,600
			SfM	3.17	0.92	21,600	2,400
		3	TLS	2.65	1.17	31,600	12,800
			SfM	32.08	1.27	24,800	6,800
	Biogenic reef	1	TLS	2.93	1.16	24,400	8,800
			SfM	46.56	1.48	24,800	6,400
		2	TLS	2.37	0.80	26,000	6,800
			SfM	31.78	0.80	23,600	4,000
		3	TLS	3.01	0.94	28,400	9,200
			SfM	31.71	0.81	22,800	4,000
	Saltmarsh	1	TLS	2.04	1.37	40,000	24,400
			SfM	22.78	1.35	33,600	27,600
		2	TLS	1.47	0.99	26,000	9,600
			SfM	21.71	1.00	25,600	6,000
		3	TLS	2.10	1.40	26,800	26,000
			SfM	23.70	1.33	23,200	25,200
Medium scale (low altitude UAV)	Rocky shore	TLS		19.07	6.77	900	400
		SfM		2.74	2.61	1,600	700
	Biogenic reef	TLS		13.94	5.06	400	400
		SfM		1.27	1.23	1,000	500
	Saltmarsh	TLS		20.02	9.75	700	400
		SfM		1.92	1.87	600	300
Broad scale (high altitude UAV)	Rocky shore	TLS		19.07	0.61	200	200
		SfM		0.26	0.22	100	100
	Biogenic reef	TLS		13.94	0.44	200	200
		SfM		0.11	0.11	<100	100
	Saltmarsh	TLS		20.02	0.96	500	400
		SfM		0.30	0.23	100	100

2.5.2 Results and discussion

We found mean absolute distance (± 1 standard deviation) between structure-from-motion and terrestrial laser scanner data ranged from 4 mm \pm 14 mm (fine-scale, rocky shore) to 56 mm \pm 111 mm (medium-scale, saltmarsh) (Figure 2.4). In all cases, distances between the point clouds clustered close to zero, indicating good average agreement, with positive and negative errors compensating each other. The spread of measured distances varied, with fine-scale and stable substrate scenes showing the least variation, while broad-scale and vegetated scenes showed the most (Figure 2.4). Visual inspection of model difference maps and cross-sections revealed that on average structure-from-motion models were accurate, but as resolution decreased, sharp features became smoothed, with cuboid reference objects being represented as mounds (Figure 2.5). Similar results are reported in other studies, with high agreement between structure-from-motion and terrestrial laser scanning at fine-scales of up to 1 m² (Cooper et al., 2017; Hillman et al., 2019) and centimetre-level accuracy at broad scales (hectares) (Cook, 2017; Mancini et al., 2013).

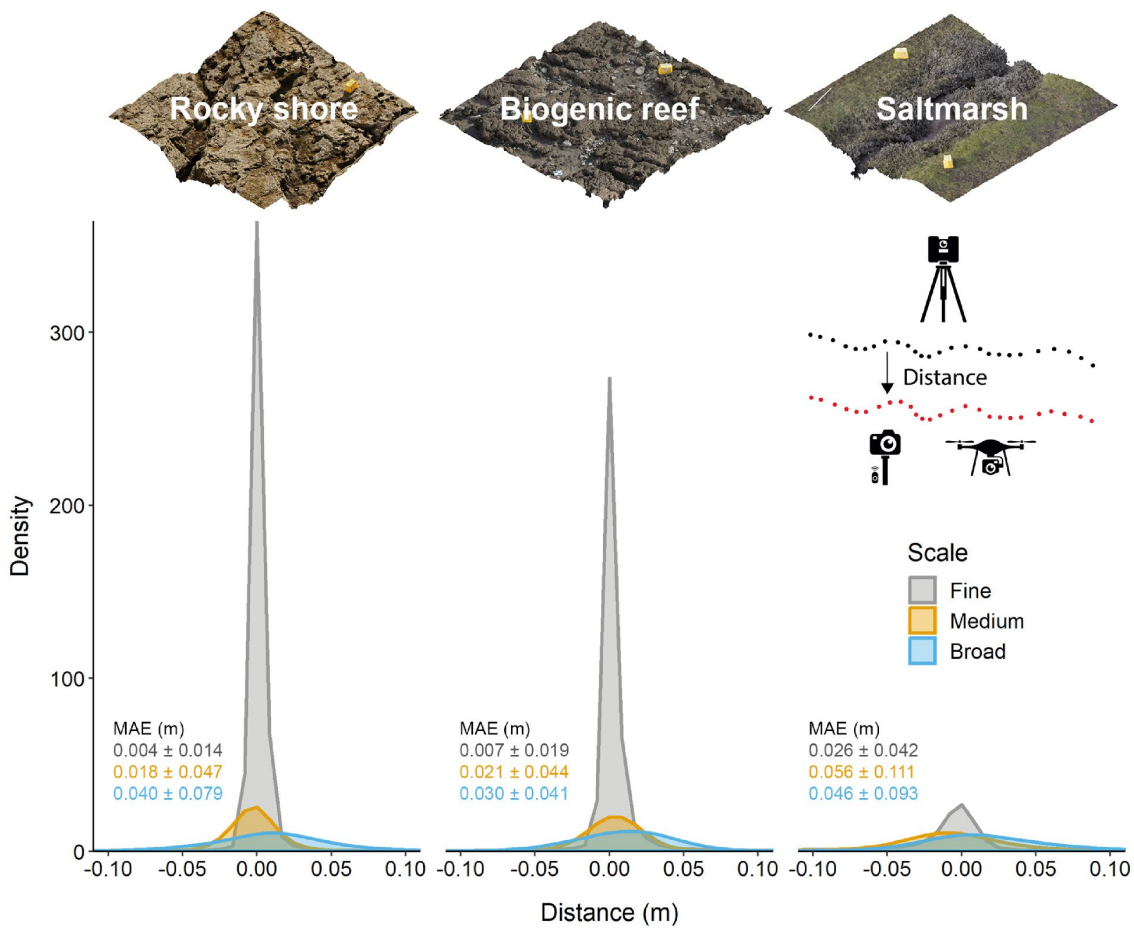


Figure 2.4 Accuracy of a structure-from-motion point cloud quantified as the point-by-point distance to a reference terrestrial laser scanning point cloud in three habitats (rocky shore, biogenic reef and saltmarsh) and at three scales (fine: 25 m² with < 1 cm resolution, medium: 2,500 m² with < 2 cm resolution and broad: 2,500 m² with 5 cm resolution). Distances were measured at 100,000 points and plotted as density curves, with the area under each curve being equal. Curve tails beyond 0 ± 0.1 m are not shown. Mean absolute error (MAE) ± 1 standard deviation (m) distance is reported.

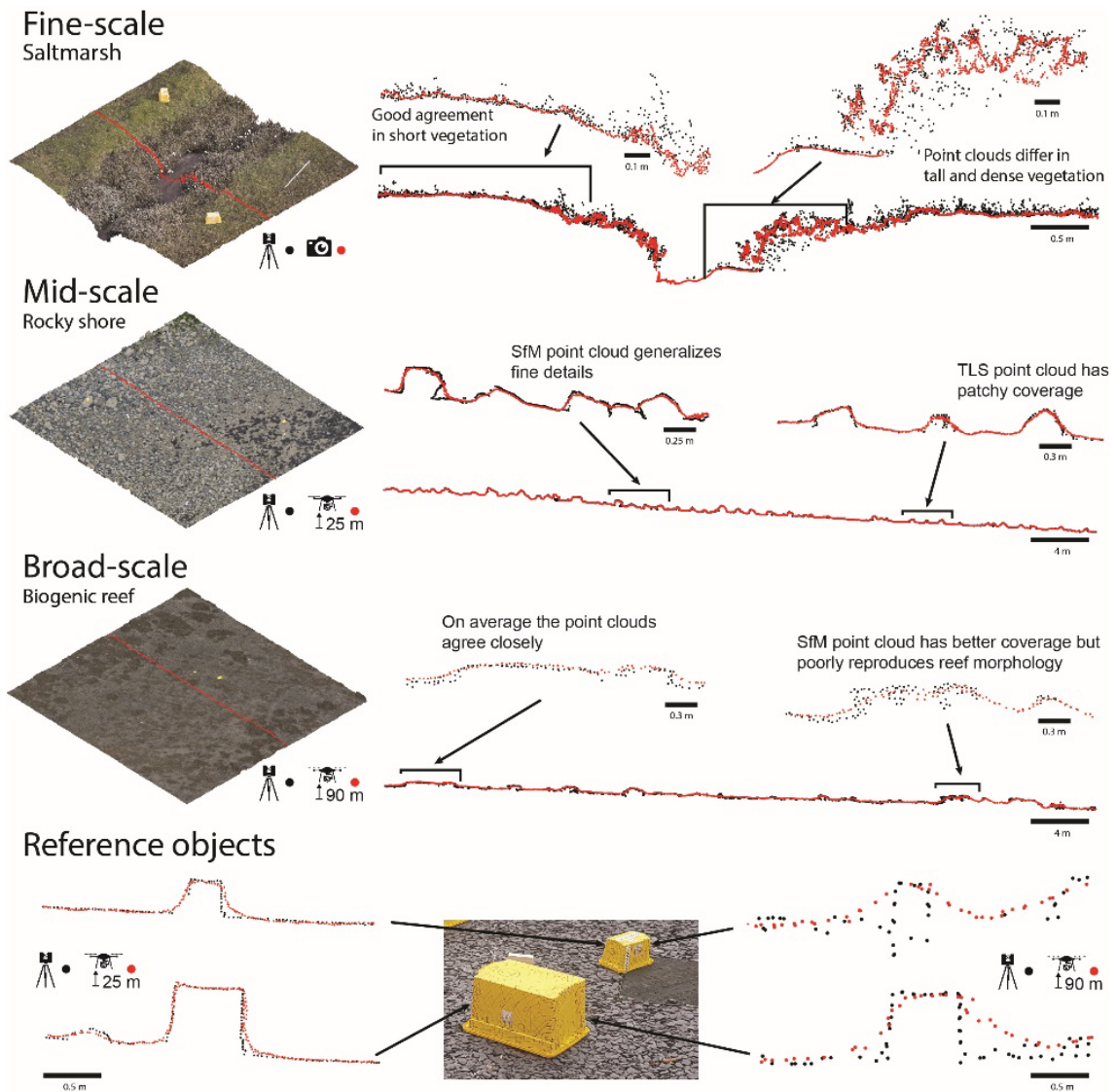


Figure 2.5 Differences in 3D point cloud models generated by terrestrial laser scanning (TLS, black points) and structure-from-motion photogrammetry (SfM, red points) at three spatial scales and three habitats. Models agree closely at fine scales (25 m² extent, <1 cm resolution) in areas of solid substrate or short vegetation. In tall and dense vegetation the models differ, with points captured from further into the feature by terrestrial laser scanning. At medium-scales (2500 m² extent, <2 cm resolution) on solid substrate average difference in models is low, but fine details are generalised by structure-from-motion. Terrestrial laser scanning data have gaps due to some areas being out of line-of-sight from any scanning position. At broad-scales (2500 m² extent, 5 cm resolution), SfM models the general form of the scene well but detailed topographic morphology is more accurate in terrestrial laser scanner data. As scale increases detailed features become smoothed by structure-from-motion, as demonstrated by models of reference objects with known shape and size.

2.6 A case for increased adoption of 3D mapping techniques in ecology

Terrestrial laser scanning and structure-from-motion photogrammetry offer rapid, detailed, continuous extent 3D mapping of ecosystems. Relieving scale-dependence of sampling and easing trade-offs in scale presents opportunities to ask new questions of the natural world and revisit classical paradigms at new scales. The potential applications for high-resolution 3D mapping techniques are vast, and like satellite remote sensing and airborne laser scanning, much of their value will likely only emerge once techniques are firmly established as standard ecological tools. Unique insights are already being generated, particularly in forest and coral reef ecosystems (Calders et al., 2020), whereas adoption has been slower in other systems such as intertidal habitats. Multiscale topography plays a critical structuring role in the intertidal zone by controlling environmental conditions and field time is constrained by tidal cycles, making rapid 3D mapping tools valuable to intertidal field ecologists. In this section we identify and discuss several themes of study in which emerging techniques have either already found innovative and transformative applications or are likely to have high impact in the near future (Figure 2.6).

2.6.1 Understanding relationships between organisms and habitat structure

Analyses of organism-habitat relationships can be hampered by our ability to quantitatively capture the environment at ecologically meaningful spatial and temporal scales. This has resulted in a diversity of definitions, metrics and methods employed to understand the mechanisms behind system-independent phenomena like habitat complexity-biodiversity relationships (Kovalenko et al., 2012). The analysis of digital representations of 3D habitat structure to derive system- and scale-independent metrics, like fractal dimension (Reichert et al., 2017), or novel organism-centric metrics (Meager and Schlacher, 2013), could lead to improved understanding by reducing the need to simplify 3D habitat structure (e.g. to 2D profiles) to facilitate analysis (Bayley et al., 2019; Dustan et al., 2013; Gratwicke and Speight, 2005; Kovalenko et al., 2012; Storlazzi et al., 2016).

Spatial patterning and the patchiness of species across a landscape can depend on topography at multiple scales. The methods used to observe and analyse topography across scales have important influence on the understanding generated (Lucieer et al., 2018a). As technologies for data collection advance, so too do methods for analysis increasingly detailed information about landscape pattern and ecosystem structure (Kedron et al., 2019; Kedron and Frazier, 2019; McGarigal et al., 2009). In tidal flats and flood plains, elevation changes in the order of centimetres can control species distributions, interactions and ecosystem services (Kalacska et al., 2017). Understanding fine-scale relationships can improve species distribution and habitat suitability modelling and lead to advances in organism-perspective landscape analysis. Terrestrial laser scanning was used to estimate topographically-controlled foraging habitat suitability for the black oystercatcher (*Haematopus bachmani*) and model how it may change under future sea-level rise (Hollenbeck et al., 2014). Fine-scale topography and 3D structure can control other variables that can be modelled in finer scales than ever before, like microclimate (Milling et al., 2018), soil pH (Baltensweiler et al., 2017) and hydrodynamic forces (Helmuth and Denny, 2003). This can enable quantification of environmental variables as continuous rather than categorical factors, which may lead to alternative or improved interpretations of organism-environment relationships (Caryl et al., 2014; Lindegarth and Gamfeldt, 2005).

2.6.2 Measuring and monitoring small, slow and complicated variation in 3D form

Improved morphological descriptions of complex natural shapes can be made with comprehensive 3D data, and variation in such shapes can be monitored through space and time at an organism-relevant resolution. Using terrestrial laser scanning, researchers found that oysters, an ecosystem engineer, can accrete reef structure at a faster rate than current sea-level rise, with important management and conservation implications (Rodriguez et al., 2014). Coral reef structure is difficult to quantify and previous methods known to poorly capture detailed topography, like the chain-and-tape method, can now be replaced with more repeatable structure-from-motion surveys with similar in-water effort (Bayley et al., 2019; Storlazzi et al., 2016). Through accurate feature modelling, terrestrial laser scanning can improve on traditional allometric equation methods to estimate above ground biomass in trees (9.68% overestimation compared to 36.57–

29.85% underestimation) (Calders et al., 2015). The low cost of operation and rapid deployment capability of terrestrial laser scanning and structure-from-motion make them suitable for opportunistic pre- and post-event change detection (Honkavaara et al., 2013) and environmental impact assessment monitoring.

2.6.3 Virtual sampling, digital archiving and addressing problems of scale in ecology

With sampling now achievable at sub-centimetre resolutions, ecosystems can be digitally represented to a degree that in some instances exceeds the resolution possible using *in situ* human observation. There are, however, still limitations of completely removing the human observer element. Macroalgal canopy cover estimates on rocky shores are indistinguishable between “virtual quadrats” from drone-derived image mosaics and *in situ* human observers using field quadrats, but understory turfing algal species are under-sampled in virtual quadrats (Murfitt et al., 2017). Sampling of cryptic species and multi-layered features will remain challenging to sample using remote sensing. Despite some limitations, the potential advantages of sub-centimetre digital mapping of ecosystems are hugely exciting, including automated species detection and identification using computer vision and machine learning (Guan et al., 2015), entire extent sampling that removes interpolation issues when scaling up from replicate samples (Estes et al., 2018), and simultaneous biological and environmental sampling (Murfitt et al., 2017) (Figure 2.6). Capturing and archiving detailed digital snapshots of ecosystems in a rapidly changing world is likely to prove invaluable for future, currently unknowable analytical approaches.

Organisms interact with their environment at a range of scales, but understanding scale-dependent patterns and processes is a long-standing challenge in ecology (Levin, 1992; Wheatley and Johnson, 2009). Observation of organisms and their environment is often conducted at spatial, temporal and thematic scales that are human-centric and chosen arbitrarily or logistically, rather than guided by the ecological processes being studied (Lecours et al., 2015; Levin, 1992; Meentemeyer, 1989; Wheatley and Johnson, 2009; Wiens, 1989). Due to the versatility of high-resolution remote sensing methods like terrestrial laser scanning and structure-from-motion, studies can now be conducted at scales that have previously been underexplored in ecology (Figure 2.1) (Estes et al., 2018).

One of the difficulties in multiscale analysis is the time and resource constraints of sampling the same extent at different resolutions (Lecours et al., 2015). With the ability to rapidly sample large extents at high-resolution, multiscale data can be digitally generated by resampling. We have increasing flexibility to move away from arbitrarily chosen sampling scales and observe ecosystems at ecologically relevant and mechanistic scales.

2.6.4 Value to managers, policy makers and the public

In a rapidly changing world, tools to efficiently record accurate, detailed snapshots of the environment and monitor ecosystem health are extremely valuable to environmental managers and policy makers. Policy makers require high quality environmental information to make evidence-based decisions aimed at limiting environmental impact, conserving ecosystems and maintaining ecosystem services, to the benefit of the public. Often availability of technology to environmental managers is not limiting, but without practical information on how to efficiently utilise tools, and analyse and interpret new data types with confidence, there may be a lag in adoption of emerging technologies in favour of more familiar methods, despite their known limitations (Ramirez-Reyes et al., 2019; Vanden Borre et al., 2011). Better information about ecosystem structure across scales may lead to improvements in predicting habitat suitability for, and monitoring performance of restoration actions for coastal habitats like mangrove forests, oyster reefs and saltmarshes where elevation and inundation cycles are crucial factors. Investigating the ecological mechanisms and consequences of patch dynamics and monitoring ecosystem change, including climate-driven change, is an area of landscape ecology that will benefit from increasingly widespread adoption of high resolution 3D mapping (Jackson et al., 2018). A benefit of high-resolution 3D mapping technologies for public facing research groups and environmental bodies is the easily interpreted visual data products generated. Photo-realistic 3D models of ecosystems aid explanation of ecological processes and issues, improving public communication and education through digitally annotated still images, animations or virtual reality systems.

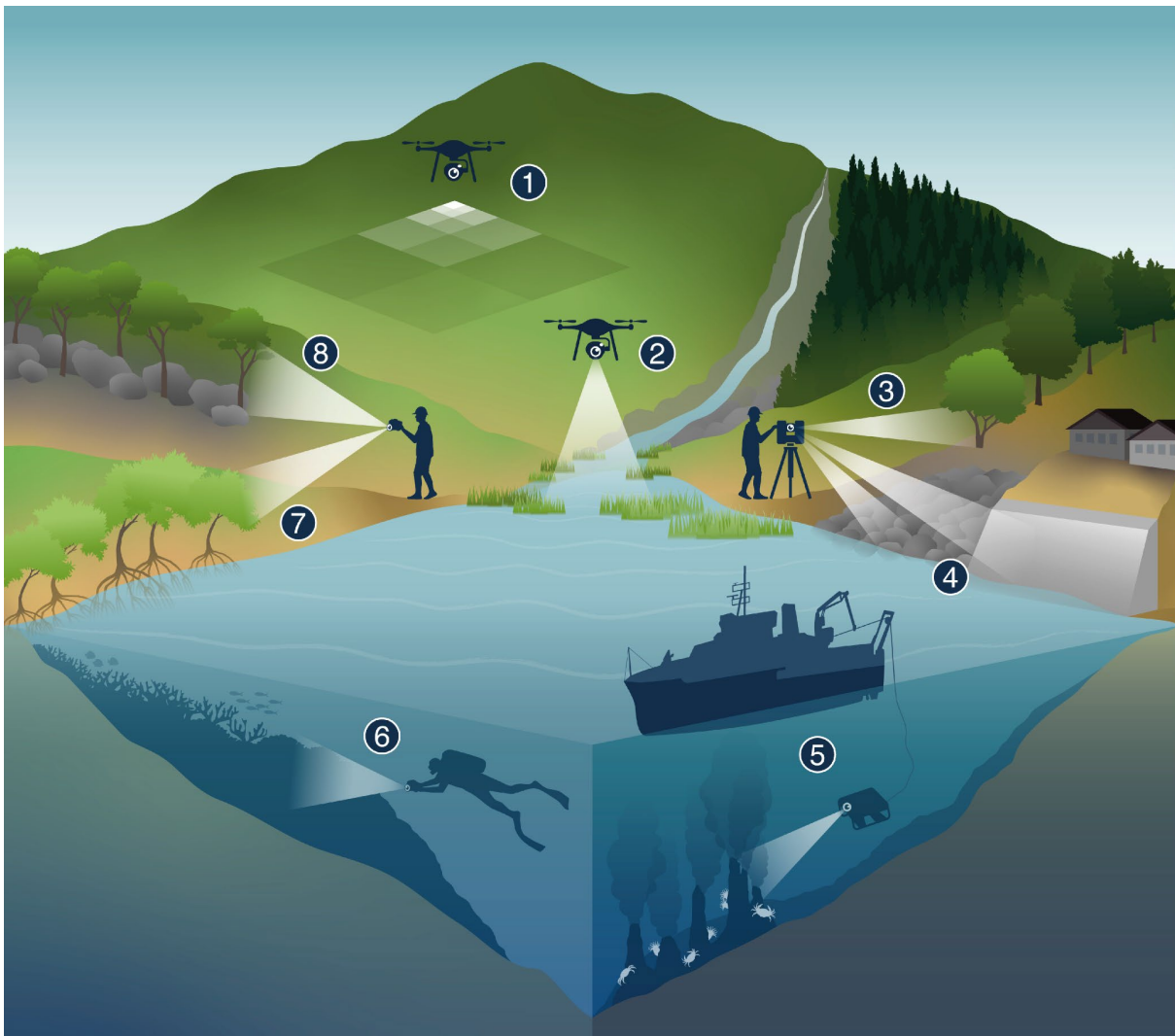


Figure 2.6 Examples in ecology and environmental management with existing or potential applications for 3D ecosystem mapping. 1) Multiscale experimental design with high-resolution 3D mapping across large extents. 2) Mapping fine-scale variation in topography across tidal flats and wetlands. 3) Automated species identification and biometric measurement in forests. 4) Comparing topographic variation in natural and artificial hard coastal substrates. 5) Digital archiving of 3D habitat structure in inaccessible ecosystems. 6) Monitoring variation in reef topography in space and time. 7) Modelling growth in complex 3D organisms like mangrove trees. 8) Mapping 3D structure in habitats with canopy cover and overhangs.

2.7 Barriers to wider uptake in ecology

While some sub-disciplines of ecology are making headway in using high-resolution remote sensing methods to answer questions and test ecological paradigms across scales (Calders et al., 2020), in general the methods remain underutilised across the discipline (Lepczyk et al., 2021). A Web of Science search conducted in December 2019 found that just 1.4% (59 out of 4348) of articles about terrestrial laser scanning or structure-from-

motion were categorised as “ecology” compared to 23.7% (1031) categorised as “geosciences multidisciplinary”. Further, 67.8% of these articles were published in the preceding three years (2017–2019), highlighting the emerging adoption of these techniques. Here we identify four perceived barriers to wider uptake in ecology.

Firstly, potential users may be unaware that such techniques exist, so a major aim of this article is to introduce ecologists and environmental managers to two of the most common and powerful techniques in an accessible manner. Second, potential users may be somewhat aware of the techniques discussed, but perceive them to be specialised tools and inaccessible due to high expertise, cost or time requirements. Technological advances in hardware and user-friendly software mean non-specialists can now be using these techniques in a basic form within a day with a small amount of training or self-learning. Equipment, software and training costs can still be significant, especially for terrestrial laser scanning, with further costs incurred for maintenance and insurance. However, the multidisciplinary applications of the techniques mean many institutions will already have access to suitable equipment and software, or can gain access to shared resources. Structure-from-motion costs can be comparable to many other field techniques, especially if using a handheld camera and open-source software. Practical field time requirements are context dependent. In coastal habitats we found that terrestrial laser scanning took 15 – 20 min between stations for a typical medium resolution (10 cm point spacing at 100 m range) survey. Structure-from-motion time requirements ranged from approximately 20 minutes for a 25 m² area surveyed using a pole mounted camera, to 2 hr for a 10 ha area surveyed at 2-cm resolution using a multi-rotor drone (45 m altitude). As a photographic technique, structure-from-motion is slowed or halted in low-light, while terrestrial laser scanning can be conducted in darkness. Processing of terrestrial laser scanning data is rapid (1 – 2 hr) and can even be conducted on a laptop in the field directly after surveying. Processing a basic structure-from-motion model can be achieved in a similar amount of time, but an accurate, detailed model typically takes a day or more to process depending on processing power and number of images. For a comparison of practical considerations for terrestrial laser scanning and structure-from-motion for geoscience see (Wilkinson et al., 2016).

A third possible barrier to uptake in ecology is that potential users are aware of 3D mapping tools and understand how they are conducted but do not see value in their use,

or are resistant to exploring technology-based alternatives to traditional field methods. Technology is unlikely to ever completely replace a human ecologist in the field for direct observation and interpretation, but can augment data collection and improve efficiency and quantification of specific variables if used appropriately (Edwards et al., 2017). By separating tasks that require human engagement from those that are more efficiently performed using technology, field time can be optimised (Murfitt et al., 2017). These technologies allow us to test existing ecological concepts at novel scales and inspire new questions that could result in novel paradigms and understanding.

Finally, potential users may be aware of the techniques and understand how they are conducted but are sceptical about the accuracy of the outputs at their spatial scales of interest; this is especially relevant for structure-from-motion photogrammetry. To address this, in this paper we have presented results from an assessment specifically to test the realistic accuracy and characteristics of structure-from-motion models in contexts and at spatial scales relevant to ecologists and environmental managers (Figure 2.4**Error! Reference source not found.**). Our results demonstrate that millimetre to centimetre scale variation in topography can be measured in space and time using high-resolution 3D mapping techniques in the field, making them valuable for numerous ecological applications (Figure 2.6).

The perceived barriers to adoption of 3D mapping techniques for ecological data collection are now low. However, system-specific challenges remain in survey design, data processing and interpretation. With terrestrial laser scanning in complex environments, line-of-sight obstructions and moving vegetation combined with the spatial characteristics of the point cloud data generates challenges for interpretation and analysis (Ashcroft et al., 2013; Hillman et al., 2019; Richardson et al., 2014). While the moving vantage aspect of structure-from-motion data capture means more homogenous data coverage, repeatability of coral reef rugosity measurements were impacted by high habitat complexity, environmental conditions and variation in methods (Bryson et al., 2017). The use of drone-mounted sensors for field ecology comes with an additional suite of considerations for training, permissions and constantly evolving regulations that govern their safe and legal usage (Duffy et al., 2018). Data processing still requires manual input at various stages, and automated workflows can be computationally demanding, especially for structure-from-motion. Various algorithms and software packages are

being developed for 3D point cloud processing, including open source projects like CloudCompare (CloudCompare, 2019). After the initial processing stages required to generate a 3D model, further processing and analysis currently requires non-trivial technical skill or novel approaches specific to the task. As 3D methods become more common in ecology, an increase in demand and funding for user-friendly and powerful processing techniques, including packages for open-source platforms like Python and R, can be expected.

2.8 Conclusion

Technology is available and accessible to non-specialist ecologists that enables the detailed mapping of habitats and organisms accurately in 3D. These techniques unlock a wealth of new spatial and temporal ecological questions that were logistically impossible to ask only a few years ago. As with any sampling method the limitations should be understood as uncertainty may not be readily detected, and there is a need for standardisation of protocols. The power of these techniques mean they are rapidly becoming standard and essential tools in various disciplines. By embracing emerging technologies, modern ecologists can overcome longstanding challenges in studying scale-dependent organism-environment relationships. Digital ecosystem analysis and multiscale 3D spatial ecology is continuing to evolve, and high-resolution remote sensing techniques are becoming instrumental as part of the modern spatial ecologist's tool kit.

3 Three-dimensional mapping reveals scale-dependent dynamics in biogenic reef habitat structure

3.1 Abstract

Habitat structure influences a broad range of ecological interactions and ecosystem functions across biomes. To understand and effectively manage dynamic ecosystems, we need detailed information about habitat properties and how they vary across spatial and temporal scales. Measuring and monitoring variation in three-dimensional (3D) habitat structure has traditionally been challenging, despite recognition of its importance to ecological processes. Modern 3D mapping technologies present opportunities to characterise spatial and temporal variation in habitat structure at a range of ecologically relevant scales. Biogenic reefs are structurally complex and dynamic habitats, in which structure has a pivotal influence on ecosystem biodiversity, function and resilience. For the first time, we characterised spatial and temporal dynamics in the 3D structure of intertidal *Sabellaria alveolata* biogenic reef across scales. We used drone-derived structure-from-motion photogrammetry and terrestrial laser scanning to characterise reef structural variation at mm to cm resolutions at a habitat scale ($\sim 35,000 \text{ m}^2$) over one year, and at a plot scale ($2,500 \text{ m}^2$) over five years (2014-2019, 6-month intervals). We found that most of the variation in reef emergence above the substrate, accretion rate and erosion rate was explained by a combination of systematic trends with shore height and positive spatial autocorrelation up to the scale of colonies (1.5 m) or small patches (up to 4 m). We identified previously undocumented temporal patterns in intertidal *S. alveolata* reef accretion and erosion, specifically groups of rapidly accreting, short-lived colonies and slow accreting, long-lived colonies. We showed that these highly dynamic colony-scale structural changes compensate for each other, resulting in seemingly stable reef habitat structure over larger spatial and temporal scales. These patterns could only be detected with the use of modern 3D mapping technologies, demonstrating their potential to enhance our understanding of ecosystem dynamics across scales.

This chapter has been published as a peer-reviewed article:

Jackson-Bué, T., Williams, G.J., Walker-Springett, G., Rowlands, S.J. and Davies, A.J., 2021. Three-dimensional mapping reveals scale-dependent dynamics in biogenic reef habitat structure. *Remote Sensing in Ecology and Conservation*, 7(4), pp.621-637 <https://doi.org/10.1002/rse2.213>

This chapter was based on a collaborative research project between SEACAMS2, Bangor University and Tidal Lagoon Power Ltd

Co-author contributions:

G.J. Williams and A.J. Davies assisted with conceptualisation, framing and commenting on drafts.

G. Walker-Springett and S.J. Rowlands assisted with data collection.

3.2 Introduction

Ecosystems are dynamic (Odum, 1969). Gradients in biophysical and human socioeconomic drivers create complex mosaics in ecosystem properties (Legendre and Fortin, 1989; Perry, 2002; Williams et al., 2019), with the patterns we observe determined by the scale of our observations (Levin, 1992; Wiens, 1989). Because ecosystem patterns and processes are intrinsically linked, we can gain a deeper understanding about ecological processes and their drivers by quantifying these underlying patterns across scales (Horne and Schneider, 1995; Underwood et al., 2000). Quantifying patterns in ecosystem properties not only advances ecological insight, but also facilitates evidence-based management by enabling us to detect change in ecosystem characteristics like habitat structure in response to disturbance (Landres et al., 1999).

Physical habitat structure can be abiotic like rocks on a shoreline, or biogenic like the trees of a forest. These features determine habitat structural complexity and influence the biodiversity and community composition of associated ecological communities through myriad processes. These include buffering organisms from extreme environmental conditions (Scheffers et al., 2014), mediating resource availability (Safriel and Ben-Eliahu, 1991), and providing shelter for prey species from predation (Stevenson et al., 2015; Warfe et al., 2008). Biogenic reefs are complex habitats in which substrate and structure is generated and amplified by engineering organisms (Jones et al., 1994). Biogenic reefs represent global biodiversity hotspots and provide a range of ecosystem services to humanity (Bruschetti, 2019; Connell, 1978; Dubois et al., 2002; Woodhead et al., 2019). Reef systems experience continuous disturbance and variation in environmental conditions across spatial and temporal scales, maintaining variation in their physical, chemical and biological structure (Connell, 1978; Gruet, 1986; Pickett et al., 1989). Spatially and temporally dynamic three-dimensional (3D) structure is critical to the biodiversity, ecological functioning and conservation value of biogenic reefs (Graham and Nash, 2013; Holt et al., 1998). Metrics of reef structure can also be an indicator of the health of the engineering species (Curd et al., 2019) and reef recovery potential following acute disturbance (Graham et al., 2015). To understand organism-habitat interactions within biogenic reef systems, we must first identify the patterns and scales of variation inherent within their structures (Holt et al., 1998; Jenkins et al., 2018).

The study of spatial patterns in ecosystems has greatly benefitted from remote sensing, providing high-resolution, spatially continuous data for a variety of properties including 3D habitat structure (Chambers et al., 2007; Vierling et al., 2008). Remote sensing of 3D structure in the marine environment from satellite or crewed aircraft improves ecological insight in clear, shallow waters (Wedding et al., 2019), but similar information is challenging and expensive to capture in deep or turbid waters (Lecours et al., 2015). Recent developments in high-resolution 3D mapping technologies including structure-from-motion photogrammetry and laser scanning offer the potential to study patterns in 3D structure from organism to habitat scales, and are practical for investigation of scale-dependent properties in marine and coastal habitats (Calders et al., 2020; Urbina-Barreto et al., 2021). This creates opportunities to apply conceptual and analytical frameworks from landscape ecology, such as identification of dominant spatial scales of variation (Legendre and Fortin, 1989), at new scales and in new systems. The ability to record spatially continuous 3D habitat structure across km-extents at mm resolution, with rapid repeats and low operating costs is sparking a revolution in the scope and scale of ecological investigations (D'Urban Jackson et al., 2020).

Here we use intertidal habitat structure built by *Sabellaria alveolata*, a reef-building annelid, as a model system to characterise scale-dependent structural dynamics in complex biogenic reef habitats using high-resolution 3D mapping. *S. alveolata* reef comprises colonies of sediment tubes biocemented together, creating extensive reefs on northeast Atlantic and Mediterranean coasts (Bruschetti, 2019; Godet et al., 2011; La Porta and Nicoletti, 2009). The reef habitat is protected under national and international conservation legislation including the Environment (Wales) Act 2016 and the European Commission Habitats Directive. Similar reefs built by other species in the Sabellariidae family are found globally (Capa et al., 2012). Our current understanding of the scale-dependent structural dynamics in biogenic reefs is hampered by a lack of spatio-temporal information about habitat structure across scales. To explore this, we quantify spatial and temporal patterns in reef structure at mm to cm resolution, at plot- (2,500 m²) to habitat-scale (~35,000 m²) extents and over temporal scales of 1-5 years. Our findings reveal previously undescribed patterns of structural variation in intertidal biogenic reefs and demonstrate the enhanced ecological insight gained from the application of modern remote sensing technologies for 3D ecosystem mapping in structurally complex habitats.

3.3 Methods

3.3.1 Data collection

3.3.1.1 Study site

To characterise variation in biogenic reef habitat structure across scales we conducted high-resolution 3D mapping at a *Sabellaria alveolata* reef habitat at Llanddulas, Wales, UK (53.294 N, 3.632 W) using two techniques between 2014 and 2019 (Figure 3.1). The reef at Llanddulas occupies the low shore for at least one kilometre along a moderately exposed, unconsolidated cobble beach with a gentle slope gradient of 3%.

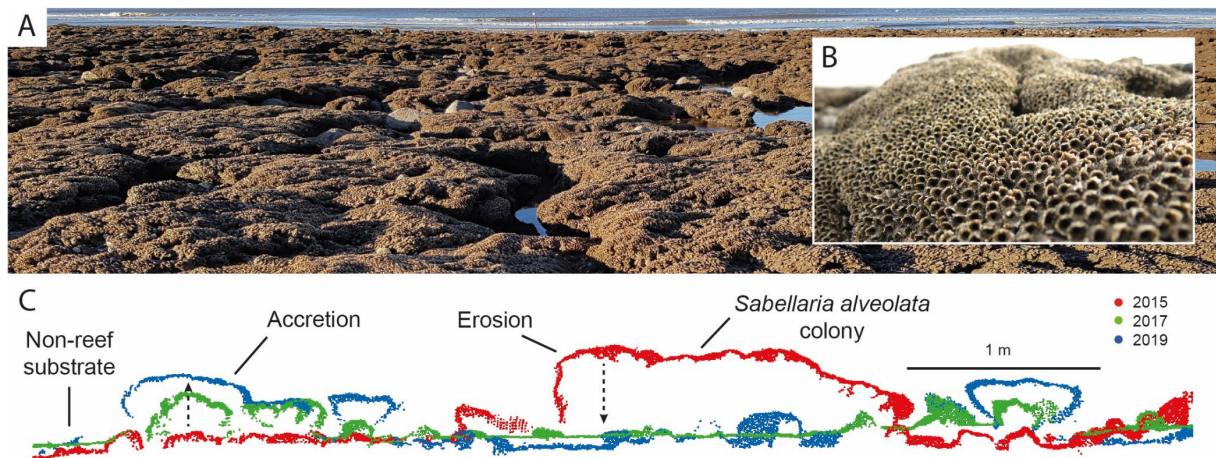


Figure 3.1 A) *Sabellaria alveolata* biogenic reef habitat comprises aggregations of sediment tubes in colonies that emerge above a hard, non-reef substrate. B) Close-up image of a prograding colony surface showing dense tube openings of ~5 mm diameter. C) Cross section of 3D terrestrial laser scan point cloud data from 3 years, demonstrating the detailed information about spatial and temporal dynamics in habitat structure that can be captured using modern 3D mapping technology. Reef colonies accrete upwards and outwards from the non-reef substrate in characteristic mushroom-like hummocks that coalesce into platforms. Erosion of reef colonies is often rapid and catastrophic.

3.3.1.2 Plot-scale (2,500 m²) 3D mapping

We collected data to investigate multi-annual temporal patterns in *S. alveolata* reef structure using terrestrial laser scanning (HDS ScanStation C10, Leica Geosystems, Switzerland) of a permanent 2,500 m² reef plot at approximately 6-month intervals (autumn and spring) over 5 years from September 2014 to October 2019. Terrestrial laser scanning generates high-resolution (thousands of points per m²) data with mm precision and was the most advanced 3D mapping technology available for field sampling at the start of the study in 2014. We conducted medium resolution (0.1 m point spacing at 100

m range) scans of the plot from several stationary positions per time point, ensuring similar data coverage among time points. We used retroreflective sphere reference targets to align scan datasets within a time point. Aligning datasets from different time points typically uses global navigation satellite system (GNSS) georeferencing or permanent reference targets. Our plot was intertidal with an unconsolidated substrate, so permanent targets could not be left and expected not to move, and alignment by GNSS georeferencing would have introduced error on the same scale (cm) as the changes we expected to detect, limiting their reliable detection and interpretation. Therefore, to enable accurate alignment of repeat surveys we increased the laser scanning data coverage to include permanent nearby features (rock groynes, cycle path and buildings), enabling us to align the datasets using the geometry of these stable features, without constraining the data across the dynamic foreshore.

We quality checked, aligned, georeferenced and manually cleaned the laser scanning point cloud data in Cyclone v9 software (Leica Geosystems, Switzerland). Within a time point, we aligned datasets from different scanner positions to 6 mm accuracy using target positions. We then aligned complete datasets from different time points to 6 mm accuracy using the geometry of permanent features. We made a final adjustment to the vertical alignment within the plot based on stable regions of non-reef substrate. We standardised datasets from different time points by cropping to the plot extent, subsampling point clouds to a minimum point spacing of 5 mm, and removing isolated points using the *statistical outlier removal* tool in the open source software CloudCompare v2.11 (CloudCompare, 2019).

3.3.1.3 Habitat-scale (~35,000 m²) 3D mapping

Terrestrial laser scanning was impractical for the larger extent of habitat-scale sampling within short low-tide windows. Therefore, to investigate spatial and temporal patterns in *S. alveolata* reef structure at a habitat scale (~35,000 m²) we used structure-from-motion photogrammetry derived from drone aerial imagery, in April 2018 and April 2019. Drone-derived structure-from-motion photogrammetry generates continuous 3D information across large extents, with comparable accuracy to terrestrial laser scanning in complex habitats like *S. alveolata* reef (D'Urban Jackson et al., 2020). We commissioned the drone surveys from a commercial survey company (OcuAir Ltd) which we specified and supervised to ensure data were collected to a high standard. Drone surveys used a

Phantom 4 Pro (DJI) with a 20 MP camera flying at 46 m altitude to capture images with 14 mm XY ground resolution (exceeding the target of 2 cm), covering approximately 150,000 m² of the coastline. The flight pattern was pre-determined and flying was automated using software (Maps Made Easy) to ensure the same survey pattern was flown in both years. To optimise the 3D modelling process, we used a high image overlap, so that every XY position in the area of interest was captured in at least 5 images. 3D models for each survey were generated by the survey company using the industry standard software Pix4Dmapper Pro v4. Unlike terrestrial laser scanning, for structure-from-motion photogrammetry we required georeferenced ground control points to scale, constrain and align the 3D models. We used 11 (2018) and 19 (2019) control points surveyed with commercial GNSS equipment (system 1200, Leica Geosystems, Switzerland). We designed the number and distribution of control points to be sufficient to adequately constrain the modelling process (James et al., 2017a), while being achievable to survey within the low tide window, incorporating redundancy as some targets were compromised by the incoming tide. Estimation of ground control point accuracy gave root mean square errors of 9 mm and 32 mm for 2018 and 2019 respectively. Because there were no permanent features within the study area, we verified vertical alignment accuracy by calculating elevation difference at 100 random points along a cycle path adjacent to the study area, giving a median difference of 23 mm and root mean square error of 26 mm. This represents a worst-case estimate because the cycle path was outside the area constrained by control points. From the 3D models and aerial images, we generated digital surface models (DSMs, 0.1 m XY resolution) and orthomosaics (0.02 m XY resolution) for 2018 and 2019.

3.3.2 Data analysis

3.3.2.1 Analysis of spatial patterns and scales of variation using variography

To identify spatial patterns and scales of spatial autocorrelation in reef emergence, accretion rate and erosion rate, we examined horizontal trends and used variography (Gringarten and Deutsch, 2001; Perry et al., 2002; Rossi et al., 1992). Variography quantifies spatial autocorrelation in a variable by fitting parametric *variogram models* to an *experimental variogram*. An experimental variogram is a plot of the variance between point samples of a spatial variable separated by a given distance (*lag*), against that lag

(Figure 3.2). In a typical simple scenario, samples that are close together are more similar than samples spaced further apart. Therefore, at small lags variance is low and positive spatial autocorrelation is high. As lag increases, variance increases until it plateaus at a lag known as the *range*, beyond which increasing lag has no effect on variance and data are no longer spatially autocorrelated. The variance value of the plateau is known as the *sill*, and in a simple scenario it is equal to the total variance in the spatial variable. To quantify the shape of the distribution of plotted points in an experimental variogram, a variogram model can be fitted. A variogram model describes the relationship between the lag and variance, with parameters including range and sill. The range of a variogram model is informative for characterising dominant scales of variation in spatial variables and interpreting their structuring processes. A short-range variogram model provides a good fit to an experimental variogram generated from a spatial variable with small-scale autocorrelation, where most of the variation is captured within short separation distances. A long-range variogram provides a good fit to an experimental variogram generated from a spatial variable with large-scale autocorrelation, where variation is spread over larger separation distances (Figure 3.2).

In natural systems a spatial variable is often structured by multiple processes at once, generating nested patterns of autocorrelation and systematic trends, collectively termed *spatial structures*, that can be identified using variogram analysis (Figure 3.2). First, trends in the spatial data are modelled using regression methods, and an experimental variogram is plotted from the residuals. Then, to identify spatial autocorrelation patterns, multiple variogram models can be fitted additively to the experimental variogram of residuals. Commonly, not all the variation in data from natural systems can be described with parametric variogram models. Interpretation of the data distribution at large lags relative to the study spatial extent should therefore be treated with caution and more emphasis is placed on modelling the dominant patterns at smaller lags. Another typical feature of natural spatial variables is anisotropy. An anisotropic variable exhibits different patterns and scales of variation depending on the orientation in which it is sampled. For example, sampling the abundance of barnacles using a transect oriented along a shore might be expected to generate a larger scale of variation compared to a transect oriented down the shore. To characterise variation in anisotropic variables, directional variogram analysis is conducted by sampling along specific axes, typically the axis with largest range (major axis) and its perpendicular axis (minor axis).

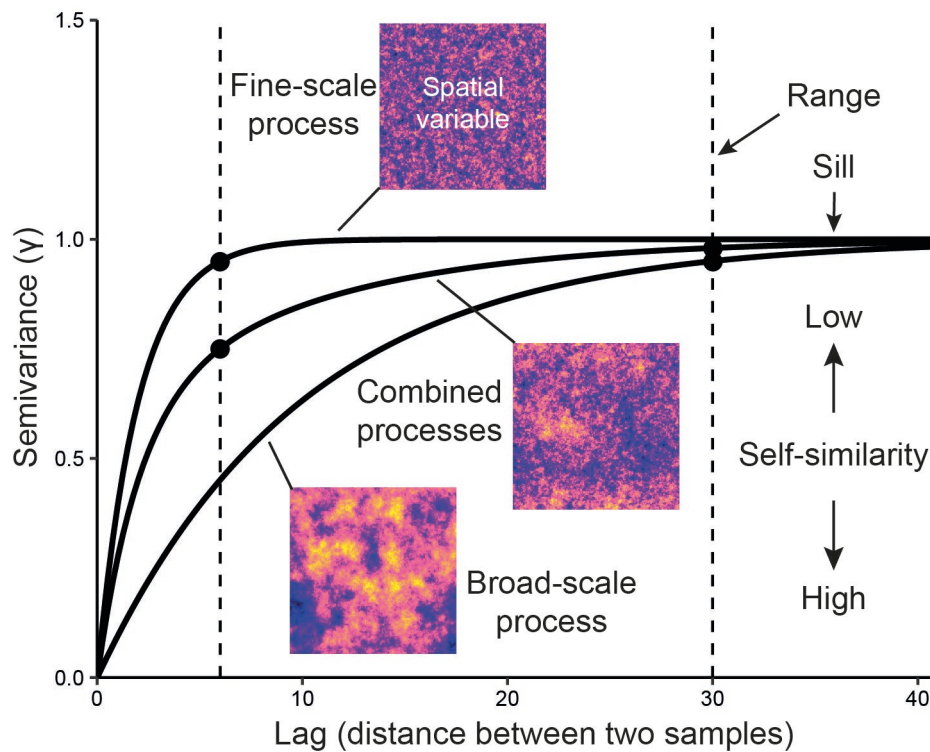


Figure 3.2 Interpreting spatial patterns in processes that generate spatial variables using variography. Variograms visualise spatial self-similarity, or autocorrelation, in a variable by plotting semivariance (γ) against lag, the distance between two samples. As lag increases samples become less similar (higher γ) until a plateau (sill) is reached at a distance (range), beyond which sample values are not autocorrelated. Here we show three simulated examples of a variable generated with different processes, and their respective variograms. Top: a fine-scale process generates a variable that is autocorrelated only over short distances, so the range (point and dashed line) is small. Bottom: a broad-scale process generates a variable that is autocorrelated over longer distances, producing a variogram with a larger range. Middle: the fine- and broad- scale processes have been added together, producing a variable with both short- and long-distance autocorrelation, generating a nested variogram with two ranges.

3.3.2.2 Habitat-scale ($\sim 35,000 \text{ m}^2$) spatial patterns in *S. alveolata* reef emergence, accretion rate and erosion rate

To study habitat-scale spatial patterns of variation in *S. alveolata* reef structure we conducted variography using the drone-derived digital surface models (DSMs) from 2018 and 2019. To investigate reef structure independently from trends in the underlying non-reef substrate, we calculated reef *emergence*, defined as the height of the DSM surfaces above a standardised digital elevation model (DEM) representing the lowest levels in the non-reef substrate (Figure 3.3). We used a threshold of emergence to classify DSM pixels as reef ($\geq 0.15 \text{ m}$) or non-reef substrate ($< 0.15 \text{ m}$) within a *reef area* polygon ($36,363 \text{ m}^2$) digitised from the 2018 orthomosaic. We validated the classification by manually

classifying 500 random points on the orthomosaic and interpreting a confusion matrix of predicted against observed classes. To study spatial patterns in accretion (positive change) and erosion (negative change) of *S. alveolata* reef we calculated the vertical difference between the DSMs from April 2018 and April 2019, to provide accretion and erosion rates as positive and negative vertical change per year.

To characterise spatial variation in habitat-scale *S. alveolata* reef structure, we modelled trends and conducted variography using emergence, accretion rate and erosion rate values of the 9140 reef pixels in a random sample of 100,000 pixels in the reef area. Our data exploration indicated that emergence, accretion rate and erosion rate had trends with shore height and along-shore distance, and were anisotropic with a major axis along the shore and minor axis down the shore. To meet the gaussian distribution requirements of linear modelling and variography, we transformed the data using ordered quantile transformation (Peterson and Cavanaugh, 2020), then modelled trends using ordinary least squares linear regression. We conducted variography on the linear model residuals along two axes: along the shore (120° from north) and down the shore (30° from north), with maximum lags of 250 m and 50 m respectively, approximately two thirds of the maximum reef area dimensions, using the *gstat* package in R (Graler et al., 2016; Pebesma, 2004; R Core Team, 2020). We fitted an initial variogram model to each experimental variogram automatically, then improved the fit by adjusting the model parameters and adding a secondary variogram model where appropriate, until a visual good fit was found to the experimental variogram (Gringarten and Deutsch, 2001). To investigate whether patterns in reef structure were related directly to patterns in the underlying non-reef substrate topography we conducted variography using emergence data from 10,000 random non-reef substrate DSM pixels.

The trend in mean emergence with shore height explained only a small amount of the variation ($R^2 = 0.043$, Table 3.1). Our data exploration showed that the reef comprised colonies at all stages of emergence, from the classification threshold of 0.15 m up to an emergence limit that was related to shore height. Therefore, shore height appeared to represent a limiting factor and so maximum emergence was a better metric for characterising habitat structure than a measure of central tendency (Kaiser et al., 1994). To examine the relationship between maximum reef emergence and shore height we used a sample of 2,000 reef pixels with a minimum point spacing of 1.5 m derived from the

variography results, 1.5 m being the dominant range of spatial autocorrelation. We modelled the relationship between maximum (99th percentile) reef emergence and DEM elevation with linear quantile regression, using the *quantreg* package in R (Koenker, 2020).

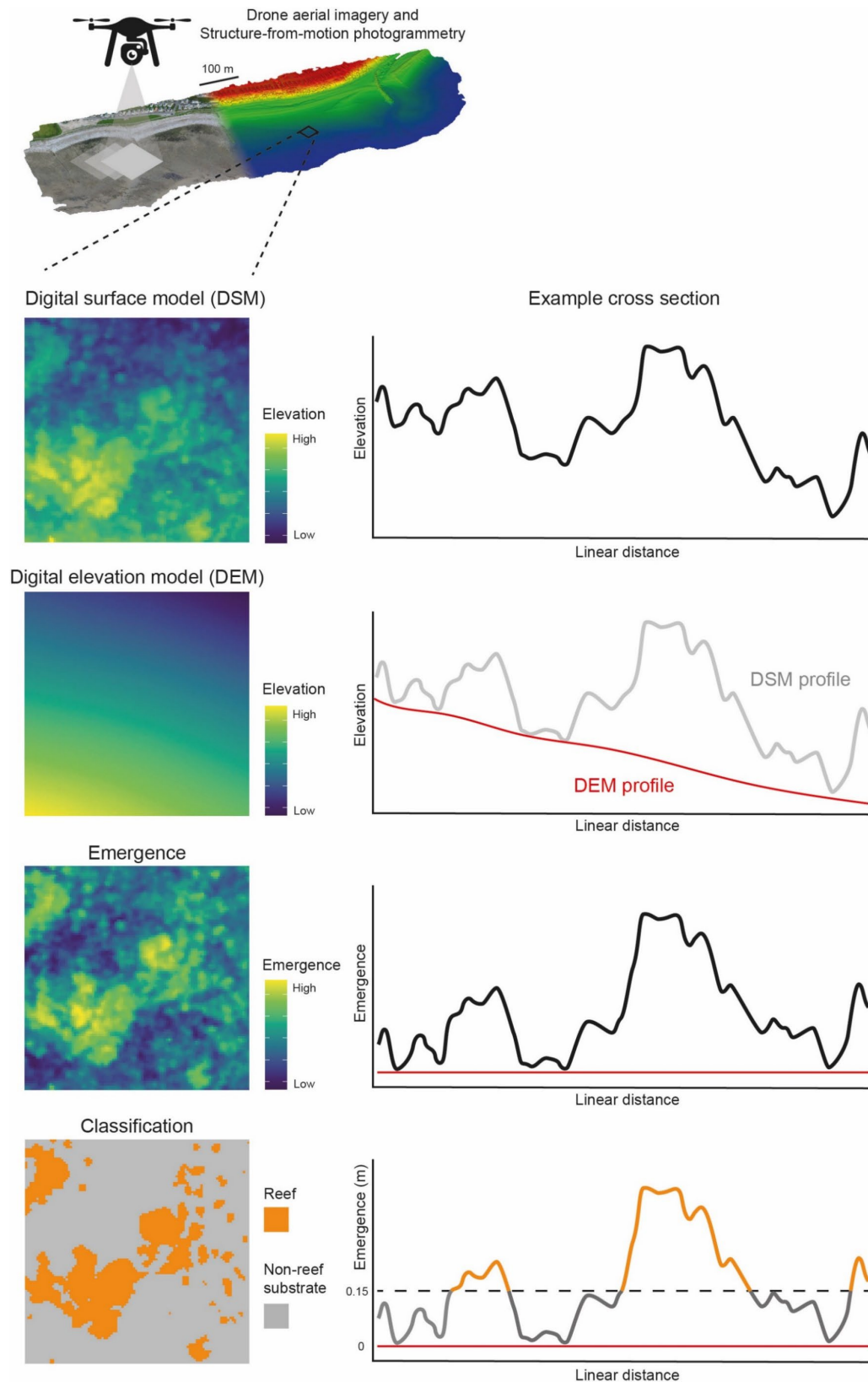


Figure 3.3 Data processing method used to classify habitat-scale digital surface models (DSMs) as reef or non-reef substrate. We generated 0.1 m XY resolution DSMs using drone aerial imagery and structure-from-motion photogrammetry. From the DSM we generated a digital elevation model (DEM) representing the ground level at the same resolution by interpolating between the lowest point in each square of a 2 m grid. We calculated emergence by subtracting the DEM from the DSM elevation. Finally, within the known reef area (Figure 3.5A) we used a binary classification of reef (≥ 0.15 m emergence) and non-reef substrate (< 0.15 m emergence).

3.3.2.3 Plot-scale (2,500 m²) temporal patterns in reef structure

To characterise multi-annual structural changes in *S. alveolata* reef structure, we used terrestrial laser scanning to survey a 2,500 m² plot each autumn and spring from September 2014 to October 2019. To track vertical changes in reef emergence through time we digitally sampled locations within the plot ($n = 454$) that had reef presence in at least one time point, avoided reef colony edges where lateral accretion and erosion would confuse interpretation, and were spatially independent (Figure 3.4). For each time point, we first generated a digital elevation model (DEM) representing the lowest levels of the non-reef substrate from the 3D point cloud data using a cloth simulation filter implemented in CloudCompare (Zhang et al., 2016). The cloth simulation filter is a tool developed to distinguish a ground surface from vertical features like trees and buildings in airborne laser scanning data (Zhang et al., 2016). To ensure we sampled upper reef surfaces and not sides or overhangs, we extracted all points more than 0.2 m above the DEM. To improve confidence in elevation measurements we gridded the density of those points at 0.1 m XY resolution, retained only the pixels containing at least 3 points, and from these points we calculated mean elevation to produce a reef digital surface model (DSM). To limit our sampling to central regions of reef colonies and avoid their edges, the reef pixels were clustered into contiguous patches with a minimum of 5 pixels and buffered inwards by 0.1 m. This gave a final reef mask raster of 0.1 m XY resolution for each time point, representing pixels suitable for sampling reef elevation.

To analyse emergence timeseries' for individual, independent reef locations, we took a stratified random sample of classified reef pixels within the plot with a minimum spacing of 1.5 m, based on the results of the habitat-scale spatial analysis. First, we combined the reef masks from all time points, giving a single raster of locations with reef presence in at least one time point. Next, to ensure spatially stratified sampling, we divided the plot with a 2 m XY grid and sampled 5 random reef pixels within each grid cell. We then subsampled the reef pixels randomly to one pixel per 2 m grid cell, specifying a minimum spacing of 1.5 m, producing a sample of 454 independent, spatially stratified pixels that contained reef in at least one of the 11 time points over 5 years (Figure 3.4). We generated a common DEM interpolated from a 2 m XY resolution minimum elevation grid of the combined ground surfaces, and at each sample location and for each time point we calculated

emergence as DSM elevation above the common DEM. These emergence values were used to plot timeseries' for each sample location (Figure 3.7).

To examine common characteristics in temporal changes in reef emergence, we derived accretion and emergence metrics from each sample timeseries. We calculated mean and maximum annual accretion rate, maximum emergence, and time spent within 80% of maximum emergence, which we termed *persistence*. We then used partitioning around medoids (PAM) clustering, a common data clustering method that is robust to outliers (Kaufman and Rousseeuw, 1990), to classify sample timeseries' into two groups with similar within-group accretion and emergence metrics using the *cluster* package in R (Maechler et al., 2019).

Following evidence of multiannual cycles of habitat-scale accretion and erosion (Gruet, 1986), we expected to observe plot-scale variation in reef emergence over the 5 year study period. We hypothesised that due to higher productivity in summer and lower growth rates coupled with more destructive wave action in winter, plot-scale emergence would be higher in autumn than in spring. We tested this hypothesis using a two fixed-factor (year and season) permutational analysis of variance (Anderson, 2001) with reef emergence as a univariate response. The permutational nature of the test removes the need to satisfy normality in the response variable as the routine permutes the raw data to generate the null distribution (Anderson, 2001). To ensure a balanced design with no missing data and no repeat sampling, we first divided reef sample locations ($n = 454$) randomly and equally among season (2 levels: autumn and spring) and year (5 levels: 2015-2019) combinations (10 combinations, $n = 45$). Some reef sample locations contained missing data for certain season and year combinations, so we iteratively exchanged these reef sample locations among groups until no missing data remained. Homogeneity of variance between factor levels was confirmed with Levene's test ($P > 0.05$). Our permutational analysis of variance was based on a Euclidean distance similarity matrix of the raw reef emergence data, with 9999 random permutations under a reduced model and Type III (partial) sums of squares. Where there was global model significance, permutational pairwise tests were used to determine where the differences occurred between factor levels.

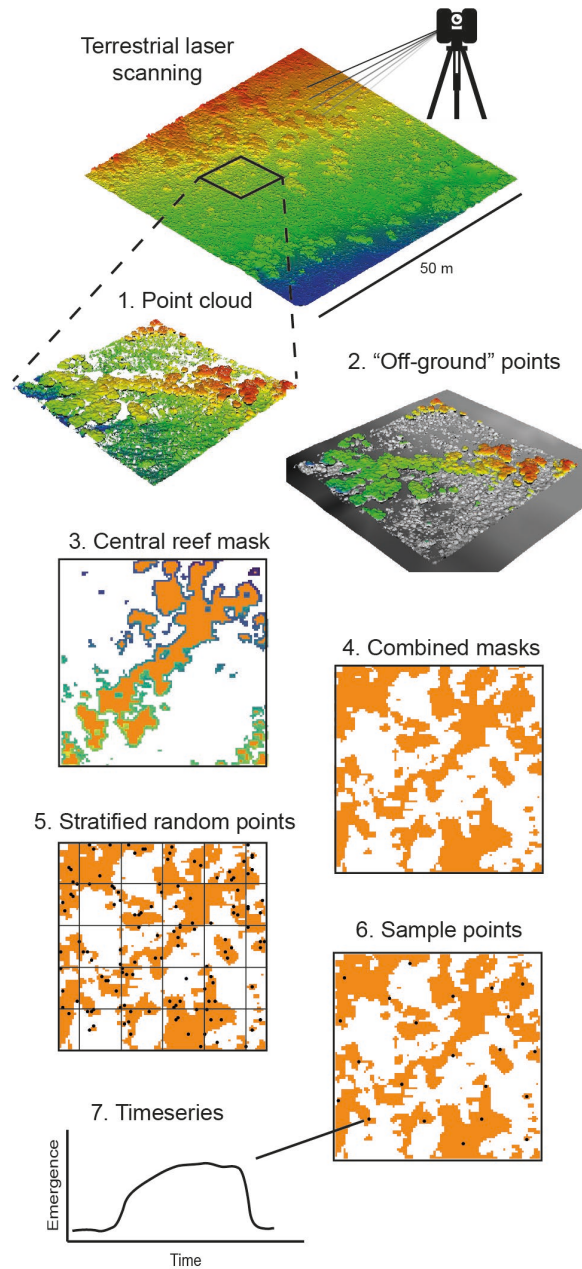


Figure 3.4 Data processing method used to sample reef emergence through time at independent reef locations within a 50 x 50 m plot mapped using terrestrial laser scanning at 6-month intervals over 5 years (Appendix B2). 1) Example section of 3D point cloud data. 2) We used a cloth simulation filter to generate a digital elevation model (DEM) for each time point and retained only points ≥ 0.2 m above the DEM. 3) We generated a digital surface model (DSM, 0.1 m XY resolution) of mean point elevation, then used the DSM to generate a mask that removed low point density pixels, isolated pixels, and colony edges. 4) We combined the masks from all time points. 5) We used a 2 m grid to generate spatially stratified random points (5 points per strata). 6) We randomly selected one point per strata with a minimum spacing of 1.5 m to generate our sample point locations. 7) At each sample location we calculated a timeseries of emergence by subtracting the elevation of a common digital elevation model representing the ground level from the DSM for each time point (Figure 3.7).

3.4 Results

3.4.1 Habitat-scale (~35,000 m²) spatial patterns in *S. alveolata* reef emergence, accretion rate and erosion rate

We estimated the percentage cover of *S. alveolata* reef within the 36,363 m² reef area as 26.8% or a total coverage of 9,745 m² based on our binary classification of the 0.1 m XY resolution emergence raster into reef or non-reef substrate (Figure 3.5A). We validated our classification method at 500 locations and found overall accuracy (correct predictions out of total predictions) was 81.2%, and precision (true positives out of total positive predictions) was 91.7% and 80.1% for reef and non-reef substrate, respectively. Maximum reef emergence (99th percentile) increased down the shore from approximately 0.2 m at 0 m ordnance datum Newlyn (ODN) to a maximum of 0.5 m above the substrate at 2.8 m below ODN (Figure 3.5B). The relationship was described by:

$$\log(emergence_{max}) = -0.308(shore\ height) - 1.551 \quad (1)$$

Reef emergence was positively spatially autocorrelated up to 1.5 m in both along shore and down shore directions, represented by a spatial structure that described 65-70% of the variance (Figure 3.5C, Table 3.1). There was a smaller amount of residual positive autocorrelation in reef emergence over larger distances along the shore (up to 110 m) and down the shore (up to 20 m) (Figure 3.5C, Table 3.1). At larger distances still, the variogram indicated additional patterns in spatial dependence of reef emergence including cyclicity, but these were not quantified because variogram model fitting becomes less reliable at larger distances relative to the study extent. The variogram of non-reef substrate emergence showed that the dominant autocorrelation pattern mostly occurred over a larger distance of 4.5 m and explained a higher proportion (90%) of the variation compared to reef emergence (Table 3.1). A small amount of spatial autocorrelation in non-reef substrate emergence was also evident over larger distances (up to 50 – 90 m).

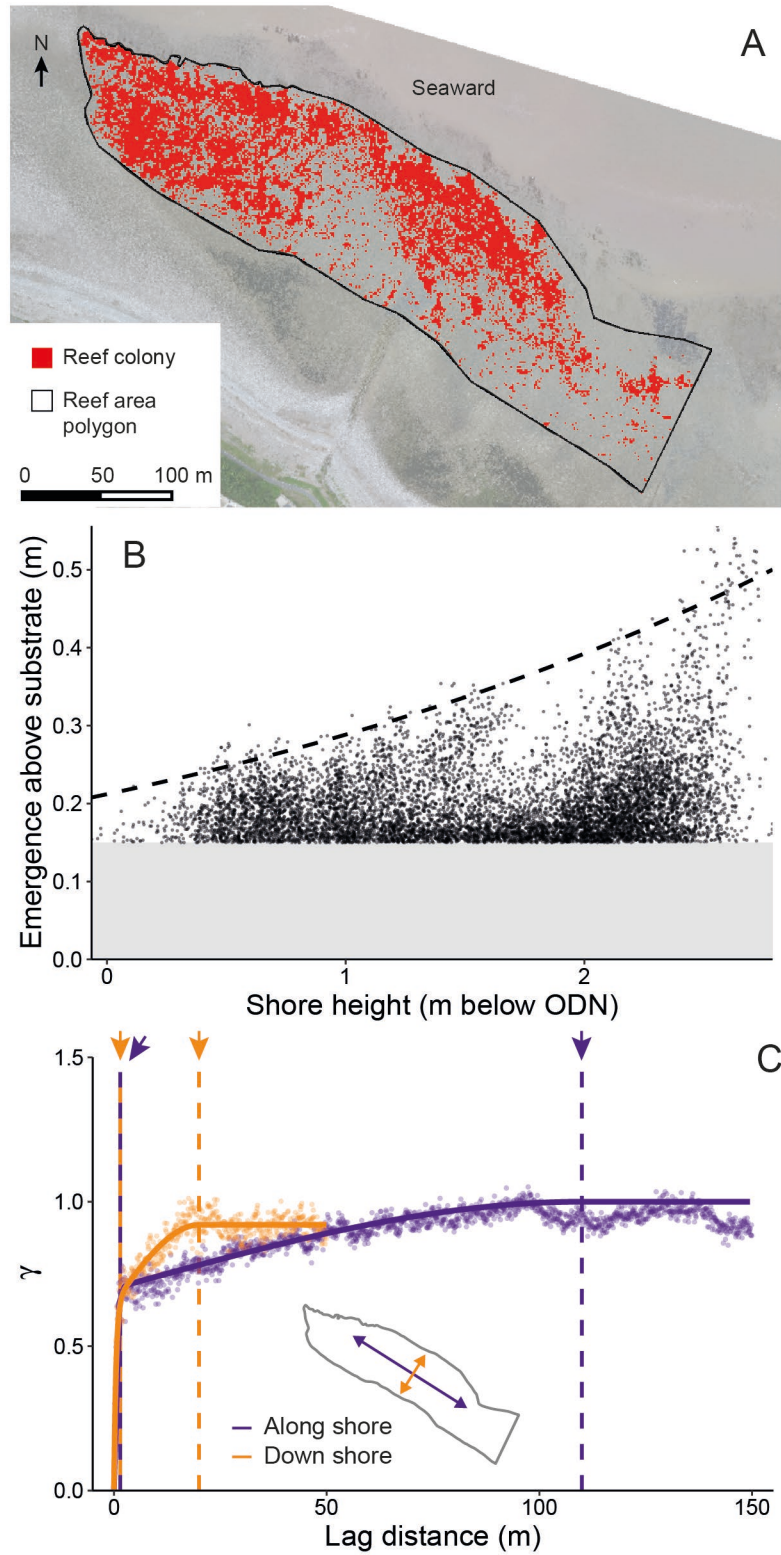


Figure 3.5 A) The foreshore at Llanddulas, Wales, UK. Habitat-scale 3D structure data were analysed within a $\sim 35,000 \text{ m}^2$ reef area polygon digitised from an aerial imagery orthomosaic. Presence of emergent reef is shown at 1 m XY resolution. B) Maximum reef colony emergence increases lower down the shore. The reef colonies that we analysed had a minimum emergence of 0.15 m. C) Reef colony emergence was spatially autocorrelated over short distances (1.5 m) both along the shore (purple) and down the shore (orange), ranges indicated by left-most vertical lines and arrows. There was a secondary autocorrelation structure that had a longer range (110 m) in the along shore direction compared to down the shore (20 m), ranges shown by right-most vertical lines and arrows.

Table 3.1 Spatial structure parameters of reef and non-reef substrate emergence within the ~35,000 m² reef area, derived from variography.

Variable	Trend model*	R ²	Direction (°)	Nugget	Model 1			Model 2		
					Model **	Partial Sill	Practical Range (m)	Model **	Partial Sill	Practical Range (m)
Reef emergence	x ~ h	0.043	120	0	Exp	0.7	1.5	Sph	0.3	110
			30	0	Exp	0.65	1.5	Sph	0.27	20
Non-reef substrate emergence	NA		120	0	Exp	0.9	4.5	Sph	0.1	90
			30	0	Exp	0.9	4.5	Sph	0.1	50

* x = variable, h = shore height

** Exp: exponential model, Sph: spherical model

At the habitat scale ($\sim 35,000 \text{ m}^2$), the elevation of *S. alveolata* reef colonies changed by $19 \pm 82 \text{ mm}$ (mean $\pm 1 \text{ sd}$) between April 2018 and April 2019 (Figure 3.6A). The small magnitude of mean elevation change across the total reef area was the result of a balance between variable positive and negative changes of individual samples (0.1 m XY resolution pixels). A high proportion of reef samples (80%) showed a small positive elevation change (accretion, $49 \pm 30 \text{ mm}$), with the remaining samples (20%) showing larger and more variable negative changes (erosion, $-99 \pm 113 \text{ mm}$). Both accretion and erosion maxima increased towards the lower shore (Figure 3.6A) and showed different spatial autocorrelation patterns. Positive spatial autocorrelation in accretion mostly occurred within short distances (up to 0.75 – 1.05 m), with a small proportion of positive autocorrelation extending over larger distances up to 40-130 m (Figure 3.6B, Table 3.2). In contrast, erosion of reef material was only positively spatially autocorrelated up to distances of 2.9 – 3.8 m, beyond which the variogram indicated spatial randomness (Figure 3.6C, Table 3.2).

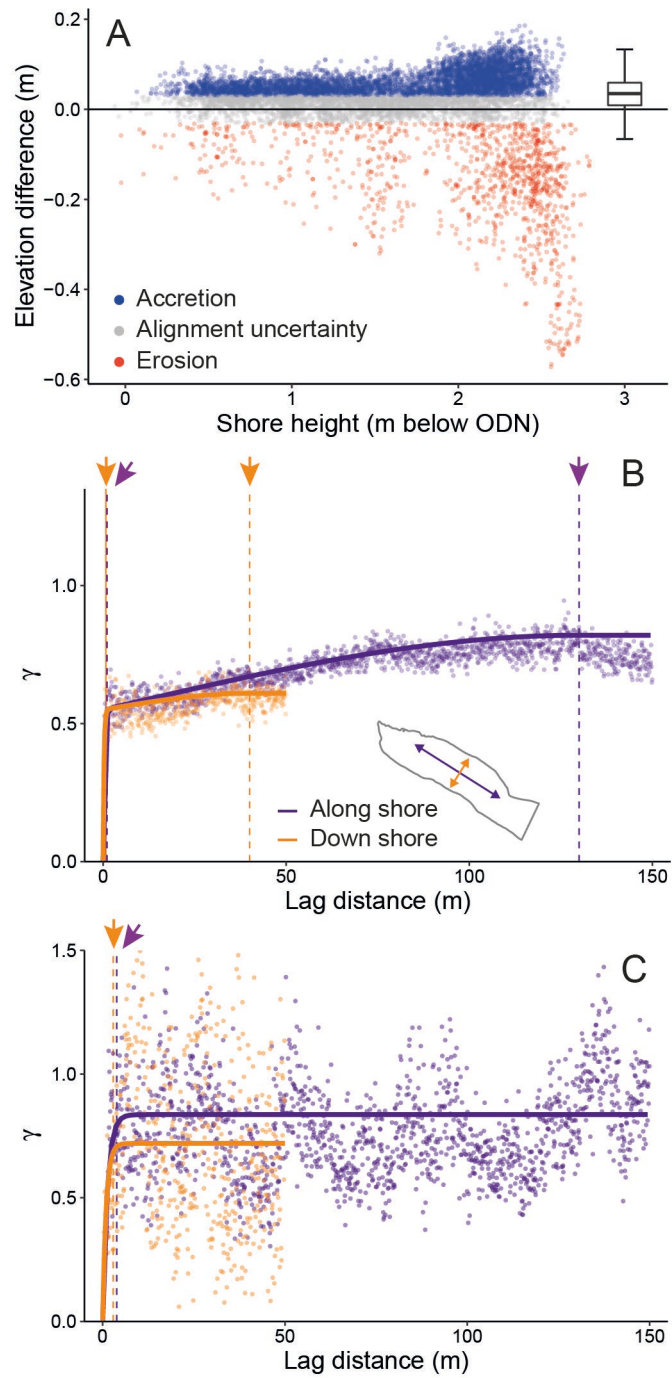


Figure 3.6 Spatial variation in *S. alveolata* reef elevation changes from April 2018 to April 2019 within the reef area (Figure 3.5A). A) Both positive and negative elevation changes increased towards the lower shore. Samples showing positive changes (blue) were greater in number than those with negative change (red), but the larger average magnitude of negative changes resulted in little change in overall elevation, shown by the boxplot of all samples crossing 0. Grey points represent samples within the alignment uncertainty estimate of ± 0.03 m. B) Variogram showing spatial autocorrelation scales of positive elevation changes (accretion) after accounting for trend (Table 3.2). The majority of spatial autocorrelation is explained by a short range (0.75 – 1.05 m) structure (left-most vertical lines and arrows), with a secondary structure showing a longer range (130 m) in the alongshore orientation compared to down the shore (30 m). C) Variogram showing spatial scales of negative elevation changes (erosion) after accounting for trend (Table 3.2). Spatial autocorrelation only occurs up to a short range (2.9 – 3.84 m, vertical lines and arrows).

Table 3.2 Spatial structure parameters of reef accretion (positive elevation change) and erosion (negative elevation change) within the ~35,000 m² reef area over one year, derived from variography

Variable	Trend model*	R ²	Dir	Nugget	Model 1			Model 2		
					Model **	PSill	Practical Range (m)	Model **	PSill	Practical Range (m)
Accretion	$x \sim h + h^2 + d$	0.328	120	0	Exp	0.55	1.05	Sph	0.27	130
			30	0	Exp	0.55	0.75	Sph	0.06	40
Erosion	$x \sim h + h^2 + h^3$	0.207	120	0	Exp	0.84	3.84	NA		
			30	0	Exp	0.72	2.9	NA		

* x: variable, h: shore height, d: distance along shore

** Exp: exponential model, Sph: spherical model

3.4.2 Plot-scale (2,500 m²) temporal patterns in reef structure

We validated our sampling strategy for selecting sampling locations for reef emergence by checking 100 random pixels classified as reef in each of 3 datasets (total $n = 300$) with corresponding drone aerial imagery (September 2017, April 2018 and April 2019), giving a precision for reef of 95%. Within the 2,500 m² plot, overall reef emergence across all 11 time points over 5 years was 0.22 ± 0.13 m (mean \pm 1 sd). We found scale dependent variation, with high variation in emergence at each sample location (colony-scale, $n = 454$) through time and high variation among samples at each time point, but low variation in plot-scale emergence through time. The coefficient of variation (mean \pm 1 sd) in sample location emergence through time was 52 ± 32.3 , and per time point was 56.5 ± 3.7 , whereas the coefficient of variation in plot-scale mean emergence through time was 8.8.

Timeseries' of emergence at reef sample locations revealed diverse temporal patterns in emergence, accretion, and erosion metrics of colonies, that we classified into two groups called *fast* and *slow* colonies (Figure 3.7). These two groups clustered moderately well, indicated by an average silhouette width of 0.35 on a scale from 0 (poorly clustered) to 1 (perfectly clustered) (Kaufman and Rousseeuw, 1990). Fast colonies were characterised by higher maximum and mean annual accretion, higher maximum emergence and shorter persistence (time spent within 80% of their maximum emergence) than slow colonies (Figure 3.7, Table 3.3). Visual assessment showed that slow colonies were evenly distributed throughout the plot, whereas fast colonies were concentrated in the northern, lower-shore half of the plot (Figure 3.8). We found that erosion of reef colonies often occurred rapidly in both groups; it was common for emergence to drop to the level of the non-reef substrate within 6 months to a year (Figure 3.7).

There was a significant interaction between 'year' and 'season' on plot-scale reef emergence ($F_{4,440} = 3.48$, $P = 0.009$, Table 3.4) driven entirely by emergence being higher in autumn than spring in 2015 ($P = 0.001$). Across season, there were no differences among years in spring emergence, but there were significant differences in autumn, with 2015, 2016 and 2019 having higher emergence than 2017 and 2018 ($P < 0.05$, Figure 3.9, Table 3.4).

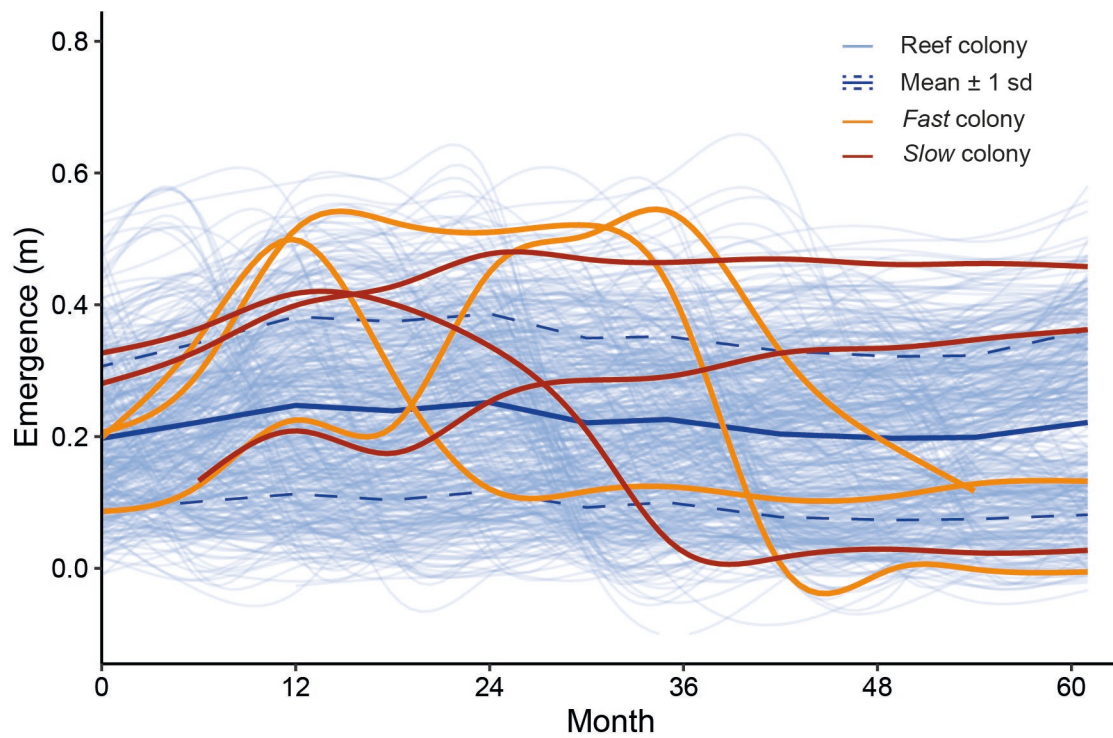


Figure 3.7 Colony-scale variation balances out to produce plot-scale stability in *S. alveolata* reef habitat structure over several years. Emergence was measured at 454 stratified random, spatially independent sample locations in a 2,500 m² plot in autumn and spring each year from September 2014 (month 0) to October 2019 (month 61). Thin blue lines show individual sample timeseries. Bold blue line and dashed lines show the mean \pm 1 sd emergence of all samples. Six example sample timeseries' are highlighted to show the diversity of fine-scale dynamics in reef accretion and loss over time, clustered into two groups: fast colonies with rapid accretion and short persistence (orange) and slow colonies with slower accretion and longer persistence (red).

Table 3.3 Average accretion and erosion metrics for two groups of reef colonies identified within the 2,500 m² plot

Colony group	N	Maximum accretion rate (m yr ⁻¹)	Mean accretion rate (m yr ⁻¹)	Maximum emergence (m)	Persistence at 80% of maximum (yr)
Fast	128	0.215	0.109	0.438	1.16
Slow	329	0.089	0.046	0.343	1.54

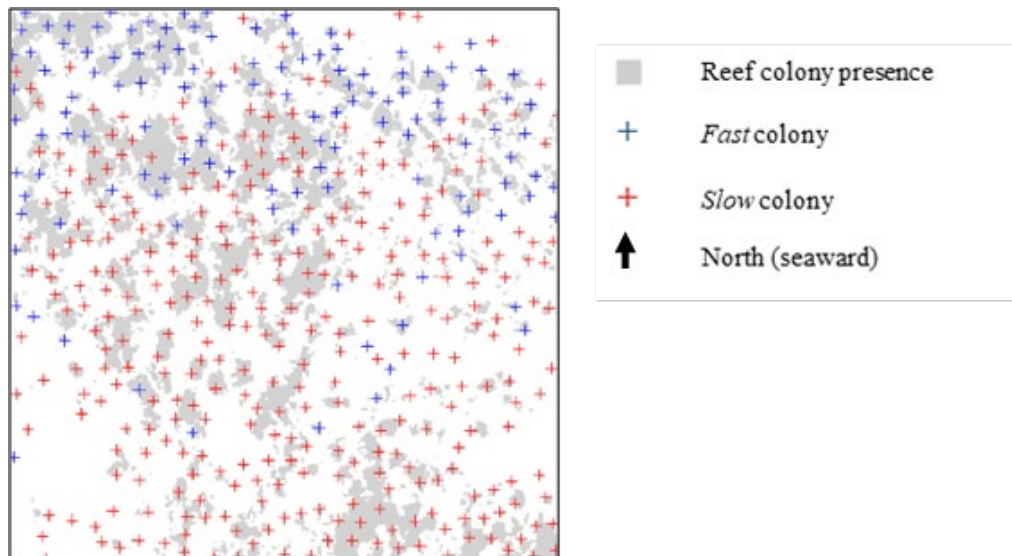


Figure 3.8 2,500 m² plot showing 0.01 m² pixels containing *S. alveolata* reef in at least one of 11 surveys over 5 years (grey) and stratified random, spatially independent samples (crosses). Cluster analysis identified two groups of colonies based on patterns of topographic change through time. *Fast* colonies (blue) have rapid accretion and short persistence at their maximum emergence above the non-reef substrate, and are more prevalent towards the lower shore. *Slow* colonies (red) have slower accretion and longer persistence at their maximum emergence, and are distributed evenly throughout the plot.

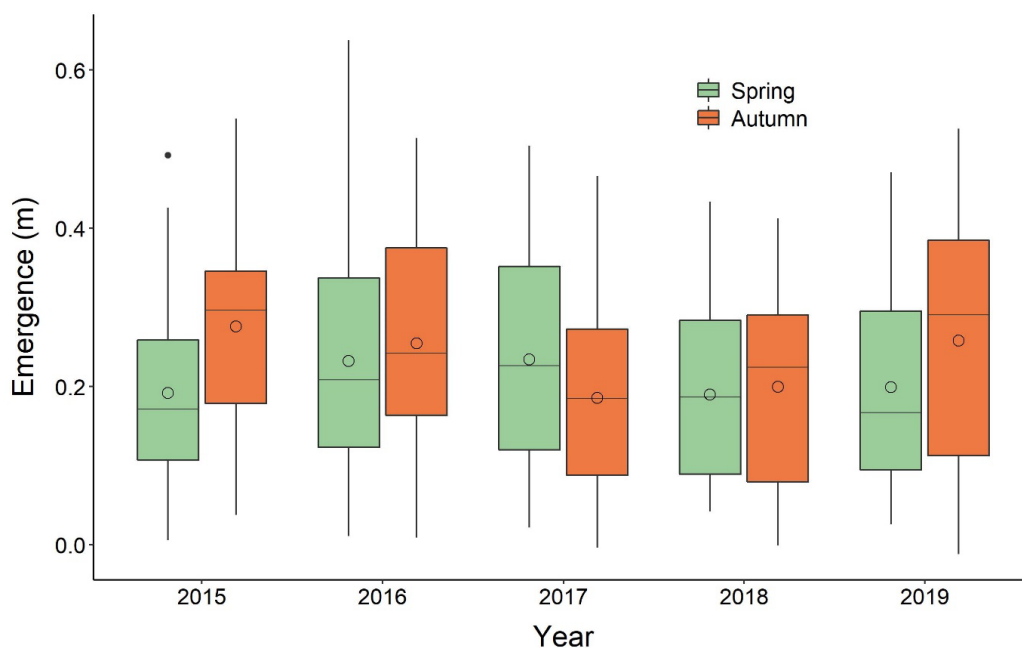


Figure 3.9 Boxplot of emergence within the 2,500 m² plot surveyed using terrestrial laser scanning at approximately 6 month intervals over 5 years, with median (bar) and mean (open circles) displayed. We used the data shown to test for effects of year, season and their interaction on emergence using permutational analysis of variance (Table 3.4). The data are balanced samples (n=45) of independent reef locations within the plot, with no missing data and no repeat sampling. To maintain a balanced design, we did not include data from autumn 2014 in this analysis.

Table 3.4 Results of permutational analysis of variance, testing for the effects of year, season and their interaction on emergence within the 2,500 m² plot. Number of permutations = 9999. Significant results ($P < 0.05$) are highlighted in **bold**.

Main test with year (5 levels: 2015-2019) and season (2 levels: spring, autumn) as fixed factors

Source	df	MS	<i>F</i>	<i>P</i>
Year	4	0.035	2.08	0.084
Season	1	0.071	4.30	0.040
Year x Season	4	0.058	3.48	0.009
Residual	440	0.017		
Total	449			

Pairwise tests of differences in season within year

Year	<i>P</i>
2015	0.001
2016	0.457
2017	0.072
2018	0.695
2019	0.051

Pairwise tests of differences in year within season

Year pair		Spring <i>P</i>	Autumn <i>P</i>
2015	2016	0.162	0.433
2015	2017	0.121	0.001
2015	2018	0.935	0.004
2015	2019	0.774	0.550
2016	2017	0.951	0.010
2016	2018	0.128	0.040
2016	2019	0.256	0.911
2017	2018	0.093	0.572
2017	2019	0.202	0.014
2018	2019	0.707	0.048

3.5 Discussion

Habitat structure strongly dictates ecological function in complex 3D ecosystems. Quantifying how 3D habitat structure varies across space and time is therefore a crucial step in understanding ecosystem dynamics and guiding their effective management. Here, for the first time, we quantified patterns of spatial and temporal variation in 3D habitat structure across scales in an ecologically important but understudied *Sabellaria alveolata* biogenic reef habitat. Our results reveal that patterns in reef emergence, accretion rate and erosion rate are spatially autocorrelated and highly scale-dependent. In this system, reef colonies formed groups of rapidly accreting short-lived colonies and slow accreting long-lived colonies, creating dynamic structure at fine spatial (m) and temporal (6 month) scales. However, these colony-scale dynamics cancel each other out at larger spatial (50m – 1 km) and temporal (5 year) scales, resulting in seemingly stable reef habitat (Figure 3.7). This habitat steady-state despite the mosaic of small-scale dynamics is akin to other biogenic systems where scale-dependent patterns in ecosystem properties have been better studied using remote sensing. In tropical forests, disturbance events with varying size distribution and return frequency generate a dynamic mosaic of patches at different successional stages that balance out to exhibit a stable system at broad spatial and temporal scales (Chambers et al., 2013). Using modern 3D mapping we have quantified spatially continuous, cross-scale habitat structure in a biogenic reef, revealing scale-dependent patterns that indicate parallels in structural dynamics between terrestrial and marine biogenic habitats.

3.5.1 Spatial patterns in biogenic reef structure

We identified predictable trends in maximum reef emergence, accretion rate and erosion rate, that all increased towards the lower shore. Shore height trends are ubiquitous in intertidal ecosystems like rocky shores and saltmarshes because numerous biological, chemical and physical structuring processes correlate with vertical position (Chappuis et al., 2014; Connell, 1972; Pennings and Callaway, 1992). The trends in our data can be explained by spatially varying hydrodynamic forces, proposed as the most important abiotic structuring factor of *S. alveolata* reef habitat (Collin et al., 2018; Gruet, 1986; Wilson, 1971). Wave forces are predicted to be greatest at the lower shore, with energy attenuated as waves travel across the rough reef surface (Bouma et al., 2014; Lowe et al.,

2005). We suggest that higher wave energy at the lower shore results in more coarse sediment being resuspended higher in the water column, enabling faster reef colony accretion and higher maximum emergence. Wave energy can also be destructive, increasing reef erosion rate towards the lower shore. In addition, longer periods of immersion experienced lower on the shore give more time for both reef accretion and erosion.

Interactions between individuals can produce spatially coherent self-organised patterns that influence ecosystem-scale processes in many natural systems, including mussel reefs (Van De Koppel et al., 2008) and arid vegetation (Klausmeier, 1999). We found evidence for self-organisation in *S. alveolata* reef emergence and accretion rate, that were spatially clustered (positively autocorrelated) up to colony scales (1.5 m). Prograding *S. alveolata* reef colonies have characteristic smooth surfaces comprising the openings of dense, parallel tubes (Figure 3.1) (Curd et al., 2019; Ventura et al., 2020). To maintain this morphology as the colony grows, within-colony accretion rate and emergence must be similar among worms. Self-organisation enhances habitat resilience (Guichard et al., 2003; Q.-X. Liu et al., 2014), and in this system the colony morphology may contribute to the remarkable wave-resistance in the friable intertidal structures (Le Cam et al., 2011), analogous to massive stony coral morphologies that can dominate wave-exposed subtidal tropical reefs (Chappell, 1980).

Spatial patterns in biogenic reef properties provide insight into the biotic and abiotic drivers of ecosystem structuring processes (Aston et al., 2019; Edwards et al., 2017; Ford et al., 2020). In our system, reef emergence and accretion rates showed secondary spatial clustering at habitat scales (20-40 m down the shore, 110-130 m along the shore), whereas erosion rates showed spatial randomness beyond 4 m. Habitat-scale spatial clustering in reef emergence and accretion rate may be due to spatial variation in resources (e.g., sediment or food quality), environmental conditions (e.g., salinity), biotic factors (e.g., recruitment density) or anthropogenic influence (e.g., trampling). Interactions between myriad drivers are likely to influence reef structure at various scales (Collin et al., 2018). Identification of the relative importance of these factors and how they vary in time and space warrants further investigation, and may help explain why *S. alveolata* reef structure is highly variable among sites (Stone et al., 2019). Spatial

clustering of erosion rates up to 4 m indicates that erosion mostly occurs as the catastrophic collapse of entire *S. alveolata* colonies and platform sections. The lack of larger scale spatial autocorrelation in erosion rates shows that colony collapse is random after accounting for shore height trends, suggesting that destructive processes are similar horizontally along the shore.

Modern remote sensing technologies are advancing our ability to describe and interrogate spatial patterns in marine reef systems. In intertidal habitats like *S. alveolata* reef, aerial methods can capture a range of ecologically relevant information at high resolution across large extents of several km² (Bajjouk et al., 2020; Collin et al., 2019, 2018). The importance of 3D ecosystem structure in ecological investigations is recognised, and tools to capture and analyse 3D structure in diverse systems including subtidal reefs are becoming increasingly powerful and accessible (D'Urban Jackson et al., 2020; Lepczyk et al., 2021).

3.5.2 Temporal patterns in biogenic reef structure

Identifying key scales of variation and their forcing processes has been a persistent challenge in ecology (Chave, 2013; Denny et al., 2004; Levin, 1992), especially in marine systems beyond the observation capabilities of traditional remote sensing (Lecours et al., 2015; Wedding et al., 2011). Our study reveals previously undescribed patterns of scale-dependent spatio-temporal variation in *S. alveolata* reef structure. We found that individual *S. alveolata* colonies on the scale of metres undergo independent and compensatory accretion and erosion cycles, resulting in stability at larger spatial (2,500 m²) and temporal (5 year) scales. Previous characterisation of *S. alveolata* reef structural dynamics have described multiannual accretion and erosion cycles operating over large areas of reef (10s – 100s m) at some sites, and multiannual stability at others (Gruet, 1986; Lecornu et al., 2016). While we recorded stability in reef structure over a period of 5 years, at decadal time scales the habitat can be transient (Firth et al., 2015). Scale-dependent structural dynamism is a feature of other systems like terrestrial forests (Chambers et al., 2013), and our results indicate that conceptual frameworks from terrestrial landscape ecology can be applied to biogenic reef systems. For instance, the stability of a forest ecosystem can be modelled as a product of the spatial and temporal scales of disturbance events that it experiences (Turner et al., 1993). Applying this concept to our study system,

disturbance events (colony collapse) were small in size (up to 4 m) relative to the habitat size ($\sim 35,000 \text{ m}^2$) and disturbance (collapse) intervals were generally longer than recovery (accretion to maximum emergence) intervals. As predicted by the conceptual model (Turner et al., 1993), we observed stability in the system at the habitat scale.

We identified two distinct types of reef colonies: “fast” colonies with rapid accretion, high maximum emergence, and short lifespan, and “slow” colonies with slower accretion, lower maximum emergence and longer lifespan. Accretion rates of “fast” *S. alveolata* colonies in our study (mean 0.109 m yr^{-1} , max 0.215 m yr^{-1}) were comparable to upper estimates of 0.105 m yr^{-1} in Cornwall, UK, and $>0.5 \text{ m yr}^{-1}$ in Normandy, France (Gruet, 1986; Wilson, 1971). These studies documented faster accretion rates in new, small colonies and a similar general pattern could be seen in our timeseries’, although variation was high and many colonies had incomplete structural cycles within our study period. We found new, low emergent colonies accreted rapidly and then accretion slowed as they approached a maximum emergence, followed by a period of persistence at the maximum emergence and eventual rapid collapse. A similar accretion pattern has been documented in oyster (*Crassostrea virginica*) reefs, with rapid accretion in deeper edges of a reef (8 m diameter) while no change was recorded in the shallowest central portions just 2 m away, indicating that reef accretion could outpace sea level rise (Rodriguez et al., 2014). This fine-scale spatial variation in structural characteristics would be lost at larger observational scales, highlighting the need for a multiscale approach when assessing the resilience of biogenic reefs to pressures like sea level rise.

Seasonal patterns of accretion and erosion in *S. alveolata* reef and their driving processes are not well understood. We did not find evidence for a consistent seasonal pattern in reef emergence, and while reef emergence measured in autumn showed some variation, spring observations were stable over 5 years (Figure 3.9, Table 3.4). However, we did find a seasonal difference in one survey year (2015). Temperature and wave energy are two dominant seasonally varying factors in intertidal habitats. The habitat is vulnerable to severe winter temperatures and damage from winter storms (Crisp, 1964; Firth et al., 2015). In summer, higher temperatures and increased food availability in summer may promote worm productivity that translates to increased accretion rate, but the availability of resuspended sediment with low summer wave action may limit accretion rate.

Hydrodynamic energy promotes both *S. alveolata* reef accretion and erosion, so the effects of seasonal variation in wave energy are difficult to predict. Higher emergence in the autumn of 2015 compared to the spring appeared to be a result of heavy recruitment during the summer of that year (TJ-B, *pers. obs.*), resulting in many new, rapidly accreting colonies. Recruitment of pelagic larvae to *S. alveolata* reefs is through a combination of continuous low-level settlement and stochastic heavy settlement events when hydrodynamic conditions are favourable (Ayata et al., 2009; Bush et al., 2015; Dubois et al., 2007). Sabellariid worms respond to storm damage with increased reproductive output in a similar way that some plants respond to fire (Barry, 1989) and *S. alveolata* larvae show high levels of retention within local geographic areas (Bush et al., 2015; Dubois et al., 2007). These factors likely result in compensatory self-recruitment to a damaged reef, contributing to long term reef persistence.

3.5.3 Conclusion

Our findings represent the most comprehensive characterisation of *S. alveolata* biogenic reef habitat structure across spatial and temporal scales to date, expanding our understanding of scale-dependent structural dynamics in this complex 3D habitat. We found that *S. alveolata* reef structure is characterised by a mosaic of different colony successional states leading to a dynamic landscape at smaller scales (m), while displaying relative stability (a steady state) at larger spatial and temporal scales. This phenomenon is characteristic of other structurally complex ecosystems like forests and we hypothesise could be true for other colonial reef systems, such as subtidal tropical coral reefs. We also identified previously undocumented temporal patterns in reef structure, specifically distinct groups of “fast and “slow” colonies. The patterns we documented could only be detected with high-resolution 3D mapping, demonstrating the enhanced ecological insight gained from the adoption of contemporary technologies in modern ecology. Scale-dependent ecosystem patterns have historically been challenging to study due to necessary trade-offs in observation scale, especially in marine systems. By embracing modern mapping technologies in ecology, these long-standing constraints can be overcome, leading to an improved understanding of ecosystem dynamics in complex 3D habitats.

4 Mapping temperate reef habitats in high energy waters

4.1 Abstract

High energy marine regions are understudied and less anthropogenically developed than lower energy waters, but host ecologically important habitats including temperate reefs. In the marine environment the spatial scale of direct habitat observation is limited, and high energy waters present additional logistical challenges and constraints. Semi-automated predictive habitat mapping is a cost-effective tool to map benthic habitats across large extents, but performance is context specific. High resolution environmental data used for predictive mapping are often limited to bathymetry, acoustic backscatter and their derivatives. However, hydrodynamic energy at the seabed is a critical structuring factor within high energy habitats and likely an important predictor of habitat composition and spatial patterning. Here, we used a machine learning classification approach to map reef substrate and biogenic reef habitat in a tidal energy development area, incorporating multiscale bathymetric derivatives and simulated tidally-induced seabed shear stress. We mapped reef substrate (four classes: sediment [not reef], stony reef [low resemblance], stony reef [medium – high resemblance] and bedrock reef) with an overall balanced accuracy (mean \pm 95% confidence interval) of $80.7\% \pm 0.8\%$ and potential biogenic *Sabellaria spinulosa* reef with a balanced accuracy of $77\% \pm 1\%$. We found that tidally induced mean bed shear stress was the most important predictor variable for both models, followed by multiscale ruggedness for the reef substrate model. We tested the influence of backscatter derivatives across a subsection of the study area, finding low influence for both models. We identify previously unresolved relationships between temperate reef spatial distribution, hydrodynamic energy and seabed three-dimensional structure in energetic waters. Our findings contribute to a better understanding of the spatial ecology of high energy marine ecosystems and will inform evidence-based decision making for sustainable development, particularly within the emerging tidal energy sector.

This chapter is in review as a peer-reviewed article:

Jackson-Bué, T., Williams, G. J., Whitton, T. W., Roberts, M. J., Goward Brown, A., Amir, H., King, J., Powell, B., Rowlands, S. J., Llewelyn Jones, G. and Davies, A. J., (in review). Seabed morphology and bed shear stress predict temperate reef habitats in a high energy marine region. *Estuarine, Coastal and Shelf Science*

This chapter was based on a collaborative research project between SEACAMS2, Bangor University and Menter Môn

Co-author contributions:

G.J. Williams and A.J. Davies assisted with conceptualisation, framing and commenting on drafts.

M.J. Roberts facilitated ship-based fieldwork, project initiation and collaboration with the industry partner.

A. Goward Brown produced the hydrodynamic model outputs.

H. Amir assisted with data collection and analysis for a preliminary study.

J. King facilitated access to resources and commented on drafts.

B. Powell assisted with ship-based data collection.

S. J. Rowlands assisted with multibeam echo sounder data processing.

G. Llewelyn Jones provided bathymetry and supplementary drop-down video data.

4.2 Introduction

To understand ecological pattern and process, reliable information about the spatial distribution of habitats is essential (Brown et al., 2011; Cogan et al., 2009; Turner, 1989). Aerial and satellite remote sensing has revolutionised spatial ecology, providing spatially continuous data on a variety of ecologically relevant variables at high resolution across broad extents (Kerr and Ostrovsky, 2003; McDermid et al., 2005). Similar information is more challenging to collect for the seabed beyond the shallow, clear waters that can be observed with optical remote sensing (Lecours et al., 2015). Advances in acoustic remote sensing now enable collection of high-resolution ($< 1\text{m}$), spatially continuous seabed bathymetry and acoustic reflectivity (commonly referred to as backscatter). However, detailed seabed mapping is still costly and inefficient compared to terrestrial remote sensing, such that less than 18% of the oceans has depth measurements at 1 km resolution or better (Mayer et al., 2018). Other seabed properties, including benthic habitat characteristics, are even more challenging to map. Methods for observing seafloor habitats and organismal communities are limited to fine to moderate spatial scales (0.01 m – 1 km) using diver, camera, crewed/uncrewed vehicle, acoustic or physical sampling (van Rein et al., 2009). To generate spatially continuous benthic habitat maps over large extents, practitioners use statistical approaches to identify relationships between discrete habitat observations and spatially continuous environmental data and extrapolate into unobserved locations (Brown et al., 2011; Pittman et al., 2009, 2007; Pittman and Brown, 2011; Wilson et al., 2007).

Temperate reefs are hard-bottom marine habitats between the tropics and the poles, and include biodiverse ecosystems that provide billions of dollars in ecosystem goods and services (Bennett et al., 2016; Taylor, 1998). Temperate reef substrate may be bedrock or stony (geogenic) or derived from organisms (biogenic), both hosting communities of sessile and mobile reef-associated species (Bué et al., 2020; Diesing et al., 2009; Holbrook et al., 1990). Due to their ecological importance reef habitats are listed in various national and international conservation legislation, including Annex 1 of the European Commission Habitats Directive (European Commission, 2013). However, a lack of information about the distribution and characteristics of reef habitats hampers effective ecosystem management (Diesing et al., 2009). Temperate reef habitats are often found in

high energy marine waters (Warwick and Uncles, 1980), areas that are challenging and costly to operate within compared to lower energy seas and as such they are less anthropogenically developed and less well studied (Shields et al., 2011). In response to the global demand for low carbon energy, these areas are now of commercial interest to the nascent marine renewable energy industry (Roche et al., 2016). To ensure sustainable development, there is a growing need for baseline ecosystem information about energetic waters. While previous attempts at mapping temperate reefs have shown some success, it has proved challenging to distinguish between specific reef types like bedrock and stony reef, and between reef and non-reef ground without considerable manual input (Dalkin, 2008; Eggleton and Meadows, 2013; Plets et al., 2012; Vanstaen and Eggleton, 2011). Biogenic temperate reefs are similarly challenging to map, typically requiring manual interpretation and digitisation of acoustic information (Jenkins et al., 2018; Lindenbaum et al., 2008; Pearce et al., 2014). There is a growing need for repeatable, cost-effective habitat mapping in high energy waters, to understand the spatial ecology of these understudied ecosystems and to support sustainable management in an evolving seascape of offshore activity (Dannheim et al., 2020; Jouffray et al., 2020; Wilding et al., 2017).

Bathymetry, backscatter intensity and their derivatives are typically the main, or only environmental predictor variables in benthic habitat models beyond shallow, clear waters, as few other variables can be recorded at similar level of detail. However, other variables can be important in structuring benthic habitats. For example, water chemistry and temperature, when modelled at appropriate spatial scales, can be important predictors of benthic habitats (Davies and Guinotte, 2011). Hydrodynamic energy at the seabed is an important structuring factor for benthic habitats and communities. As well as imparting mechanical stress (Gove et al., 2015; Koehl, 1999), water flow controls water chemistry (Gutiérrez et al., 2008), particulate food supply (Rosenberg, 1995; Sebens et al., 1998) and larval dispersal (Cowen and Sponaugle, 2009). Alteration of flow regimes affects feeding efficiency, growth rates and settlement of benthic species that are adapted to specific flow conditions (Eckman and Duggins, 1993). Critically, hydrodynamic energy affects substrate composition through sediment transport (Shields, 1936), which in turn controls benthic community composition and imparts temporal variation within the system (Coggan et al., 2012; Warwick and Uncles, 1980). Hydrodynamic energy has

proved be an important variable for mapping benthic habitat spatial distribution at regional and national scales with resolution of kilometres (Huang et al., 2011; Robinson et al., 2011), but it is often overlooked or unavailable for predictive mapping at finer scales (Brown et al., 2011; Pearman et al., 2020). The inclusion of simulated wave induced seabed energy improved predictive habitat mapping for a wave exposed region in temperate southern Australia (Rattray et al., 2015), and it follows that tidally induced seabed energy is likely to be an important predictor of high energy habitats in regions with fast tidal currents. However, to our knowledge no study has incorporated tidally induced energy at the seabed with high-resolution bathymetry for predictive habitat mapping in temperate, high tidal energy waters.

Tidally induced hydrodynamic energy is likely to influence the distribution of geogenic and biogenic reefs in different ways. Strong tidal currents erode and transport sediment, leaving stable substrates that may be colonised by epibiota to form geogenic reefs. For biogenic reefs, the effects of hydrodynamic energy depend on the reef-forming organism. *Sabellaria spinulosa* is a reef-forming annelid that builds aggregations of tubes from suspended coarse sediment that support diverse associated communities (Pearce, 2017). *S. spinulosa* reef distribution is likely to be influenced by the availability of resuspended sediment as tube-building material, in turn driven by hydrodynamic energy (Davies et al., 2009; Holt et al., 1998). We used semi-automated predictive mapping, parameterized with multibeam derived variables and incorporating simulated hydrodynamic energy data, to map previously unresolved potential reef habitats in a marine area of interest for tidal energy development. We show that tidally induced bed shear stress is a highly important variable for predicting high energy reef habitats. Our findings provide a deeper understanding of the relationships between hydrodynamic conditions, seabed morphology and reef habitats, with implications for sustainable development of understudied, high tidal energy waters.

4.3 Method

4.3.1 Study site

We mapped potential reef habitats in a 49 km² area to the west of Sir Ynys Môn (Isle of Anglesey), Wales, UK (Figure 4.1B). Our study area included a 35 km² area leased for tidal energy device demonstration, and a surrounding 500 m buffer. Tidal current speeds reach 3.7 m s⁻¹ and annual mean significant wave height is 1.26 to 1.5 m (Royal Haskoning DHV, 2019). Water depth within the study area ranges from 3-79 m (Figure 4.1B) and the seabed comprises a range of benthic habitats from mobile sediment to stable cobble and bedrock colonised by slow growing epifauna (Whitton, 2014). The site is known to contain potential reef, but the spatial distribution of different reef types in the area is unresolved (MarineSpace, 2019).

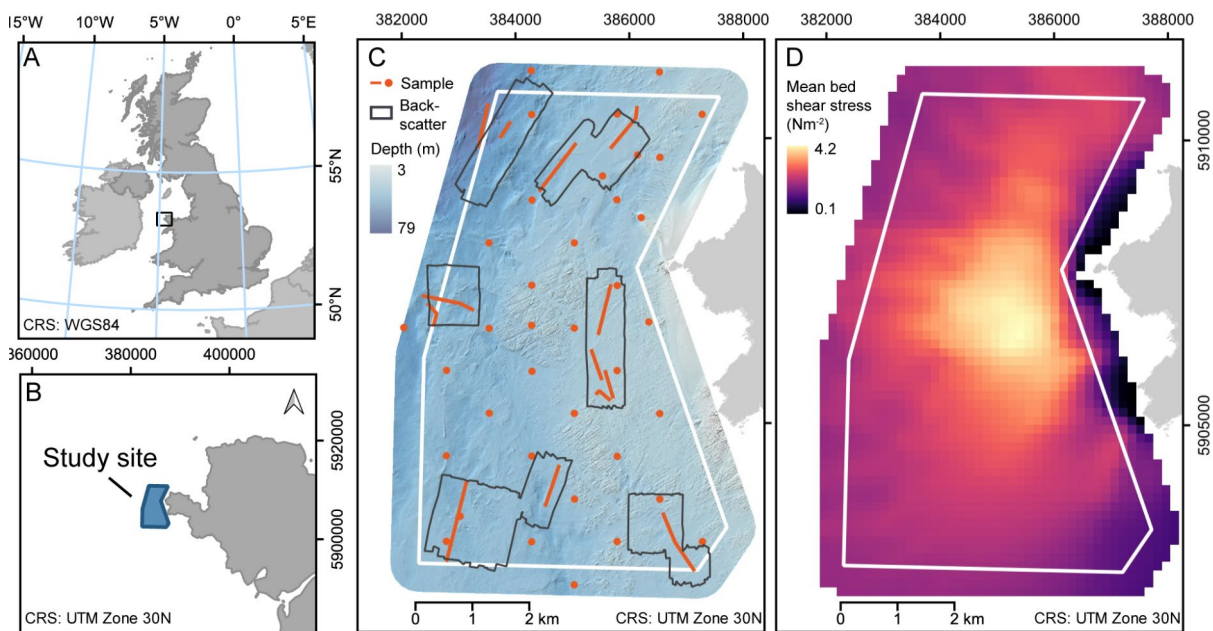


Figure 4.1 A & B) Location of the study site in north west Wales, UK. C) Bathymetry of the study area showing point and transect drop-down video sampling locations, extent of backscatter data and the leased area boundary (white). D) Modelled tidally induced mean bed shear stress across the study site.


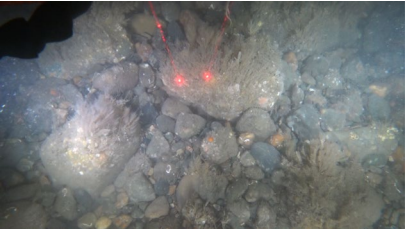


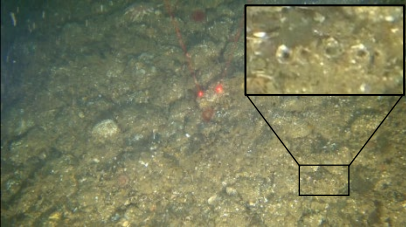

4.3.2 Habitat observations

We collected seabed video samples within the study site in June and July 2019 using the RV Prince Madog (Figure 4.1C, transects), with further samples obtained from a commercial ecological survey of the study site (Figure 4.1C, points). Sampling locations were spatially well-distributed, captured a range of energy conditions, and targeted areas of the study site with visually different bathymetric features. For transect video samples we used high-resolution (1080p, 60 frames per second) video with a forward facing (45° to the seabed), mechanically stabilised camera (FDR X3000, Sony), with dive lights for illumination and parallel lasers for scaling. To record sampling positions, we used an ultra-short baseline (USBL) system (EasyTrak Nexus Lite, Applied Acoustics) calibrated to a horizontal accuracy of 8 m. We sampled transects by drifting for 1 hour or 1 km within an hour either side of slack water, in current speeds of less than 1 kt.

To extract discrete observation data without introducing multiple operator errors, a single operator reviewed and classified the transect video footage. Starting from 1 min after the frame started moving steadily on the seabed, we assigned a class for reef substrate and a class for potential *S. spinulosa* reef (Table 4.1) for each 30 s section, with classes derived from the Habitats Directive Annex 1 definitions (European Commission, 2013). We only recorded observations for sections in which the seabed was visible at close enough range to confidently assess particle size using the parallel lasers for at least 50% of the section. We classified reef substrate as sediment (not reef), stony reef (low resemblance), stony reef (mid-high resemblance) or bedrock reef (Irving, 2009). While we initially classified stony reef into three resemblance classes, there were few high resemblance observations, so we combined mid and high resemblance records (Table 4.1). We classified potential biogenic (*Sabellaria spinulosa*) reef separately to substrate because *S. spinulosa* can colonise a range of substrates, and initial data exploration indicated that the predictor variables we used, mainly geomorphological descriptors, were unlikely to distinguish between, stony reef and stony reef colonised by *S. spinulosa*. We classified *S. spinulosa* observations as not seen, present, or potential reef based on percent cover of worm tubes and tube height (Hendrick and Foster-Smith, 2006). As there were few observations of potential *S. spinulosa* reef, low, medium and high resemblance observations were combined (Table 4.1). We extracted positions of the video observations to within 8 m horizontal accuracy by matching the video timestamps to the

USBL timestamps. Data from one transect were discarded due to low positional accuracy. We reclassified an additional point video sample dataset obtained from a commercial ecological survey of the study site to our classification system based on the percent cover of substrates and *S. spinulosa* reef recorded. These data were derived from drop down video sampling of the study area in 2018 and had been analysed for biotope mapping with percent cover of species and substrates quantified. We gridded the combined transect and point video observations on a 10 m resolution grid, assigning the class with the highest rank (Table 4.1) where there were multiple observations in a grid cell, giving a total of 675 observations (Figure 4.1C).

Table 4.1 Classification system for video samples. Each 30 second section of video was assigned a class for reef substrate and potential biogenic reef. Distance between laser points = 50 mm

CLASS	QUALIFIER	RANK	EXAMPLE
REEF SUBSTRATE			
SEDIMENT (NOT REEF)	Less than 10% particles of 64 mm or more.	1	
STONY REEF (LOW RESEMBLANCE)	10 – 40% particles of 64 mm or more. Epifauna present.	2	
STONY REEF (MID-HIGH RESEMBLANCE)	Over 40 % particles of 64 mm or more. Epifauna present.	3	
BEDROCK REEF	Bedrock present	4	
POTENTIAL BIOGENIC REEF			
<i>S. SPINULOSA</i> NOT SEEN	No <i>S. spinulosa</i> tubes seen	1	NA
<i>S. SPINULOSA</i> PRESENT	<i>S. spinulosa</i> tubes present	2	
POTENTIAL <i>S. SPINULOSA</i> REEF	<i>S. spinulosa</i> colonies of over 2 cm height or with over 10% cover	3	

4.3.3 Environmental predictor variables

To predict the spatial distribution of potential reef habitats we used geomorphological derivatives from bathymetry data and a measure of seabed energy as environmental predictor variables. Bathymetry data (1 m horizontal resolution) were collected using a multibeam echo sounder (MBES) for the study site in 2018 during a commercial survey (Royal Haskoning DHV, 2019) (Figure 4.1C). We generated geomorphological derivatives from the bathymetry data using ArcGIS 10.6 (ESRI) and the Benthic Terrain Modeller v3.0 plugin (Table 4.2) (Walbridge et al., 2018; Wright et al., 2005). We selected derivatives based on their demonstrated predictive power in the literature, and their hypothesised predictive power within the context of this study (Lecours et al., 2017b). Geomorphological derivatives are typically calculated using a square window with an edge length of 3 pixels, but the scale at which they are generated can influence their predictive power (Porskamp et al., 2018). Therefore, we generated vector ruggedness measure at scales (square window width) of 3, 27 and 81 m, representing uncorrelated intervals, and bathymetric position index at scales (circular window diameter) of 50 and 500 m (Table 4.2). Derivatives were generated from the 1 m resolution bathymetry data and then resampled (using mean-aggregation) to 10 m horizontal resolution to match the spatial accuracy of the observation data. Multi-collinearity in predictor variables was tested and resolved by removing highly colinear derivatives until the variance inflation factor for all predictors was below 10 (Dormann et al., 2013; Naimi et al., 2014) (Figure 4.2). All derivative data were generated across the full extent of the bathymetry data at 10 m resolution and then cropped to the study area.

Table 4.2 Bathymetric and backscatter derivatives used as predictor variables following removal of colinear variables. Scale mostly indicates the edge length of a square observation window. For BPI, scale indicates the diameter of a focal circle. Derivatives are calculated by operations on matrix or raster format data, for details see references in the methods column.

Derivative	Scale (m)	Method
Slope	3	Planar method ArcGIS 10 https://pro.arcgis.com/en/pro-app/2.8/tool-reference/3d-analyst/how-slope-works.htm
Curvature	3	Standard curvature ArcGIS 10 https://pro.arcgis.com/en/pro-app/2.8/tool-reference/3d-analyst/how-curvature-works.htm
Northness	3	cos(aspect) ArcGIS 10 For aspect see: https://pro.arcgis.com/en/pro-app/latest/tool-reference/spatial-analyst/how-aspect-works.htm
Eastness	3	sin(aspect) ArcGIS 10
	3	
Vector ruggedness measure (VRM)	27	Benthic Terrain Modeler v3 for ArcGIS 10 (Sappington et al., 2007; Walbridge et al., 2018)
	81	
Bathymetric position index (BPI)	50	Benthic Terrain Modeler v3 for ArcGIS 10 (Walbridge et al., 2018; Weiss, 2001)
	500	
Backscatter grey level co-occurrence matrix mean (GLCM)	3	<i>glm</i> package in R (Haralick et al., 1973; R Core Team, 2021; Zvoleff, 2020)
Backscatter position index (BS BPI)	20	Benthic Terrain Modeler v3 for ArcGIS 10 (Walbridge et al., 2018; Weiss, 2001)
	200	

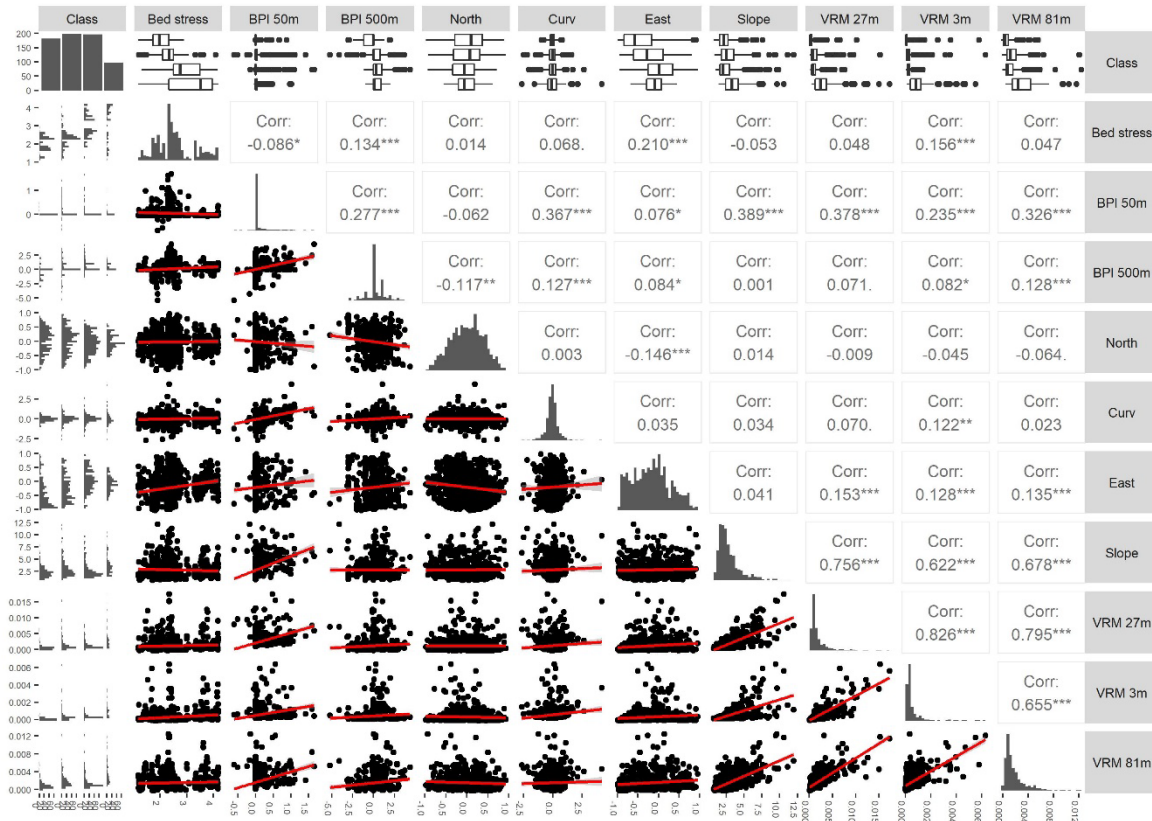


Figure 4.2 Correlation matrix of variables included in the full extent predictive models.

To generate a predictor variable of seabed energy, we used a 3D Regional Ocean Modelling System hydrodynamic model with a horizontal resolution of 150 m, covering the north-west Wales region, derived from a well-validated Irish Sea scale model (Ward et al., 2015). We calculated mean tidally induced bed shear stress over a typical spring-neap tidal cycle (Figure 4.1D). Mean bed shear stress is a good predictor of substrate composition at regional scales (Ward et al., 2015) and is likely to have a mechanistic influence on substrate and benthic communities. Ocean boundary conditions were taken from the TOPEX/POSEIDON global tidal model (TPXO). The model validates well against the Holyhead tide gauge harmonic data (Figure 4.3). The 150 m resolution model data were resampled using nearest neighbour (no interpolation) to 10 m resolution. As the hydrodynamic model incorporated bathymetry, and raw bathymetry within the depth range of the study site was not expected to have a mechanistic effect on benthic substrate or biogenic reef distribution, raw bathymetry was not included as a predictor variable.

High quality backscatter data were not available for the entire study area, but to investigate whether the inclusion of backscatter could improve predictive models of high energy benthic habitats we conducted a dedicated backscatter survey (SeaBat 7125, Reson) for six discrete patches in the area sampled by the camera sled transects, covering 9.8 km², 20% of the study area (Figure 4.1C). We collected backscatter data at low vessel speed (< 4 kt) with high swath overlap ensuring the entire seabed within the patches was insonified at least twice from different angles, and with settings fixed within a patch (Lamarche and Lurton, 2018). Backscatter data were processed using industry standard software FMGT (QPS) to generate a 1 m horizontal resolution raster. Because environmental conditions differed among patches and raw backscatter response was not calibrated, local derivatives were generated to provide relative metrics that could be analysed across non-overlapping patches (Table 4.2). Backscatter derivatives were resampled to 10 m resolution and collinear variables were removed.

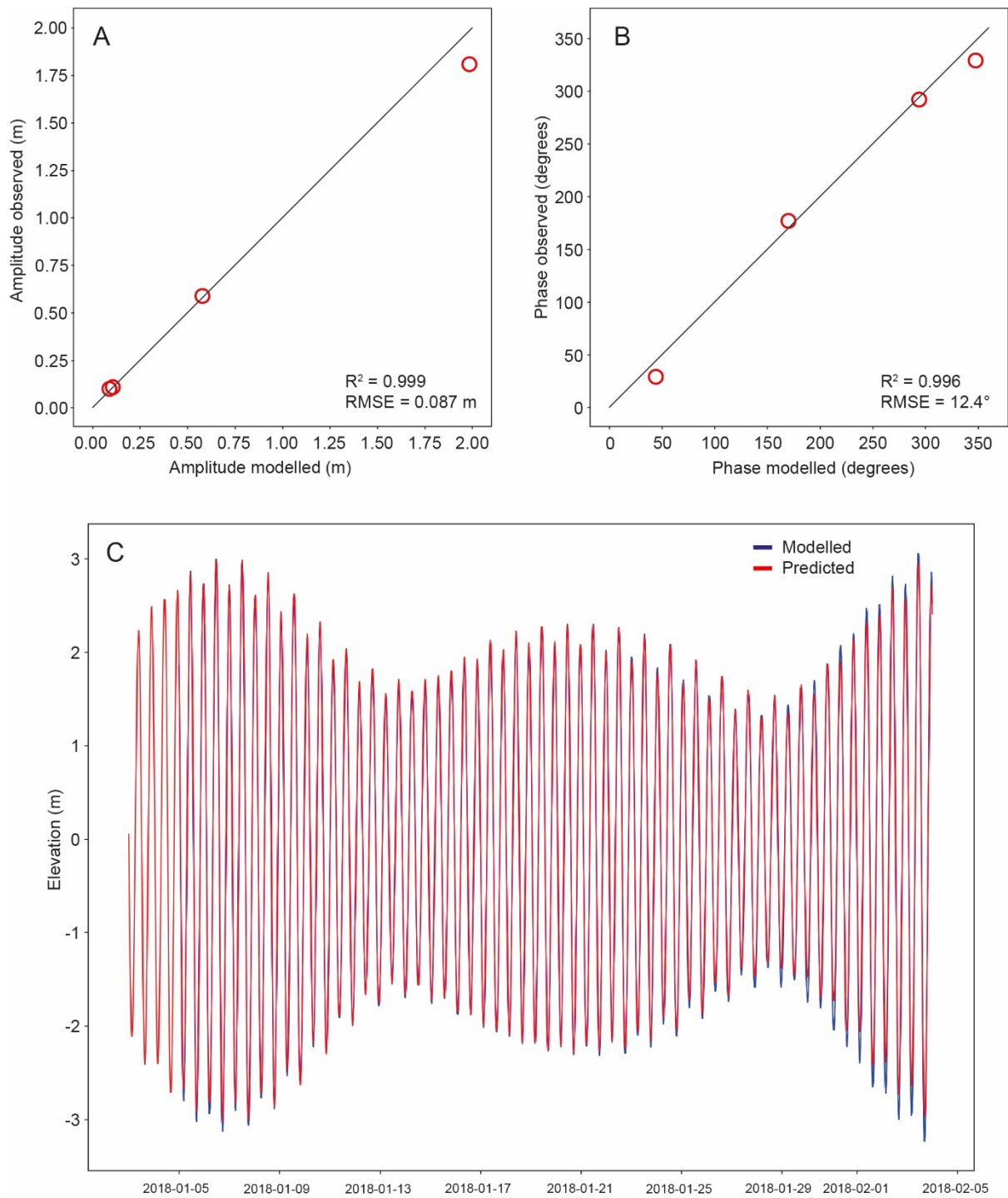


Figure 4.3 Our hydrodynamic model validates well against Holyhead tidal gauge harmonic data in A) amplitude, B) phase and C) elevation. Tidal elevation was processed in Python using `ttide_py` (https://github.com/moflaher/ttide_py) for tidal analysis and `numpy` to calculate r-squared values.

4.3.4 Classification model and predictive mapping

For classification and predictive mapping of reef substrate and potential biogenic reef we used Random Forests, an ensemble machine learning algorithm based on bootstrap aggregated classification trees (Breiman, 2001; Cutler et al., 2007), that performs consistently well for benthic habitat mapping in a range of contexts (Mitchell et al., 2018; Wicaksono et al., 2019). The approach has no assumptions of data distribution, making it a suitable choice given the characteristics of our sampling design and data. We implemented the algorithm using the *randomForest* and *caret* packages in R (Kuhn, 2008; Liaw and Wiener, 2002; R Core Team, 2021). We investigated the alternative classifier XGBoost, a tree-based algorithm that employs gradient boosting (Chen et al., 2018), but found that it gave no performance improvement while being less interpretable and more computationally demanding as it requires extensive tuning of several hyperparameters. To assess model performance we used a repeated modelling and cross-validation approach (Mitchell et al., 2018). We generated 25 training and test sets (7:3 ratio) from bootstrap samples of our observation data with replacement. We used each set to train and test a random forest classification model with 1000 trees and 3 variables tested at each split, hyperparameters that were defined by a preliminary tuning stage. We calculated average estimated performance metrics from cross validation of each of the model runs. We used each model run to predict the spatial distribution of benthic classes in the study area and produced maps representing the most frequent class predicted for each pixel from all model runs. We mapped spatially explicit uncertainty as confidence maps. Confidence for each pixel was quantified by multiplying the proportion of the most common predicted class from all model runs with the average probability of the most common class (Mitchell et al., 2018). To assess the influence of backscatter derivatives on model performance, we ran models with and without backscatter derivatives as predictor variables for the extent of the backscatter data.

To assess the performance of a predictive mapping model, an error matrix and a selection of metrics should be considered in the context of the aims of the model and the user's interests (Foody, 2002; Olofsson et al., 2014). The error matrix documents the predicted and observed classes of the test samples, giving an estimate of the model performance for new, unknown observations. We generated a selection of standard and recommended performance metrics from the error matrix (Foody, 2002; Mitchell et al., 2018; Olofsson

et al., 2014; Pontius and Millones, 2011). No single measure can fully describe performance of a classification model, but here we present balanced accuracy as an overall measure that accounts for imbalance in class prevalence (Brodersen et al., 2010). For consistency with other studies we also present overall accuracy as the proportion of correct predictions out of total predictions, and Cohen's kappa coefficient (Cohen, 1960), although their use has been discouraged (Brodersen et al., 2010; Foody, 2020; Pontius and Millones, 2011). To give context to the overall accuracy value, the no information rate is provided, equal to the proportion of the most prevalent class and therefore being the accuracy value that would be achieved by predicting all observations as one class. User's and producer's accuracies provide class-wise insight. The user's accuracy estimates the reliability of the map for a user, describing the proportion of the predictions of a class that were actually observed to be that class. The producer's accuracy, also known as sensitivity, or true positive rate, estimates the ability of a model to correctly map the land- or seascape, describing the proportion of known observations of a particular class that were correctly predicted as that class. The complement of sensitivity is specificity. Specificity, or true negative rate, describes how many observations that were known to not be a class were correctly predicted to not be that class. Finally, we present quantity disagreement and allocation disagreement (Pontius and Millones, 2011). These measures provide information about the way in which the observations and predictions differ. High quantity disagreement indicates large differences in class prevalence while a high allocation disagreement indicates a large proportion of misclassifications. To examine whether inclusion of backscatter derivatives improved the substrate and *S. spinulosa* predictive models, we used Mann-Whitney U tests to test for differences in class-wise and overall balanced accuracy, sensitivity (producer's accuracy), specificity and user's accuracy of model runs ($n = 25$) with and without backscatter derivatives, using alpha of 0.05.

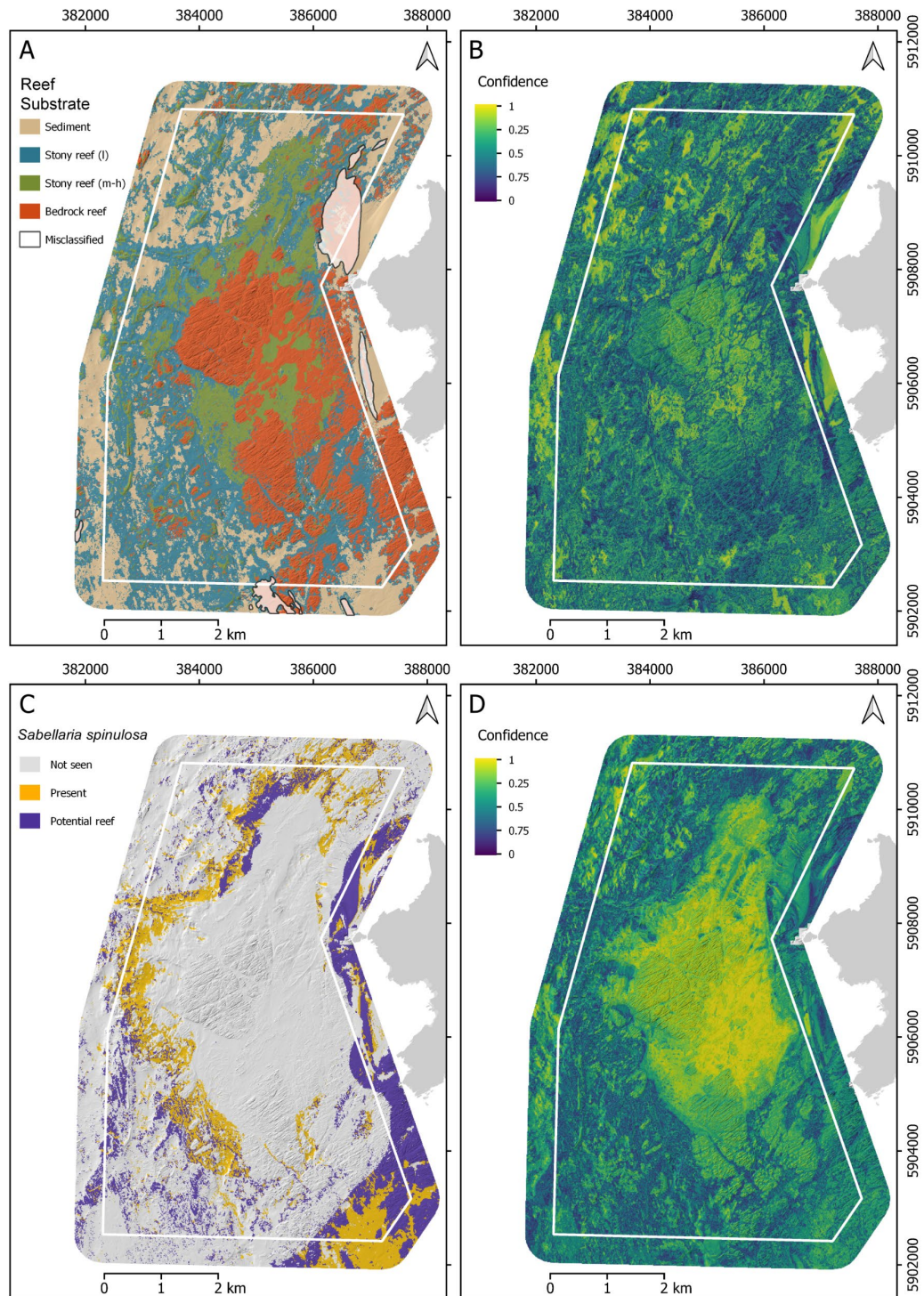


Figure 4.4 A) Predicted reef substrate map with visually identified misclassified areas masked out. B) Confidence map for substrate, calculated by multiplying the frequency of the most commonly predicted class with the average probability of the most common class. C) Predicted *Sabellaria spinulosa* presence and potential reef with D) associated confidence map.

4.4 Results

4.4.1 Reef substrate

We predicted the spatial distribution of reef substrate in the study area by classifying the substrate into four classes: sediment (not reef), stony reef (low resemblance), stony reef (mid-high resemblance) and bedrock reef (Figure 4.4A). The model performed well, with most observations correctly predicted (Table 4.3), reflected in the overall balanced accuracy (mean \pm 95% CI) of $80.7\% \pm 0.8\%$ (Table 4.4). Producer's and user's accuracies were higher in sediment and stony reef (mid-high resemblance) compared to stony reef (low resemblance) and bedrock. The observed and predicted classes differed due to misclassification (allocation disagreement = $23.7\% \pm 1.2\%$), more than due to differences in class prevalence (quantity disagreement = $4.6\% \pm 0.9\%$). The error matrix showed that the majority of misclassifications were in the classes most similar to the target class (Table 4.3). For example, sediment was mostly misclassified as stony reef (low resemblance) and rarely as bedrock. We identified visually apparent misclassifications and masked these out on the final predictive map (Figure 4.4A).

The most important variable for predicting reef substrate classes in the study area was mean bed shear stress, followed by vector ruggedness measure at multiple scales (Figure 4.5A). Partial dependence plots of the three most important variables showed that areas with low mean bed shear stress (up to approximately 2.5 Nm^{-2}) and low ruggedness at multiple scales were more likely to be classified as sediment or stony reef (low resemblance), and less likely to be classified as bedrock (Figure 4.5B-D). Areas with high bed shear stress and moderate to high fine-scale (3 m window) ruggedness were less likely to be classified as sediment. The confidence map showed that areas of sediment and stony reef (mid to high resemblance) were predicted with the most consistency among model runs (Figure 4.4B). Less consistency was seen at transition zones between different classes and areas where a mixture of classes was predicted in a small area.

Table 4.3 Error matrix of a model to predict reef substrates. Cross validation of each bootstrap model run (n = 25) was used to generate an error matrix normalised by the number of test observations in each class. The normalised values from all error matrices are summarised here as mean \pm 95% confidence interval. True positives are highlighted in grey

	Observed			
	Sediment	Stony reef (l)	Stony reef (m-h)	Bedrock reef
Predicted Sediment	0.75 \pm 0.026	0.174 \pm 0.023	0.009 \pm 0.006	0.004 \pm 0.004
Stony reef (l)	0.215 \pm 0.023	0.66 \pm 0.02	0.144 \pm 0.021	0.145 \pm 0.019
Stony reef (m-h)	0.011 \pm 0.005	0.103 \pm 0.019	0.769 \pm 0.023	0.189 \pm 0.028
Bedrock reef	0.025 \pm 0.009	0.062 \pm 0.011	0.077 \pm 0.014	0.662 \pm 0.03

Table 4.4 Performance metrics for the reef substrate model. Values calculated from the error matrices from each bootstrap model run cross validation are summarised here as mean \pm 95% confidence interval.

	Overall	Sediment	Stony reef (l)	Stony reef (m-h)	Bedrock reef
Total observations	202	55	59	59	29
User's accuracy	0.718 \pm 0.012	0.794 \pm 0.021	0.616 \pm 0.018	0.791 \pm 0.02	0.672 \pm 0.023
Producer's accuracy / Sensitivity	0.71 \pm 0.013	0.75 \pm 0.026	0.66 \pm 0.02	0.769 \pm 0.023	0.662 \pm 0.03
Specificity	0.903 \pm 0.004	0.925 \pm 0.01	0.829 \pm 0.013	0.915 \pm 0.009	0.945 \pm 0.006
Quantity disagreement	0.046 \pm 0.009	0.027 \pm 0.008	0.029 \pm 0.009	0.02 \pm 0.006	0.017 \pm 0.004
Allocation disagreement	0.237 \pm 0.012	0.095 \pm 0.011	0.192 \pm 0.009	0.108 \pm 0.012	0.079 \pm 0.006
Balanced accuracy	0.807 \pm 0.008				
Accuracy	0.717 \pm 0.012				
Kappa	0.614 \pm 0.017				
No information rate	0.292 \pm 0				

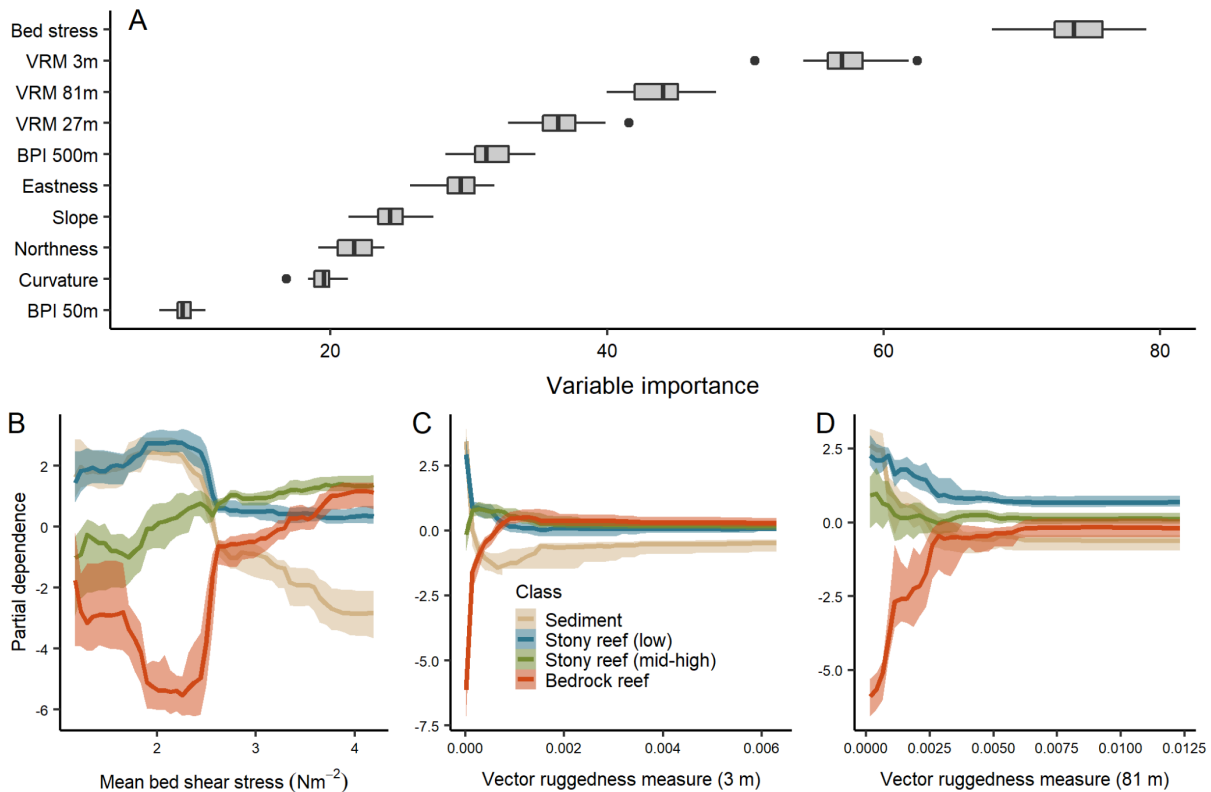


Figure 4.5 A) Relative importance of predictor variables in the reef substrate model. B) Partial dependence plots for the three variables with highest importance. The plots visualise the response of the model to an individual variable. The plots visualise the influence of each variable on the likelihood that an observation is predicted to be each of four classes. For example, observations with low mean bed shear stress are less likely to be classified as bedrock reef and more likely to be classified as sediment or stony reef (low resemblance).

4.4.2 Potential *Sabellaria spinulosa* biogenic reef

Our classification model predicted the spatial distribution of three classes for *Sabellaria spinulosa*: not seen, present, and potential reef (Figure 4.4C). The model predicted most observations correctly and had an overall balanced accuracy of $77\% \pm 1\%$, indicating good performance (Table 4.5, Table 4.6). The high accuracy reported appeared to be strongly influenced by the model's ability to correctly predict the "not seen" class, which represented the highest proportion of observations. Our model accuracy was higher than the no information rate, indicating that it provided useful additional information (Table 4.6). The "potential reef" class had a low producer's accuracy ($47.2\% \pm 3.4\%$) but higher user's accuracy ($67.6\% \pm 3.7\%$) (Table 4.6), indicating that while not all areas of potential reef were mapped, the areas that were mapped were likely to be correct. Potential reef

had a high specificity ($95.1\% \pm 0.7\%$), indicating that most non-reef observations were correctly mapped (Table 4.6).

Mean bed shear stress was the most important variable for predicting potential *S. spinulosa* reef, with the remaining variables having much lower importance (Figure 4.6A). The partial dependence plot for the effect of mean bed shear stress on class predictions showed that the potential *S. spinulosa* reef class was most likely to be predicted at very low ($< 1.5 \text{ Nm}^{-2}$) and moderate (approx. 2.4 and 2.9 Nm^{-2}) mean bed shear stress, with low likelihood of prediction above 3 Nm^{-2} (Figure 4.6B). Inspection of the spatial prediction shows that *S. spinulosa* species presence observations were predicted to occupy a band approximately following the 2.5 Nm^{-2} mean bed shear stress contour, in an area predicted to be a mixture of stony reef and sediment substrates (Figure 4.4C). The model predicted a low likelihood of *S. spinulosa* reef in the highest energy areas in the centre of the study area with high confidence, an area that was dominated by bedrock and stony reef (mid-high resemblance) (Figure 4.4C & D). Potential reef was predicted to be found in the north west and south west of the study area, and in denser patches in the east and south east of the study area. However, we did not have any observations from the shallow eastern edge so these results should be considered with caution.

Table 4.5 Error matrix of the model predicting *S. spinulosa* presence and potential reef. Cross validation of each bootstrap model run ($n = 25$) was used to generate an error matrix normalised by the number of test observations in each class. The normalised values from all error matrices are summarised here as mean \pm 95% confidence interval. True positives are highlighted in grey.

		Observed		
		Not reef	Present	Reef
Predicted	Not reef	0.941 \pm 0.007	0.257 \pm 0.028	0.247 \pm 0.023
	Present	0.043 \pm 0.005	0.606 \pm 0.023	0.281 \pm 0.027
	Reef	0.015 \pm 0.004	0.137 \pm 0.018	0.472 \pm 0.034

Table 4.6 Performance metrics for the potential *S. spinulosa* reef model. Values calculated from the error matrices from each bootstrap model run cross validation are summarised here as mean \pm 95% confidence interval.

	Overall	Not seen	Present	Potential reef
Total observations	206	123	47	36
User's accuracy	0.725 \pm 0.017	0.847 \pm 0.009	0.651 \pm 0.022	0.676 \pm 0.037
Producer's accuracy / Sensitivity	0.673 \pm 0.015	0.941 \pm 0.007	0.606 \pm 0.023	0.472 \pm 0.034
Specificity	0.867 \pm 0.006	0.747 \pm 0.018	0.903 \pm 0.008	0.951 \pm 0.007
Quantity disagreement	0.07 \pm 0.008	0.067 \pm 0.008	0.02 \pm 0.006	0.052 \pm 0.008
Allocation disagreement	0.148 \pm 0.011	0.07 \pm 0.008	0.144 \pm 0.01	0.081 \pm 0.011
Balanced accuracy	0.77 \pm 0.01			
Accuracy	0.783 \pm 0.01			
Kappa	0.593 \pm 0.02			
No information rate	0.597 \pm 0			

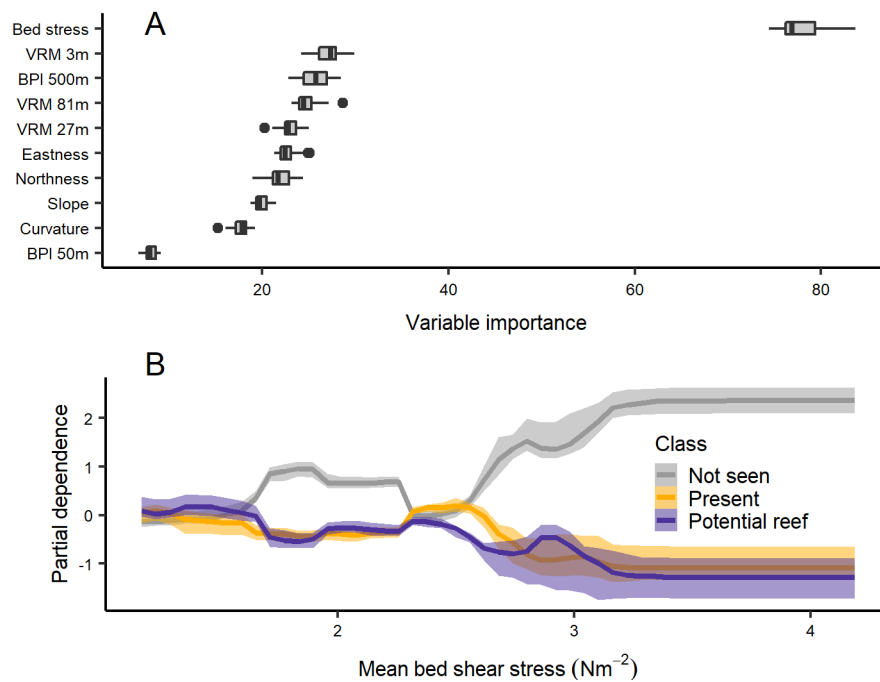


Figure 4.6 A) Relative importance of predictor variables in the potential *S. spinulosa* reef model. B) Partial dependence plots for mean bed shear stress, the variable with highest importance.

4.4.3 The influence of backscatter

To investigate the influence of backscatter derivatives on model performance we compared models with and without backscatter derivatives for the spatial extent of backscatter data (Figure 4.1C). We found a low influence of backscatter derivatives on model performance that varied with class and performance metric. For the model predicting reef substrate, backscatter derivatives had moderate to low importance (Figure 4.7). There were some significant differences in class-wise performance metric medians, but differences were limited to 3 percentage points (Table 4.7) and there was no significant difference in overall metrics.

In the model predicting *S. spinulosa* distribution, backscatter grey level co-occurrence matrix (GLCM) mean had the second highest importance after mean bed shear stress (Figure 4.7). However, the only significant difference in model performance metrics between the models with and without backscatter derivatives was in the sensitivity of the “present” class, in which the median of the model excluding backscatter derivatives was higher by 6.6 percentage points (Table 4.7).

Figure 4.7 Variable importance plots for models of reef substrate and *Sabellaria spinulosa* presence and potential reef, with and without backscatter derivatives (underlined) included

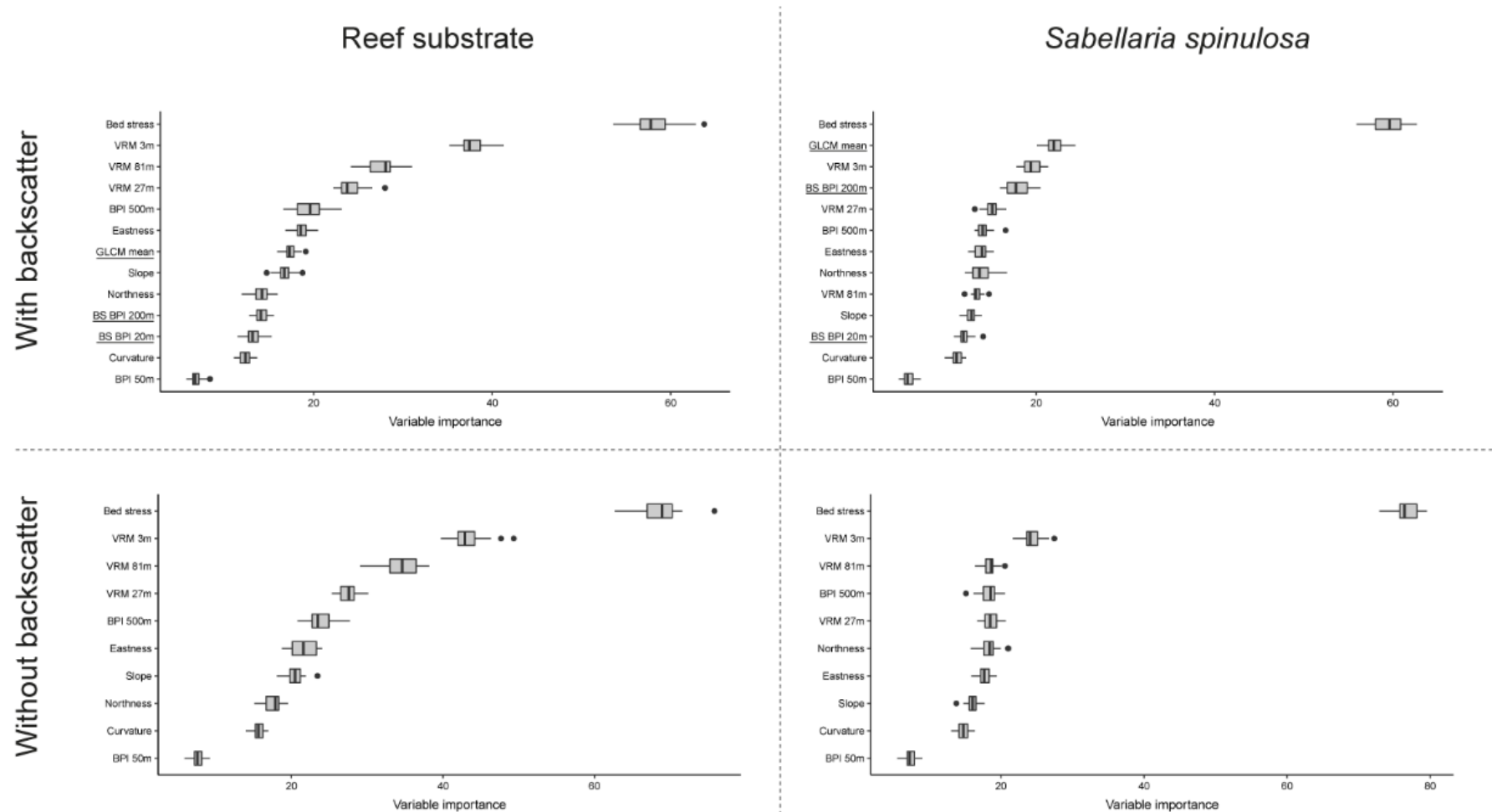


Table 4.7 Results of Mann-Whitney U tests comparing performance metrics of predictive models that excluded (BS -) and included backscatter derivatives (BS +). Significant differences are indicated in **bold**.

Substrate		Sediment			Stony reef (l)			Stony reef (m-h)			Bedrock reef			Overall		
Metric	BS	Median	<i>U</i>	<i>P</i>	Median	<i>U</i>	<i>P</i>	Median	<i>U</i>	<i>P</i>	Median	<i>U</i>	<i>P</i>	Median	<i>U</i>	<i>P</i>
Sensitivity	-	0.730	428.5	0.023	0.694	306	0.907	0.804	432.5	0.019	0.792	217	0.062	0.745	325	0.818
	+	0.757			0.694			0.804			0.750			0.739		
Specificity	-	0.930	304.5	0.884	0.846	413.5	0.049	0.918	287	0.626	0.965	393.5	0.113	0.911	369	0.280
	+	0.938			0.855			0.918			0.972			0.913		
User's accuracy	-	0.757	331	0.727	0.640	415.5	0.047	0.831	295	0.741	0.769	358	0.382	0.753	361	0.352
	+	0.788			0.661			0.825			0.792			0.758		
Balanced accuracy	-	0.836	415.5	0.047	0.769	334.5	0.677	0.852	400	0.091	0.871	232	0.120	0.828	335	0.672
	+	0.855			0.780			0.865			0.857			0.826		

Sabellaria spinulosa

		Not seen			Present			Potential reef			Overall		
Metric	BS	Median	<i>U</i>	<i>P</i>	Median	<i>U</i>	<i>P</i>	Median	<i>U</i>	<i>P</i>	Median	<i>U</i>	<i>P</i>
Sensitivity	-	0.922	363.5	0.323	0.733	160	0.003	0.516	298	0.784	0.717	244.5	0.190
	+	0.933			0.667			0.484			0.706		
Specificity	-	0.882	222	0.079	0.851	390.5	0.131	0.948	238	0.148	0.890	245	0.195
	+	0.855			0.860			0.941			0.890		
User's accuracy	-	0.900	228	0.103	0.642	317	0.938	0.690	254.5	0.264	0.750	248	0.216
	+	0.885			0.640			0.682			0.729		
Balanced accuracy	-	0.896	272	0.438	0.791	215.5	0.061	0.737	282.5	0.567	0.807	241	0.170
	+	0.888			0.767			0.717			0.798		

4.5 Discussion

We used a machine learning approach to predict the spatial distribution of previously unresolved potential temperate reef habitats in a high tidal energy marine region, finding that hydrodynamic energy at the seabed was the most important predictor of potential reef habitats. Multiscale bathymetric derivatives were also important for predicting reef substrate, whereas backscatter derivatives had low influence on model performance when included.

Mean tidally induced bed shear stress was the most important variable in predictive models for both reef substrate and potential *Sabellaria spinulosa* biogenic reef. Our results support findings from wave exposed coastal regions (Porskamp et al., 2018; Rattray et al., 2015), showing that hydrodynamic energy is an important predictor of reef habitats in high energy waters. After bed shear stress, ruggedness calculated at three scales (9 m, 27 m and 81 m) were the next most important variables for predicting reef substrate. These results support an increasingly recognised need to include predictor variables across scales for benthic habitat mapping (Lecours et al., 2015; Porskamp et al., 2018). As with bathymetric indices, the ability of bed shear stress to structure and predict benthic habitats and communities is likely to differ across spatial scales. Variation in water flow influences species distribution by controlling proximal factors across scales. For instance, suspended food availability is influenced by topographically driven turbulence at the centimetre scale (Prado et al., 2020), and by oceanographic processes like upwelling at the kilometre scale (Navarrete et al., 2005). Hydrodynamic energy information with metre or finer resolution across regional extents would enhance the performance of fine-scale habitat mapping and marine species distribution modelling to better understand patterns and processes at organism-centric scales. Unlike bathymetry and backscatter that are relatively stable through time, hydrodynamic conditions are highly variable, making simulating and validating them at fine spatial scales logistically and computationally challenging with current technology.

Backscatter intensity derivatives had limited impact on model performance, likely for several reasons. First, the surficial substrates we observed by camera may represent veneers over different underlying substrates, adding variability to the acoustic reflectivity of substrates with similar appearance (Lucieer et al., 2013). Second, we were only able to

capture high quality backscatter data for discrete patches within the study area due to the added time and calmer sea conditions required for collection of high-quality backscatter data compared to a purely bathymetric survey (Lamarche and Lurton, 2018). Backscatter data can be valuable for seabed substrate discrimination, particularly for sediments (Lucieer et al., 2018b). However, a lack of standardisation in data collection and processing protocols limits repeatability in backscatter data (Lamarche and Lurton, 2018; Lucieer et al., 2018b), and presents challenges in combining data from different surveys (Lacharité et al., 2018; Misiuk et al., 2020). For our aims of predicting the spatial distribution of reef habitats, our results indicated that the lack of full-coverage, high quality backscatter data was not a substantial limitation on model performance.

Accuracy metrics are useful for assessing the performance and usefulness of a model for a specific application but should not be used in isolation to compare different models and studies (Bennett et al., 2013; Mitchell et al., 2018). The performance of benthic habitat mapping varies with decisions made throughout planning, data collection and analysis, leading to a lack of standardisation (Strong, 2020). For instance, choices in model framework, scale and choice of environmental variables, the number of observation classes used and whether to use a geomorphic or biological basis to classes, all affect different aspects of the resulting map product (Ierodiaconou et al., 2018; Porskamp et al., 2018; Smith et al., 2015). A predicted map should therefore be considered along with its error matrix, several performance metrics and spatially explicit uncertainty estimates in a case-by-case basis to determine its suitability for a particular user and purpose (Foody, 2020, 2002). Our model performance (balanced accuracy of 81-84%) was sufficient to provide useful information about the spatial distribution of potential temperate reef habitats in our study site, and was comparable to other studies with similar contexts and model frameworks, having overall accuracies of 81-93% (Haggarty and Yamanaka, 2018), and 69.7% (Porskamp et al., 2018). Improvements could be made to the modelling approach we used. In particular, Random Forests are sensitive to class imbalance which was present in our data (Table 4.4, Table 4.6). Sampling methods including up-sampling minority classes, down-sampling majority classes or hybrid methods like synthetic minority over sampling (SMOTE) can be incorporated to counteract the influence of class imbalance (Chawla et al., 2002; Kuhn and Johnson, 2013). Alternatively, a different model algorithm that is more robust to class imbalance like gradient boosting may show better

performance (Lawrence et al., 2004), although preliminary tests with the XGBoost algorithm (Chen et al., 2018) did not improve our results. Our results demonstrate that predictive mapping using machine learning is a valuable tool to support mapping of stony and biogenic reef habitats in high tidal energy temperate seas.

Misclassifications were identified both in the error matrices and through manual inspection of the generated predicted maps. Most misclassifications were in classes most similar to the target class, which is to be expected with a classification system that maps a continuously varying natural environment as discrete categories (Foody, 2002; Wang, 1990). Misclassification of sediment wave bedforms as bedrock were visually identified and can largely be explained by a paucity of observations in these areas. As the classification algorithm can only learn from the training data, with no rugged sediment observations in the training data, rugged ground was most likely to be predicted as bedrock. This suggests that semi-automated and manual interpretation mapping methods are complementary and the use of multiple methods will ultimately improve the quality of benthic habitat maps (Diesing et al., 2014). Other sources of uncertainty included the limited field of view of video observations (approx. 1 x 1 m) relative to the pixel size of the final map (10 x 10 m), and the potential for the observed substrate (e.g., sediment) to be a veneer over another substrate (e.g., bedrock or biogenic reef). This is a particular concern in areas with strong tidal currents where high volumes of sediment are periodically transported and deposited during a tidal cycle and a single observation in time cannot capture such transience.

Our predictive model for *Sabellaria spinulosa* distribution was largely driven by the singular important variable of bed shear stress. *S. spinulosa* presence and reef were not predicted to occur in the areas with highest energy, suggesting that bed shear stress was a limiting factor for the species above $\sim 3 \text{ Nm}^{-2}$. Higher flow rates may present barriers to larval settlement, tube building or feeding for the species, but there is little existing information on its environmental limits (Davies et al., 2009). Bathymetric and backscatter predictor variables had low importance, suggesting that they were insufficient to explain the spatial variation in *S. spinulosa* distribution. *S. spinulosa* is difficult to detect using multibeam bathymetry acoustic data and expert interpretation of higher resolution side scan sonar data is recommended to locate potential reefs (Limpenny et al., 2010).

Although our original acoustic data resolution was 1 m, it may have still been too coarse to distinguish *S. spinulosa* reef morphology in an area dominated by stony reef, especially with a relatively low number of positive observations of the species or reef presence to train the model. Sabellariid reefs are dynamic in both space and time in terms of their emergence, density and patchiness (Jackson-Bué et al., 2021; Jenkins et al., 2018; Pearce et al., 2014), and can survive periods of burial due to sediment transport (Hendrick et al., 2016). This presents further challenges in both detecting reef habitats and identifying its environmental niche with a limited temporal resolution. Observations through time are needed for an improved understanding of the environmental conditions suitable for *S. spinulosa* reef habitat development.

This study supports the use of predictive mapping as an efficient and repeatable tool for ecosystem management in logistically challenging environments like high tidal energy waters. These traditionally less anthropogenically developed and understudied regions are seeing novel industrial interest from the nascent marine renewable energy industry, generating demand for cost effective means to gather baseline ecosystem information (Shields et al., 2011; Wilding et al., 2017). We found that tidally-induced seabed shear stress was a powerful variable for predicting reef habitats in high tidal energy temperate seas, and highlighted the importance of multiscale bathymetric indices for benthic habitat mapping. Our results will contribute to a better understanding of the spatial ecology of temperate reef ecosystems and will inform evidence-based decision making for ecosystem management in high energy marine areas.

5 General discussion

5.1 Overview

We are entering a new era in spatial ecology. Contemporary advances in tools and techniques for observing ecosystems present unprecedented opportunities for investigating patterns and processes in new ways, across novel scales and in challenging environments. In this thesis, I examined some of the most powerful tools and applications for high-resolution three-dimensional (3D) ecosystem mapping currently available to ecologists, focussing their application within temperate reef habitats. In chapter 2 I reviewed and tested the potential of modern 3D mapping tools for field ecology in various systems and scales. In chapter 3 I applied those tools to examine cross-scale structural dynamics in a complex biogenic reef habitat. In chapter 4 I integrated acoustic 3D mapping with hydrodynamic information to predict previously unresolved spatial patterns in subtidal reef habitats. Through the course of these studies many lessons were learned about the practicalities, opportunities, and limitations of using modern remote sensing tools to ask ecological questions.

The aims and objectives of the thesis were mostly met, although challenges were encountered and further work would be needed to explore questions that arose though the course of the study. My first aim was to assess the performance and potential applications of contemporary and emerging tools for investigating 3D ecosystem structure to advance understanding of patterns and processes in marine and coastal ecology. I reviewed state-of-the-art technological solutions for 3D mapping in ecology. My review was timely and novel as the technologies examined had only recently emerged as accessible field methods for non-specialists. Due to the extremely rapid pace of innovation in the 3D reality capture and geospatial technology sectors, the technologies I focussed on could now be considered established rather than emerging, and some of the barriers I identified like a lack of awareness of methods are already being overcome. An updated review of the field will be necessary in the next few years to help field ecologists stay up to date with technology. As methods and technologies advance, it is critical to maintain rigorous testing of their capabilities and limitations, and the uncertainty in the data they

generate in specific contexts. The findings from my tests of the accuracy of 3D models generated by different technologies will therefore remain relevant and informative going forward. My second aim was to characterise patterns of spatial and temporal variation in the 3D structure of temperate intertidal biogenic reef built by *Sabellaria alveolata*. Achieving this aim benefitted from having a relatively long period of data collection (5 yrs) and having access to state-of-the-art 3D mapping technologies. My findings indicated that a still longer timeseries of high-resolution 3D data could provide a more complete understanding of *S. alveolata* reef structural dynamics by capturing more complete cycles of colony initiation, accretion and erosion. Further work would also be needed to identify the environmental and biological drivers behind structural variation in the habitat. My third aim was to predict the spatial distribution of temperate reef habitats in a high energy marine area, using information about 3D ecosystem structure. I had success in predicting potential geogenic reef substrates, but potential biogenic reef distribution was more challenging to predict. I discussed limitations of the study and suggested methodological improvements that could be incorporated into further work to improve both the performance of the models and the confidence in the model predictions.

The scope and scale of spatio-temporal ecological investigation is rapidly expanding with the emergence of new capabilities in observation and analysis, paving the way for step changes in our understanding of natural systems. This thesis highlights the huge potential for 3D mapping in ecological investigation and provides an accessible demonstration of the advanced insights that can be gained from its adoption as part of the modern ecologist's toolbox. In this section I discuss the relevance of my findings in the context of key themes that emerge from the collective works. I highlight important limitations of the methods used and consider improvements and extensions to the work completed. Finally, I discuss future research priorities, opportunities and challenges for the use of 3D ecosystem mapping in ecology and environmental management.

5.2 New insight from 3D mapping of ecosystems

The findings of the individual chapters of this thesis are relevant to diverse research avenues, but two major themes run through the collective works. First, the work demonstrates that emerging remote sensing tools are making recording and analysing 3D structure practical and accessible for field ecologists. The data products have a broad

range of applications, from enhanced observation to overcoming long-standing technological barriers to examining fundamental ecological questions. Second, my findings highlight that the scale of observations and analyses have important effects on the patterns detected, with knock-on implications for interpretation of results and subsequent evidence-based decision making. Cross-scale data collection and analysis mitigates bias in observation scale and advances our understanding of scale-dependent patterns and processes in ecosystems.

5.2.1 Recording and analysing 3D structure

Organisms are 3D entities that inhabit 3D ecosystem space. An organism's physical structure, or morphology, provides information about its evolutionary and developmental history, while habitat structure provides information about environmental conditions, resource availability and organism-environment interactions. Recording and analysing structure, therefore, forms an important component of many studies in ecology and evolution. However, measuring and analysing complex 3D structure has traditionally been challenging, and is commonly simplified to metrics that can be more easily handled (Reichert et al., 2017). For example, a typical model system may include organisms with size represented by length, inhabiting a landscape represented as a 2D patch-mosaic. This simplification of organisms and ecosystem structure is necessary for analysis within established frameworks, but may be limiting our understanding of ecosystem functioning and interactions (Lepczyk et al., 2021). With the ability to measure and record organisms and ecosystems in 3D, novel analyses can be explored, potentially revealing new or advanced insight (Kedron et al., 2019).

In chapter 2 I found that 3D mapping could generate digital 3D ecosystem reconstructions with millimetre-scale resolution and accuracy. By testing tools in various habitats and quantifying their performance, the findings help to address a key barrier to widespread adoption of 3D mapping in field ecology, the question of quantifying the accuracy of models generated using structure-from-motion photogrammetry. The algorithms used for structure-from-motion photogrammetry are complex, and uncertainty can propagate through the data collection and processing pipeline (Clapuyt et al., 2016). It is important, therefore, to test and validate the method in a variety of situations relevant to the field. My findings complement those of other researchers testing 3D mapping methods in

different contexts. My results of structure-from-motion accuracies of 4-56 mm agree with previous studies testing in-air structure-from-motion reporting a range of accuracies from millimetres to decimetres, although context differences prevent direct comparison. Accuracy in these models is influenced by methodological factors including equipment specification (Clapuyt et al., 2016), observation distance (James and Robson, 2012), ground control point configuration and quality (Sanz-Ablanedo et al., 2018) and processing decisions (James et al., 2017a). Capturing underwater ecosystem structure using structure-from-motion photogrammetry comes with additional sources of error including varying optical and ambient light conditions, refraction at the air-glass-water interface of camera lenses, and a lack of high-precision ground control points (Bayley et al., 2019; Bryson et al., 2017).

Understanding direct and indirect effects of 3D ecosystem structure on organisms is central to understanding organism-environment interactions (Davies and Asner, 2014). One area of research that will benefit from tools that can rapidly and accurately record 3D morphology is in the study of habitat complexity and its influence on communities. There is a long history of researchers attempting to determine the causes driving the common observation that organismal diversity and abundance are enhanced in more complex habitats, but system and scale-independent mechanisms have proved elusive (Kovalenko et al., 2012). The difficulties partly stem from challenges in defining habitat complexity consistently as a measurable metric and measuring it at appropriate scales. Habitat complexity has been defined in many ways in the literature (Kovalenko et al., 2012; Lazarus and Belmaker, 2021). One metric that has become attractive for system-independent analysis is fractal dimension (D). Fractal dimension can be measured using diverse methods to suit a system, incorporates information across scales into a single value, and can be measured for 1, 2 and 3D features (Halley et al 2004). Several studies have calculated fractal dimension of 2D transects or cross-sections to quantify surface complexity of habitats, for example in rocky shores (Kostylev et al., 2005), mussel beds (Commito and Rusignuolo, 2000) and coral reefs (Nash et al., 2013). Before 3D methods were widely available, sampling a 3D surface using 2D transects was appropriate, but variation among replicates could be high and values from the same surface measured using different methods varied (Frost et al., 2005). With the ability to capture a 3D digital snapshot of a site, 2D fractal dimension can be estimated efficiently by digitally sampling

any number of transects, and 3D fractal dimension can be calculated, which cannot be measured in the field (Reichert et al., 2017). Fractal dimension is just one of several metrics that can be derived from 3D models to evaluate complexity. New metrics are being explored and general relationships with biodiversity are emerging (Meager and Schlacher, 2013; Torres-Pulliza et al., 2020). However habitat complexity is defined, digital ecosystem reconstructions with validated accuracy enable interrogation, measurement, and characterisation of a scene in more detail than is possible with field measurements.

Efficient and reliable means for recording structure are particularly valuable for ecology and conservation in reef systems, whether geogenic or biogenic, intertidal or subtidal, temperate or tropical. Structure-from-motion photogrammetry is showing huge potential in subtidal reef ecology, for rapid recording of highly complex scenes within limited dive time and often with limited resources (Bayley and Mogg, 2020; Young et al., 2017). High resolution remote sensing also enables detailed sampling of large extents within low tide windows for sampling intertidal reefs (This thesis chapters 2 and 3, Collin et al., 2018; Hollenbeck et al., 2014).

5.2.2 Scale-dependence in ecological patterns and processes

A recurring theme in ecology and one that has seen growing interest in recent decades is in examining the scales at which processes operate and how scale of observation and analysis shapes our interpretation and conclusions (Chave, 2013; Levin, 1992). Studying scale dependence in ecological phenomena requires comparable measurement of a variable of interest at several scales in time or space, needing versatile, efficient, scalable methods (Schneider, 2001). Historically, study designs had to incorporate trade-offs in observation scale to record the necessary information to test a hypothesis or characterise a phenomenon within a sensible timeframe. With modern and emerging techniques, these trade-offs are eased, enabling higher resolution information to be collected across large extents, both in time and space (Estes et al., 2018). The availability of such data presents opportunities to examine the scale dependence of patterns and interactions in ecosystems. In terrestrial landscape ecology, with the benefit of airborne and satellite remote sensing, studying scale-dependent patterns provides insight into structuring processes (Lausch et al., 2015). Marine systems are more challenging to observe across

scales, but contemporary approaches have revealed scale-dependent patterns here too (Aston et al., 2019; Ford et al., 2020; Pittman and Brown, 2011; Wedding et al., 2011).

The findings of this thesis contribute to a deeper understanding of scale-dependent patterns in reef systems, using modern mapping techniques to overcome traditional sampling constraints. For example, Gruet (1986) observed spatial and temporal changes in *Sabellaria alveolata* reef structure, taking high resolution (mm) vertical measurements. To achieve such measurements within low-tide windows in the intertidal habitat, the extent of the study was limited to two transects of approximately 60 m. Using 3D mapping tools, I demonstrated that measurements of the same resolution can be recorded in the same habitat but across a much larger, spatially continuous extent. Gruet (1986) concluded that the reef structure showed cyclical growth and decay over a decadal cycle, whereas I concluded that cyclical changes occurring in small patches were balanced out across the extent of the habitat, which showed broad-scale stability over 5 years. It may, of course be that both conclusions are correct, and that the reefs studied at different sites and times had differing patterns in their structural dynamics. However, while measurement of further transects in the French reef study may have led to different conclusions, by mapping at high-resolution across large, continuous extents we can have more confidence that we are seeing the whole picture within a site.

Understanding spatial and temporal dynamics in habitat structure is important to understand the resilience of systems to disturbance (Landres et al., 1999; Q. X. Liu et al., 2014; Turner, 2010; Wedding et al., 2019). Disturbance and recovery patterns and processes have been studied in-depth in terrestrial forests, with the use of earth observation datasets that span large spatial and temporal extents. In some forest systems, stability over different time scales can be predicted by from the intensity and lag between disturbance events (Turner et al., 1993), and the landscape patterns that emerge following disturbance subsequently influence properties of future disturbance events (Turner, 1989). We can expect a similar feedback system of landscape pattern and process to exist in biogenic reefs, which may respond to damage in a similar way to vegetation responding to fire (Barry, 1989). The structure of reef systems is changing in response to climate change, as a result of both persistent change in conditions and increasingly frequent and severe disturbance events (Agostini et al., 2021; Alvarez-Filip et al., 2009)

with associated threats to biodiversity and ecosystem services (Rogers et al., 2014). 3D mapping enables recording and analysis of long term and post-event changes in ecosystem structure (Cook, 2017), helping make predictions about future functioning in chronically perturbed ecosystems (Perry and Alvarez-Filip, 2019).

Ecological processes commonly operate and interact across scales, generating scale-dependent patterns in ecosystems. By identifying key scales in patterns, insight can be gained about their generating processes (Legendre and Fortin, 1989). Identification of scale-dependent patterns requires scalable observation and analysis methods, like those demonstrated in this thesis. The results of chapter 4 revealed that multiscale structural metrics provided uncorrelated predictor information for mapping reef habitats. In chapter 2 I used the geostatistical method of variography to identify key scales of variation in reef structure. A range of other analytical methods can be exploited to investigate scale-dependence phenomena when high resolution, spatially continuous data are available (Perry et al., 2002). Correlograms can be used in a similar way to variography to test for statistically significant autocorrelation patterns and clustering in spatially varying ecosystem properties (Ford et al., 2020). Wavelet analysis can be used to identify scale- and location-specific variation in 1D or 2D data (Dale and Mah, 1998; James et al., 2011). Lacunarity analysis can provide information about dominant textural scales in a spatial variable (Plotnick et al., 1993). The combination of several of these analytical procedures provides complementary information to build a detailed understanding of ecological pattern and structuring processes in ecosystems (Saunders et al., 2005). The high quality, cross-scale data produced by modern remote sensing tools are versatile and well-suited to interrogation by multifaceted analysis (Lecours et al., 2015).

5.3 Limitations

Several advances and novel insights emerged from this thesis, but it is important to acknowledge the limitations. Some limitations were inherent to the technologies used and were unavoidable with the equipment available, while others were due to constraints on time, budget person power or environmental conditions. Here I will discuss technical and methodological limitations discovered during my research and how these can be

addressed with future studies. I will also consider limitations of my conclusions and questions that emerged along the way that require further research to address.

5.3.1 Limitations of technologies used

The modern remote sensing tools tested and employed during this research generate visually and technically impressive data products. With the capability to produce high-resolution, photorealistic digital ecosystem reconstructions it is easy to assume that these models are accurate replications of a field site. It is true that analysis of digital models can mimic and even surpass what is possible in field measurements. However, no technology can record a perfect reconstruction of the environment, and it is important to have some understanding of the data collection technology to correctly interpret how the digital model represents, or misrepresents, the environment. The three remote sensing tools used in this thesis: terrestrial laser scanning, structure-from-motion photogrammetry and multibeam echo sounder, all reconstruct the environment using different technology and have their own limitations.

Laser scanning is an active remote sensing technology, emitting laser pulses and analysing their reflections to build up a model of the environment comprising millions of measured points. Terrestrial laser scanning, used in this thesis, involves scanning from several stationary positions using a tripod-mounted instrument, followed by combining data from several scans to construct a more complete model of the scene. Due to the stationary vantage points and radial emission of laser pulses, an important limitation of terrestrial laser scan data is systematic spatial variation in data density. Regions of the scene close to a scanning station have higher point density than those further away. For surfaces perpendicular to the line-of-sight data density decreases linearly, such that if a surface 10 m away is recorded with a point spacing of 1 cm, a surface 100 m away will have a point spacing of 10 cm. The fixed vantage point, typically no more than 2 m above the ground, means that the angle of incidence of a laser pulse becomes more acute with distance from the scanner, so that data penetration into depressions is limited and “shadows” become larger. Data from a single scanning station therefore, has characteristically lower density and less vertical sampling with range (Gruszczyński et al., 2017). By combining data from several scanning stations and subsampling by point spacing, variation in data density across the scene can be reduced, but spatial artefacts will still be evident. Depending on

the questions being asked and the analysis conducted, being aware of systematic variation in sampling density may be important. For example, if the data are used to measure rugosity on a rocky shore as the standard deviation of elevation, rugosity will be artificially lower in regions at a greater distance from any scanning station. This limitation can be accounted for by careful study design, and mitigated during analysis but requires some understanding of the technology and data characteristics (Muir et al., 2017). To demonstrate how this limitation can be mitigated, in my study of temporal dynamics in *Sabellaria alveolata* I used a high density of scanning stations to capture a relatively small area of reef (up to 8 stations in 2500 m²) and limited my analysis of reef structure change to data from the upper reef surfaces, that were visible from the scanner positions. An improvement to the study design would have been to use the same scanning positions for each survey to limit variation in data density among surveys. This would have also enabled analysis of lateral accretion in colonies as the same colony sides would be visible in each survey. Mobile laser scanning platforms, including wearable, vehicle-mounted and drone-mounted devices are now available that can overcome some of these issues by using a moving vantage point, but at the cost of some precision and range (Cabo et al., 2018).

Structure-from-motion photogrammetry is a passive remote sensing technology that relies on reflected light from an external source, typically sunlight in outdoor scenes. The method reconstructs a 3D model from overlapping photographs taken with any digital camera, from any platform, making it a very versatile, but unstandardised technique. The visually impressive outputs can have serious systematic error, artefacts and spatially variable uncertainty that can be hard to constrain and quantify. To confound the problem, software packages used to process the data and generate outputs use closed-source algorithms and provide misleading error quantification metrics (Sanz-Ablanedo et al., 2018). The result is that the accuracy of a model generated using structure-from-motion is hard to determine, making change detection challenging (James et al., 2017b). Structure-from-motion photogrammetry also suffers from systematic variation in data density, but in different ways to terrestrial laser scanning. Typically using a moving vantage point like a drone or diver, data density across a scene is more homogenous than terrestrial laser scanning. However, as data density is related to the pixel size and sharpness of the original images, density is reduced with a greater range from the scene

and varies with light conditions and image quality (Bryson et al., 2017). A key difference between structure-from-motion photogrammetry and terrestrial laser scanning outputs is that the data point positions in the former are estimated using comparative geometry of features in several images, rather than directly measured. This can result in a model with interpolated surfaces that span real-life gaps and smooth complex features, as demonstrated in chapter 2. For example, if using downward-facing images over a coral reef, empty space under overhanging features like table corals and between branches of corals may be filled and be represented as solid blocks, especially when using a broad-scale protocol (Bayley and Mogg, 2020). Again, these data characteristics may or may not be a problem depending on the questions being asked and can be mitigated during study design and analysis. Continuing with the coral reef example, a comparison of complexity of two reef areas using structure-from-motion photogrammetry would need to ensure that images were collected with the same specification camera and lens, in similar light conditions, from the same range and viewing angle, and interpretation of the results would need to acknowledge the potential missing complexity information from underneath and between fine-scale features.

Gathering data from surfaces below water is a challenge for both terrestrial laser scanning and structure-from-motion photogrammetry due to refraction at the air-water interface. Methods to correct for refraction in both terrestrial laser scanning and structure-from-motion photogrammetry models exist but are not routinely applied within processing software (Skarlatos and Agrafiotis, 2018; Smith et al., 2012). No attempt was made to correct data in my studies because below-water surfaces were not of primary interest.

In chapter 4 I used multibeam echo sounder technology to capture the 3D structure of the subtidal seabed. Multibeam echo sounders are acoustic swath remote sensing instruments that emit sound pulses and analyse their reflections to build up a map of the seafloor bathymetry. As with other remote sensing technologies, post processing is required to obtain useful data products from the raw data, including making tidal corrections, manually cleaning the data of spurious points and interpolating the data to a regular grid. Through data collection and processing, care must be taken to minimise error propagation (Calder and Mayer, 2003). For example, adverse sea conditions can produce artefacts that can be difficult to distinguish from real bedforms, and details of

bed morphology can be lost through interpolation and cleaning, impacting further analysis (Erikstad et al., 2013; Lecours et al., 2017a). Multibeam echo sounder is widely used in industry so there are well-developed standardised workflows to achieve accurate bathymetry data. In addition to bathymetry, multibeam echo sounders can collect backscatter information, a measure of the reflectivity of the seabed which can give some insight into the composition and texture of the substrate. Unlike bathymetry, backscatter data generation is not currently standardised so it can be challenging or impossible to compare data from non-overlapping areas or times (Lacharité et al., 2018). Although backscatter can be a powerful explanatory variable in some studies, standardisation and a better understanding of seabed acoustic mechanics is needed before its potential can be fully exploited (Lamarche and Lurton, 2018).

5.3.2 Study limitations and extensions

In chapter 2 I identified barriers to widespread adoption of 3D mapping in field ecology and assessed the accuracy and practicality of two of the most accessible 3D mapping tools available. My assessment of barriers to uptake was based on a review of the literature and discussion with academic and industry colleagues over several years, which may have resulted in a biased opinion. A more thorough way to address this question would be to conduct a well-designed survey of opinions from a cross-section of academic and industry practitioners, from all career stages, and global regions.

In testing the accuracy and practicality of structure-from-motion photogrammetry and terrestrial laser scanning for field ecology, I focussed on three intertidal habitats where fine-scale 3D structure plays an important role in controlling environmental conditions and structuring communities. Since the study was conducted, further advances have been made in 3D mapping technologies. Further work should continue to test new technologies like drone-mounted (Lin et al., 2019) or wearable laser scanning (Cabo et al., 2018) and structure-from-motion photogrammetry using aerial images from drones equipped with real time kinematic global navigation satellite systems (Forlani et al., 2018), in real-world situations against independent reference data, to understand the limitations of their data before using them in ecological studies.

In chapter 3 I studied the spatial and temporal dynamics of *Sabellaria alveolata* reef habitat, concluding that the habitat is dynamic at fine spatial and temporal scales, while being simultaneously stable at larger scales. The methods used in this study required large spring tides coinciding with favourable weather conditions of low wind speed and no precipitation, so survey opportunities were limited and meant only one site could be studied in detail. A primary question that emerges from the study is whether the structural dynamics observed at this site are representative of other sites of the same habitat. *S. alveolata* reef habitat characteristics are highly variable between sites separated by only short distances (Stone et al., 2019) and the environmental controls on the habitat structure and dynamics are poorly understood (Collin et al., 2018; Desroy et al., 2011). My study site was at the northern range edge of the habitat (Firth et al., 2015) so may experience a different balance of pressures to more southerly sites.

A useful outcome of this thesis is that I showed that with a carefully controlled workflow, drone-derived structure from motion photogrammetry data can have equivalent accuracy to terrestrial laser scan data. Collecting drone aerial imagery is faster than terrestrial laser scanning and the equipment is cheaper, so the *S. alveolata* reef study could be efficiently extended to further sites using only drone data. However, drone imagery requires daylight, so daytime spring tides would be required and local restrictions on flying drones may be a constraint (Duffy et al., 2018). By extending this study to further sites, the drivers of structural dynamics in the habitat could be explored. It is not known how the various factors acting on the habitat including air and water temperature, wave and current forces, sediment supply, immersion cycle, nutrient input, water chemistry, human activity, bioerosion and predation interact with the life history of *S. alveolata* to influence the balance of accretion and erosion of the reef colonies (Collin et al., 2018). Sediment supply is likely to be the most important factor controlling the maximum height and accretion rate of reef colonies (Gruet, 1986). This means that changes to the sediment supply and transport regime to an area caused by natural processes and anthropogenic activities like cliff erosion, storms, dredging and coastal construction may change the environmental suitability for the species, and the reef habitat that it can create. To test the influence of sediment supply on reef structural dynamics, an experiment could be conducted to sample coarse sediment in the water column from close to the substrate and at the maximum reef height at several locations in a habitat, and at several sites. Sampling

sediment from the water column is challenging and usually requires bulky equipment or expensive optical laser diffraction instruments, neither of which is appropriate for replication at this scale on wave-exposed shores. I designed a low-cost prototype sediment trap that could be used for this purpose after testing in controlled conditions. The contents of the sediment traps would need to be regularly retrieved and the study would need to continue for at least a year to understand the general conditions at each site. I determined that this study was outside the scope of my thesis.

In chapter 4 I used bathymetry, backscatter and simulated hydrodynamic energy to predict the distribution of ecologically important classes of reef habitat in a high energy marine region. Predictive mapping can be conducted using many frameworks (Brown et al., 2011) and it is important to recognise that there will always be a degree of uncertainty in the maps produced (Foody, 2002; Strong, 2020), especially when mapping natural systems with discrete classes (Fiorentino et al., 2018). Best practice for assessing map accuracy involves an independent reference survey of observations using a statistically robust sampling design, followed by constructing an error matrix of reference and predicted classes and calculating a selection of accuracy metrics (Congalton, 1991; Foody, 2002; Stehman and Czaplewski, 1998). However, due to time and resource constraints, independent datasets for producing, or training, the map and testing the accuracy are rarely collected. Instead, statistical routines like cross-validation used here, are used to estimate accuracy using subsets of the training data (Mitchell et al., 2018). Further, in this study as in many others, it was not feasible to design a fully randomised spatial distribution of sample points to use for ground truth data due to the practical constraints of sampling at sea in a challenging environment. While the Random Forest framework I used is non-parametric and makes no assumptions about input data characteristics, it is sensitive to spatial autocorrelation and a fully randomised sampling design would be more desirable (Millard and Richardson, 2015). There is ongoing debate about the best way to estimate model performance for spatial mapping without a probability sample of reference data (Meyer and Pebesma, 2022, 2021; Ploton et al., 2020; Wadoux et al., 2021). A further key limitation of this study was not having high quality backscatter data for the full extent of the study area, which may have improved the accuracy of the model.

The outcomes of chapter 4 highlighted that hydrodynamic energy is an important predictor for reef habitat distribution. Further work in environmentally similar sites elsewhere would be useful to determine the generality of this conclusion. I found that predicting the spatial distribution of *Sabellaria spinulosa* reef was challenging with the environmental information available. The habitat can be visually identified in the higher resolution data from side scan sonar but these data cannot be automatically analysed as a spatially continuous mosaic (Limpenny et al., 2010). It is expected that as the discriminatory power of multibeam echo sounders improves, increasingly fine-scale features will be detectable. Future work aiming to improve the detection of *S. spinulosa* reef habitat should examine whether higher resolution bathymetry and calibrated backscatter from a more advanced system can detect a characteristic acoustic signature from this ecologically important reef habitat. An important consideration with benthic habitat mapping is temporal dynamics of the substrate composition. As discussed in chapter 2, trade-offs in spatial, temporal and thematic resolution and extent are necessary with any sampling approach. Benthic ecosystems are dynamic over several timescales (Southward et al., 2004), but the high costs of sea going surveys and time required to survey large spatial extents of seabed mean that while the data are high in spatial resolution, temporal resolution of benthic maps is often limited to a single snapshot. For biogenic reefs like *S. spinulosa* reef, the emergent reef features can be transient over various timescales, and the conditions that lead to reef building in some locations and presence of isolated individuals in others are not well understood (Pearce et al., 2014). For these reasons, benthic habitat mapping would be improved with regular repeat surveys to capture the scale of temporal as well as spatial variation in a seascape.

5.4 Future research priorities, opportunities, and challenges

In an age of rapid technological development, advanced data collection tools and sources of detailed ecosystem data are becoming increasingly accessible to ecologists. Emerging technologies can quickly move from being niche tools used only by specialist user groups to being familiar to many. The rise of drones as scientific tools exemplifies this. A decade ago, for many, the term “drone” referred to military aircraft, while prototypes were being developed for scientific imaging (Colomina and Molina, 2014; Koh and Wich, 2012). Just

few years later, drones are now commonplace, consumer-grade technology, in diverse forms for countless applications. They are familiar features in the methods of conference presentations and articles as low-cost remote sensing platforms, even having dedicated journals (Gonzalez-Aguilera and Rodriguez-Gonzalvez, 2017). Since embarking on my research for this thesis, the technologies I have exploited for ecological mapping, including drones, laser scanning, structure-from-motion photogrammetry and multibeam echo sounders have gone through similarly rapid development. Recent years have seen rapid emergence of the technologies as commonplace tools within certain fields in ecology. To highlight this, results from a Web of Science search in June 2021 show that 87% (118 out of 135) of articles about “structure from motion” or “photogrammetry”, and “coral”, were published since 2015. This thesis serves to both test the technologies and demonstrate their applications, showing how 3D mapping can be used to characterise variation in habitat structure in space and time across scales, and highlighting the value of structural metrics in characterising and mapping reef habitats. The ability to collect detailed, accurate, spatially continuous data about ecosystem structure is no longer limiting for ecological studies in many contexts. The major challenges for the discipline now lie in handling, processing, analysing and interpreting the large volumes of data generated to extract information that can advance our understanding of ecosystems to support ecosystem management and conservation. Several studies have demonstrated the potential of emerging technologies for 3D ecosystem mapping, now there is a need to apply them to answer key research questions in full-scale observational and experimental studies.

There is a bottleneck between 3D data collection and usable outputs, at the data analysis stage. Capturing a detailed digital reconstruction of a scene is now relatively easy but quantifying its structural characteristics for various statistical analyses is more challenging. Mapping has traditionally been conducted in 2D and so decades of development of analytical techniques for spatial data have been based on this format. For example, metrics based on a patch-mosaic landscape model can be extracted and analysed with the widely used FRAGSTATS software (McGarigal and Marks, 1995). Where they are collected, 3D ecosystem data are often analysed as 2.5D elevation models, with each 2D position having a single elevation value. This may be appropriate for analysing relatively planar environments across large extents, like a sedimentary seabed, but information is

lost from more complex environments with vertical and overhanging features. Just as metrics have been developed for analysis of 2D models, there is a need to develop 3D structural metrics to quantify and compare 3D landscape and seascape models. Procedures are being developed to quantify structural metrics of 3D objects and analyse differences in complex 3D shapes (Kedron et al., 2019; Reichert et al., 2017).

With increasing collection and use of high-resolution remote sensing data across sectors and access to high powered cloud-based computing, novel analytical approaches are rapidly emerging, especially on open source platforms (Hesselbarth et al., 2021). At present, processing and analysis of 3D data requires high levels of specialist manual input to extract useful information. In the future, with standardised processing pipelines and analyses exploiting machine learning and artificial intelligence, many of the more commonly required tasks may be automated. For example, it is conceivable that a repeat survey of an intertidal reef site could be conducted and analysed with minimal human input. A drone could be deployed, collect imagery and upload it to cloud storage automatically. Generation of 3D models could take place in the cloud following a standard processing workflow. Automated analysis could then be conducted to extract useful information including spatially explicit 3D complexity, segmentation and identification of species and substrate, organism or feature volume distribution, and spectral analysis to assess the health of certain species. Automated workflows are valuable to many users, improving efficiency and standardisation for common tasks (Hopkinson et al., 2020). Indeed, drone survey flight paths are commonly automated to ensure sufficient overlap in images, automated, uncrewed vessel systems are in use for seabed mapping (Zwolak et al., 2020) and data extraction from point clouds can be automated for common tasks (Maas et al., 2008). However, there will always be a demand for bespoke data collection and analysis, particularly in academia, making the current rapid development of accessible open-source solutions encouraging.

With increasingly advanced and automated data collection, huge volumes of data are being collected by countless parties for different uses in academia and industry. Many datasets are collected, analysed, and used for a single purpose before being archived. Often, access to the data, and even knowledge of their existence is restricted to the owners. Collection and storage of large volumes of data has monetary and environmental

cost (Dutta and Hasan, 2013), so efforts should be made to improve the accessibility of datasets for others to use. In an age of big data and cloud-based computing, complex models and analyses benefit from large volumes of data, so access to archived data from multiple sources could help improve our understanding of natural systems without the need for new data collection. As an example of what can be achieved by multisource data collection and access efforts, the Nippon Foundation-GEBCO Seabed 2030 Project aims to produce a map of the entire globe's seabed by 2030, having increased the coverage from 8% in 2017 to 19% in 2020 (Mayer et al., 2018, seabed2030.org). Another ambitious project that will benefit from detailed information about ecosystem structure across scales is the European Space Agency's Digital Twin Earth. This project aims to make improved simulations and predictions and future environmental scenarios using high volumes of earth observation data integrated with high powered computing and artificial intelligence, with one of several precursor projects focussing on a Digital Twin Ocean (esa.int/Applications/Observing_the_Earth/Working_towards_a_Digital_Twin_of_Earth). Collation of data from different sources is not without difficulty, and quality control is essential. For this reason there is an urgent need for standardisation of data collection by emerging technologies like structure-from-motion photogrammetry, or at a minimum, guidelines for recording sufficient metadata to assess the quality of the data.

As big data forms an increasingly important resource in ecology, ecologists will benefit from working collaboratively with specialists from other fields to optimise the information gained from large datasets and to overcome challenges. Working with data scientists can help ecologists interrogate large datasets efficiently and optimise the pipeline from data to information to impact (Li et al., 2020). Working collaboratively with experts from other disciplines can expand the scope of investigation and provide added insight into natural systems (Shiklomanov et al., 2019). In chapter 4 I collaborated with oceanographers to integrate bathymetric and seafloor backscatter information with simulated hydrodynamic information. The hydrodynamic energy data were generated from a custom model run at a relatively high spatial resolution compared to many readily available sources of similar data. The outcomes of this study showed that the hydrodynamic information was a key variable structuring ecological processes and interactions in the study area, providing insight that would have been challenging to examine without this collaboration. Similar collaboration would be valuable to integrate

3D ecosystem information with other information sources to ask important questions. For example, heterogeneity in 3D ecosystem structure creates a variety of habitats that can provide thermal refuges buffered from broad-scale temperature (Milling et al., 2018). By integrating 3D ecosystem structure information with spatially explicit climate change projections, spatial variation in the vulnerability of ecosystems to climate change can be examined, enabling environmental managers to plan distribution of resources and act to protect their local biodiversity (Hooidonk et al., 2016). Finally, a persistent challenge in science is bridging the gap between academia and the public or decision makers, a critical step to maximise the impact of new findings. The modern world of high-volume, fast paced information sharing via social media can be at odds with the quality controlled but lengthy process of academic publishing. Collaboration with science communication professionals can help academics disseminate their work to reach specific target audiences efficiently (Groffman et al., 2010). With visually impressive outputs from 3D mapping tools, research from this field can be particularly engaging, helping to educate the public about current global environmental challenges and convince decision makers to enact positive change. Low cost, versatile 3D mapping tools like structure-from-motion photogrammetry and consumer-grade laser scanners now found in the latest mobile phones create opportunities for widespread engagement through citizen science, empowering the public to take ownership of their local ecosystems and the challenges they face.

6 References

- Agostini, S., Harvey, B.P., Milazzo, M., Wada, S., Kon, K., Floc'h, N., Komatsu, K., Kuroyama, M., Hall-Spencer, J.M., 2021. Simplification, not “tropicalization”, of temperate marine ecosystems under ocean warming and acidification. *Glob. Chang. Biol.* 00, gcb.15749. <https://doi.org/10.1111/GCB.15749>
- Alvarez-Filip, L., Dulvy, N.K., Gill, J.A., Côté, I.M., Watkinson, A.R., 2009. Flattening of Caribbean coral reefs: region-wide declines in architectural complexity. *Proc. R. Soc. B Biol. Sci.* 276, 3019–3025. <https://doi.org/10.1098/rspb.2009.0339>
- Anderson, K., Gaston, K.J., 2013. Lightweight unmanned aerial vehicles will revolutionize spatial ecology. *Front. Ecol. Environ.* 11, 138–146. <https://doi.org/10.1890/120150>
- Anderson, M.J., 2001. A new method for non-parametric multivariate analysis of variance. *Austral Ecol.* 26, 32–46. <https://doi.org/10.1111/j.1442-9993.2001.01070.pp.x>
- Ashcroft, M.B., Gollan, J.R., Ramp, D., 2013. Creating vegetation density profiles for a diverse range of ecological habitats using terrestrial laser scanning. *Methods Ecol. Evol.* 5, 263–272. <https://doi.org/10.1111/j.2041-210X.2013.12157.x>
- Asner, G.P., Martin, R.E., Mascaro, J., 2017. Coral reef atoll assessment in the South China Sea using Planet Dove satellites. *Remote Sens. Ecol. Conserv.* 3, 57–65. <https://doi.org/10.1002/rse2.42>
- Aston, E.A., Williams, G.J., Green, J.A.M., Davies, A.J., Wedding, L.M., Gove, J.M., Jouffray, J.-B., Jones, T.T., Clark, J., 2019. Scale-dependent spatial patterns in benthic communities around a tropical island seascape. *Ecography* 42, 578–590. <https://doi.org/10.1111/ecog.04097>
- Ayata, S.-D., Ellien, C., Dumas, F., Dubois, S., Thiébaud, É., 2009. Modelling larval dispersal and settlement of the reef-building polychaete *Sabellaria alveolata*: Role of hydroclimatic processes on the sustainability of biogenic reefs. *Cont. Shelf Res.* 29, 1605–1623. <https://doi.org/10.1016/j.csr.2009.05.002>

- Azmy, S.N., Sah, S.A.M., Shafie, N.J., Ariffin, A., Majid, Z., Ismail, M.N.A., Shamsir, M.S., 2012. Counting in the dark: Non-intrusive laser scanning for population counting and identifying roosting bats. *Sci. Rep.* 2, 524. <https://doi.org/10.1038/srep00524>
- Bajjouk, T., Jauzein, C., Drumetz, L., Dalla Mura, M., Duval, A., Dubois, S.F., 2020. Hyperspectral and Lidar: Complementary Tools to Identify Benthic Features and Assess the Ecological Status of *Sabellaria alveolata* Reefs. *Front. Mar. Sci.* 7, 804. <https://doi.org/10.3389/fmars.2020.575218>
- Baltensweiler, A., Walthert, L., Ginzler, C., Sutter, F., Purves, R.S., Hanewinkel, M., 2017. Terrestrial laser scanning improves digital elevation models and topsoil pH modelling in regions with complex topography and dense vegetation. *Environ. Model. Softw.* 95, 13–21. <https://doi.org/10.1016/j.envsoft.2017.05.009>
- Barry, J., 1989. Reproductive response of a marine annelid to winter storms: an analog to fire adaptation in plants? *Mar. Ecol. Prog. Ser.* 54, 99–107. <https://doi.org/10.3354/meps054099>
- Bayley, D.T.I., Mogg, A.O.M., 2020. A protocol for the large-scale analysis of reefs using Structure from Motion photogrammetry. *Methods Ecol. Evol.* 11, 1410–1420. <https://doi.org/10.1111/2041-210X.13476>
- Bayley, D.T.I., Mogg, A.O.M., Koldewey, H., Purvis, A., 2019. Capturing complexity: Field-testing the use of “structure from motion” derived virtual models to replicate standard measures of reef physical structure. *PeerJ* 7, e6540. <https://doi.org/10.7717/peerj.6540>
- Beck, M.W., 2000. Separating the elements of habitat structure: Independent effects of habitat complexity and structural components on rocky intertidal gastropods. *J. Exp. Mar. Bio. Ecol.* 249, 29–49. [https://doi.org/10.1016/S0022-0981\(00\)00171-4](https://doi.org/10.1016/S0022-0981(00)00171-4)
- Bennett, N.D., Croke, B.F.W., Guariso, G., Guillaume, J.H.A., Hamilton, S.H., Jakeman, A.J., Marsili-Libelli, S., Newham, L.T.H., Norton, J.P., Perrin, C., Pierce, S.A., Robson, B., Seppelt, R., Voinov, A.A., Fath, B.D., Andreassian, V., 2013. Characterising performance of environmental models. *Environ. Model. Softw.* 40, 1–20. <https://doi.org/10.1016/j.envsoft.2012.09.011>
- Bennett, S., Wernberg, T., Connell, S.D., Hobday, A.J., Johnson, C.R., Poloczanska, E.S.,

2016. The “Great Southern Reef”: social, ecological and economic value of Australia’s neglected kelp forests. *Mar. Freshw. Res.* 67, 47.
<https://doi.org/10.1071/MF15232>
- Borsje, B.W., van Wesenbeeck, B.K., Dekker, F., Paalvast, P., Bouma, T.J., van Katwijk, M.M., de Vries, M.B., 2011. How ecological engineering can serve in coastal protection. *Ecol. Eng.* 37, 113–122.
<https://doi.org/10.1016/J.ECOLENG.2010.11.027>
- Bouma, T.J., van Belzen, J., Balke, T., Zhu, Z., Airolidi, L., Blight, A.J., Davies, A.J., Galvan, C., Hawkins, S.J., Hoggart, S.P.G., Lara, J.L., Losada, I.J., Maza, M., Ondiviela, B., Skov, M.W., Strain, E.M., Thompson, R.C., Yang, S., Zanuttigh, B., Zhang, L., Herman, P.M.J., 2014. Identifying knowledge gaps hampering application of intertidal habitats in coastal protection: Opportunities & steps to take. *Coast. Eng.* 87, 147–157.
<https://doi.org/10.1016/j.coastaleng.2013.11.014>
- Breiman, L., 2001. Random forests. *Mach. Learn.* 45, 5–32.
<https://doi.org/10.1023/A:1010933404324>
- Brodersen, K.H., Ong, C.S., Stephan, K.E., Buhmann, J.M., 2010. The balanced accuracy and its posterior distribution, in: *Proceedings - International Conference on Pattern Recognition*. pp. 3121–3124. <https://doi.org/10.1109/ICPR.2010.764>
- Brown, C.J., Smith, S.J., Lawton, P., Anderson, J.T., 2011. Benthic habitat mapping: A review of progress towards improved understanding of the spatial ecology of the seafloor using acoustic techniques. *Estuar. Coast. Shelf Sci.* 92, 502–520.
<https://doi.org/10.1016/j.ecss.2011.02.007>
- Bruschetti, M., 2019. Role of Reef-Building, Ecosystem Engineering Polychaetes in Shallow Water Ecosystems. *Diversity* 11, 168. <https://doi.org/10.3390/d11090168>
- Bryson, M., Ferrari, R., Figueira, W., Pizarro, O., Madin, J., Williams, S., Byrne, M., 2017. Characterization of measurement errors using structure-from-motion and photogrammetry to measure marine habitat structural complexity. *Ecol. Evol.* 7, 5669–5681. <https://doi.org/10.1002/ece3.3127>
- Buckley, S.J., Howell, J.A., Enge, H.D.D., Kurz, T.H.H., 2008. Terrestrial laser scanning in geology: data acquisition, processing and accuracy considerations. *J. Geol. Soc.*

London. 165, 625–638. <https://doi.org/10.1144/0016-76492007-100>

Bué, M., Smale, D.A., Natanni, G., Marshall, H., Moore, P.J., 2020. Multiple-scale interactions structure macroinvertebrate assemblages associated with kelp understory algae. *Divers. Distrib.* 26, 1551–1565. <https://doi.org/10.1111/ddi.13140>

Bush, L., Balestrini, S., Robins, P., Davies, A., 2015. NRW Evidence Report No 049 - The reproduction and connectivity of *Sabellaria alveolata* reefs in Wales – MAR4REF Bangor University.

Cabo, C., Del Pozo, S., Rodríguez-Gonzálvez, P., Ordóñez, C., González-Aguilera, D., Cabo, C., Del Pozo, S., Rodríguez-Gonzálvez, P., Ordóñez, C., González-Aguilera, D., 2018. Comparing Terrestrial Laser Scanning (TLS) and Wearable Laser Scanning (WLS) for Individual Tree Modeling at Plot Level. *Remote Sens.* 10, 540. <https://doi.org/10.3390/rs10040540>

Calder, B.R., Mayer, L.A., 2003. Automatic processing of high-rate, high-density multibeam echosounder data. *Geochemistry, Geophys. Geosystems* 4, 1048. <https://doi.org/10.1029/2002GC000486>

Calders, K., Newnham, G., Burt, A., Murphy, S., Raunonen, P., Herold, M., Culvenor, D., Avitabile, V., Disney, M., Armston, J., Kaasalainen, M., 2015. Nondestructive estimates of above-ground biomass using terrestrial laser scanning. *Methods Ecol. Evol.* 6, 198–208. <https://doi.org/10.1111/2041-210X.12301>

Calders, K., Phinn, S., Ferrari, R., Leon, J., Armston, J., Asner, G.P., Disney, M., 2020. 3D Imaging Insights into Forests and Coral Reefs. *Trends Ecol. Evol.* 35, 6–9. <https://doi.org/10.1016/j.tree.2019.10.004>

Capa, M., Hutchings, P., Peart, R., 2012. Systematic revision of Sabellariidae (Polychaeta) and their relationships with other polychaetes using morphological and DNA sequence data. *Zool. J. Linn. Soc.* 164, 245–284. <https://doi.org/10.1111/j.1096-3642.2011.00767.x>

Carrington Bell, E., Denny, M.W., 1994. Quantifying wave exposure - a simple device for recording maximum velocity and results of its use at several field sites. *J. Exp. Mar. Biol. Ecol.*

- Caryl, F.M., Hahs, A.K., Lumsden, L.F., Van der Ree, R., Wilson, C., Wintle, B.A., 2014. Continuous predictors of species distributions support categorically stronger inference than ordinal and nominal classes: An example with urban bats. *Landscape Ecol.* 29, 1237–1248. <https://doi.org/10.1007/s10980-014-0062-7>
- Chambers, J.Q., Asner, G.P., Morton, D.C., Anderson, L.O., Saatchi, S.S., Espírito-Santo, F.D.B., Palace, M., Souza, C., 2007. Regional ecosystem structure and function: ecological insights from remote sensing of tropical forests. *Trends Ecol. Evol.* 22, 414–423. <https://doi.org/10.1016/j.tree.2007.05.001>
- Chambers, J.Q., Negron-Juarez, R.I., Marra, D.M., Di Vittorio, A., Tews, J., Roberts, D., Ribeiro, G.H.P.M., Trumbore, S.E., Higuchi, N., 2013. The steady-state mosaic of disturbance and succession across an old-growth Central Amazon forest landscape. *Proc. Natl. Acad. Sci. U. S. A.* 110, 3949–54. <https://doi.org/10.1073/pnas.1202894110>
- Chappell, J., 1980. Coral morphology, diversity and reef growth. *Nature* 286, 249–252. <https://doi.org/10.1038/286249a0>
- Chappuis, E., Terradas, M., Cefalì, M.E., Mariani, S., Ballesteros, E., 2014. Vertical zonation is the main distribution pattern of littoral assemblages on rocky shores at a regional scale. *Estuar. Coast. Shelf Sci.* 147, 113–122. <https://doi.org/10.1016/j.ecss.2014.05.031>
- Chave, J., 2013. The problem of pattern and scale in ecology: what have we learned in 20 years? *Ecol. Lett.* 16, 4–16. <https://doi.org/10.1111/ele.12048>
- Chawla, N. V., Bowyer, K.W., Hall, L.O., Kegelmeyer, W.P., 2002. SMOTE: Synthetic Minority Over-sampling Technique. *J. Artif. Intell. Res.* 16, 321–357. <https://doi.org/10.1613/JAIR.953>
- Chen, T., He, T., Benesty, M., 2018. XGBoost : eXtreme Gradient Boosting. R Packag. version 0.71-2.
- Chiba, S., Noda, T., 2000. Factors maintaining topography-related mosaic of barnacle and mussel on a rocky shore. *J. Mar. Biol. Assoc. United Kingdom* 80, 617–622. <https://doi.org/10.1017/S0025315400002435>

- Clapuyt, F., Vanacker, V., Oost, K. Van, 2016. Reproducibility of UAV-based earth topography reconstructions based on Structure-from-Motion algorithms. *Geomorphology* 260, 4–15. <https://doi.org/10.1016/j.geomorph.2015.05.011>
- CloudCompare, 2019. CloudCompare (version 2.11) [GPL software] retrieved from <http://www.cloudcompare.org/>.
- Cogan, C.B., Todd, B.J., Lawton, P., Noji, T.T., 2009. The role of marine habitat mapping in ecosystem-based management. *ICES J. Mar. Sci.* 66, 2033–2042. <https://doi.org/10.1093/icesjms/fsp214>
- Coggan, R., Barrio Froján, C.R.S., Diesing, M., Aldridge, J., 2012. Spatial patterns in gravel habitats and communities in the central and eastern English Channel. *Estuar. Coast. Shelf Sci.* 111, 118–128. <https://doi.org/10.1016/j.ecss.2012.06.017>
- Cohen, J., 1960. A Coefficient of Agreement for Nominal Scales. *Educ. Psychol. Meas.* 20, 37–46. <https://doi.org/10.1177/001316446002000104>
- Cohen, W.B., Goward, S.N., 2004. Landsat's role in ecological applications of remote sensing. *Bioscience* 54, 535–545. [https://doi.org/10.1641/0006-3568\(2004\)054\[0535:LRIEAO\]2.0.CO;2](https://doi.org/10.1641/0006-3568(2004)054[0535:LRIEAO]2.0.CO;2)
- Collin, A., Dubois, S., James, D., Houet, T., 2019. Improving Intertidal Reef Mapping Using UAV Surface, Red Edge, and Near-Infrared Data. *Drones* 3, 67. <https://doi.org/10.3390/drones3030067>
- Collin, A., Dubois, S., Ramambason, C., Etienne, S., 2018. Very high-resolution mapping of emerging biogenic reefs using airborne optical imagery and neural network: the honeycomb worm (*Sabellaria alveolata*) case study. *Int. J. Remote Sens.* 39, 5660–5675. <https://doi.org/10.1080/01431161.2018.1484964>
- Colomina, I., Molina, P., 2014. Unmanned aerial systems for photogrammetry and remote sensing: A review. *ISPRS J. Photogramm. Remote Sens.* 92, 79–97. <https://doi.org/10.1016/j.isprsjprs.2014.02.013>
- Comito, J.A., Rusignuolo, B., 2000. Structural complexity in mussel beds: the fractal geometry of surface topography. *J. Exp. Mar. Bio. Ecol.* 255, 133–152.
- Congalton, R.G., 1991. A review of assessing the accuracy of classifications of remotely

- sensed data. *Remote Sens. Environ.* 37, 35–46. [https://doi.org/10.1016/0034-4257\(91\)90048-B](https://doi.org/10.1016/0034-4257(91)90048-B)
- Connell, J.H., 1978. Diversity in Tropical Rain Forests and Coral Reefs. *Science* 199, 1302–1310.
- Connell, J.H., 1972. Community Interactions on Marine Rocky Intertidal Shores. *Annu. Rev. Ecol. Syst.* 3, 169–192. <https://doi.org/10.1146/annurev.es.03.110172.001125>
- Connell, J.H., Sousa, W.P., 2015. On the Evidence Needed to Judge Ecological Stability or Persistence. <https://doi.org/10.1086/284105> 121, 789–824.
<https://doi.org/10.1086/284105>
- Cook, K.L., 2017. An evaluation of the effectiveness of low-cost UAVs and structure from motion for geomorphic change detection. *Geomorphology* 278, 195–208.
<https://doi.org/10.1016/J.GEOMORPH.2016.11.009>
- Cooper, S., Roy, D., Schaaf, C., Paynter, I., 2017. Examination of the Potential of Terrestrial Laser Scanning and Structure-from-Motion Photogrammetry for Rapid Nondestructive Field Measurement of Grass Biomass. *Remote Sens.* 9, 531.
<https://doi.org/10.3390/rs9060531>
- Cowen, R.K., Sponaugle, S., 2009. Larval Dispersal and Marine Population Connectivity. *Ann. Rev. Mar. Sci.* 1, 443–466.
<https://doi.org/10.1146/annurev.marine.010908.163757>
- Crisp, D.J., 1964. The Effects of the Severe Winter of 1962-63 on Marine Life in Britain. *J. Anim. Ecol.* 33, 165. <https://doi.org/10.2307/2355>
- Cunliffe, A.M., Brazier, R.E., Anderson, K., 2016. Ultra-fine grain landscape-scale quantification of dryland vegetation structure with drone-acquired structure-from-motion photogrammetry. *Remote Sens. Environ.* 183, 129–143.
<https://doi.org/10.1016/j.rse.2016.05.019>
- Curd, A., Pernet, F., Corporeau, C., Delisle, L., Firth, L.B., Nunes, F.L.D., Dubois, S.F., 2019. Connecting organic to mineral: How the physiological state of an ecosystem-engineer is linked to its habitat structure. *Ecol. Indic.* 98, 49–60.
<https://doi.org/10.1016/J.ECOLIND.2018.10.044>

- Cutler, D.R., Edwards, T.C., Beard, K.H., Cutler, A., Hess, K.T., Gibson, J., Lawler, J.J., 2007. Random forests for classification in ecology. *Ecology* 88, 2783–2792. <https://doi.org/10.1890/07-0539.1>
- D'Urban Jackson, T., Williams, G.J., Walker-Springett, G., Davies, A.J., 2020. Three-dimensional digital mapping of ecosystems: A new era in spatial ecology. *Proc. R. Soc. B Biol. Sci.* 287, 1–10. <https://doi.org/10.1098/rspb.2019.2383>
- Dale, M.R.T., Mah, M., 1998. The use of wavelets for spatial pattern analysis in ecology. *J. Veg. Sci.* 9, 805–814. <https://doi.org/10.2307/3237046>
- Dalkin, M., 2008. Mid Irish Sea reefs habitat mapping report. Eur. Environ. Agency 306.
- Dannheim, J., Bergström, L., Birchenough, S.N.R., Brzana, R., Boon, A.R., Coolen, J.W.P., Dauvin, J.C., De Mesel, I., Derweduwen, J., Gill, A.B., Hutchison, Z.L., Jackson, A.C., Janas, U., Martin, G., Raoux, A., Reubens, J., Rostin, L., Vanaverbeke, J., Wilding, T.A., Wilhelmsson, D., Degraer, S., 2020. Benthic effects of offshore renewables: Identification of knowledge gaps and urgently needed research. *ICES J. Mar. Sci.* 77, 1092–1108. <https://doi.org/10.1093/icesjms/fsz018>
- Danson, F.M., Disney, M.I., Gaulton, R., Schaaf, C., Strahler, A., 2018. The terrestrial laser scanning revolution in forest ecology. *Interface Focus* 8, 20180001. <https://doi.org/10.1098/rsfs.2018.0001>
- Dassot, M., Constant, T., Fournier, M., 2011. The use of terrestrial LiDAR technology in forest science: Application fields, benefits and challenges. *Ann. For. Sci.* 68, 959–974. <https://doi.org/10.1007/s13595-011-0102-2>
- Davies, A.B., Asner, G.P., 2014. Advances in animal ecology from 3D-LiDAR ecosystem mapping. *Trends Ecol. Evol.* <https://doi.org/10.1016/j.tree.2014.10.005>
- Davies, A.J., Guinotte, J.M., 2011. Global Habitat Suitability for Framework-Forming Cold-Water Corals. *PLoS One* 6, e18483. <https://doi.org/10.1371/journal.pone.0018483>
- Davies, A.J., Last, K.S., Attard, K., Hendrick, V.J., 2009. Maintaining turbidity and current flow in laboratory aquarium studies, a case study using *Sabellaria spinulosa*. *J. Exp. Mar. Bio. Ecol.* 370, 35–40. <https://doi.org/10.1016/j.jembe.2008.11.015>
- Denny, M.W., Helmuth, B., Leonard, G.H., Harley, C.D.G., Hunt, L.J.H., Nelson, E.K., 2004.

- Quantifying scale in ecology: Lessons from a wave-swept shore. *Ecol. Monogr.* 74, 513–532. <https://doi.org/10.1890/03-4043>
- Desroy, N., Dubois, S.F., Fournier, J., Ricquiers, L., Le Mao, P., Guerin, L., Gerla, D., Rougerie, M., Legendre, A., 2011. The conservation status of *Sabellaria alveolata* (L.) (Polychaeta: Sabellariidae) reefs in the bay of mont-saint-michel. *Aquat. Conserv. Mar. Freshw. Ecosyst.* 21, 462–471. <https://doi.org/10.1002/aqc.1206>
- Diesing, M., Coggan, R., Vanstaen, K., 2009. Widespread rocky reef occurrence in the central English Channel and the implications for predictive habitat mapping. *Estuar. Coast. Shelf Sci.* 83, 647–658. <https://doi.org/10.1016/j.ecss.2009.05.018>
- Diesing, M., Green, S.L., Stephens, D., Lark, R.M., Stewart, H.A., Dove, D., 2014. Mapping seabed sediments: Comparison of manual, geostatistical, object-based image analysis and machine learning approaches. *Cont. Shelf Res.* 84, 107–119. <https://doi.org/10.1016/j.csr.2014.05.004>
- Dormann, C.F., Elith, J., Bacher, S., Buchmann, C., Carl, G., Carré, G., Marquéz, J.R.G., Gruber, B., Lafourcade, B., Leitão, P.J., Münkemüller, T., McClean, C., Osborne, P.E., Reineking, B., Schröder, B., Skidmore, A.K., Zurell, D., Lautenbach, S., 2013. Collinearity: a review of methods to deal with it and a simulation study evaluating their performance. *Ecography* 36, 27–46. <https://doi.org/10.1111/j.1600-0587.2012.07348.x>
- Dubois, S., Comtet, T., Retière, C., Thiébaud, É., 2007. Distribution and retention of *Sabellaria alveolata* larvae (Polychaeta: Sabellariidae) in the Bay of Mont-Saint-Michel, France. *Mar. Ecol. Prog. Ser.* 346, 243–254. <https://doi.org/10.3354/meps07011>
- Dubois, S., Retiere, C., Olivier, F., 2002. Biodiversity associated with *Sabellaria alveolata* (Polychaeta: Sabellariidae) reefs: effects of human disturbances. *J. Mar. Biol. Assoc. UK* 82, 817–826. <https://doi.org/10.1017/S0025315402006185>
- Duffy, J.P., Cunliffe, A.M., DeBell, L., Sandbrook, C., Wich, S.A., Shutler, J.D., Myers-Smith, I.H., Varela, M.R., Anderson, K., 2018. Location, location, location: considerations when using lightweight drones in challenging environments. *Remote Sens. Ecol. Conserv.* 4, 7–19. <https://doi.org/10.1002/rse2.58>

- Dustan, P., Doherty, O., Pardede, S., 2013. Digital Reef Rugosity Estimates Coral Reef Habitat Complexity. *PLoS One* 8, e57386.
<https://doi.org/10.1371/journal.pone.0057386>
- Dutta, A.K., Hasan, R., 2013. How much does storage really cost? Towards a full cost accounting model for data storage, in: *Lecture Notes in Computer Science (Including Subseries Lecture Notes in Artificial Intelligence and Lecture Notes in Bioinformatics)*. Springer, Cham, pp. 29–43. https://doi.org/10.1007/978-3-319-02414-1_3
- Eckman, J.E., Duggins, D.O., 1993. Effects of Flow Speed on Growth of Benthic Suspension Feeders. *Biol. Bull.* 185, 28–41. <https://doi.org/10.2307/1542128>
- Edwards, C.B., Eynaud, Y., Williams, G.J., Pedersen, N.E., Zgliczynski, B.J., Gleason, A.C.R., Smith, J.E., Sandin, S.A., 2017. Large-area imaging reveals biologically driven non-random spatial patterns of corals at a remote reef. *Coral Reefs* 36, 1291–1305.
<https://doi.org/10.1007/s00338-017-1624-3>
- Eggleton, J., Meadows, W., 2013. Offshore monitoring of Annex I reef habitat present within the Isles of Scilly Special Area of Conservation (SAC). Natural England Commissioned Report NECR125.
- Eitel, J.U.H., Höfle, B., Vierling, L.A., Abellán, A., Asner, G.P., Deems, J.S., Glennie, C.L., Joerg, P.C., LeWinter, A.L., Magney, T.S., Mandlbürger, G., Morton, D.C., Müller, J., Vierling, K.T., 2016. Beyond 3-D: The new spectrum of lidar applications for earth and ecological sciences. *Remote Sens. Environ.* 186, 372–392.
<https://doi.org/10.1016/j.rse.2016.08.018>
- Eitel, J.U.H., Vierling, L.A., Magney, T.S., 2013. A lightweight, low cost autonomously operating terrestrial laser scanner for quantifying and monitoring ecosystem structural dynamics. *Agric. For. Meteorol.* 180, 86–96.
<https://doi.org/10.1016/J.AGRFORMET.2013.05.012>
- Elsherif, A., Gaulton, R., Mills, J., 2018. Estimation of vegetation water content at leaf and canopy level using dual-wavelength commercial terrestrial laser scanners. *Interface Focus* 8, 20170041. <https://doi.org/10.1098/rsfs.2017.0041>
- Eltner, A., Kaiser, A., Castillo, C., Rock, G., Neugirg, F., Abellán, A., 2016. Image-based

- surface reconstruction in geomorphometry-merits, limits and developments. *Earth Surf. Dyn.* 4, 359–389. <https://doi.org/10.5194/esurf-4-359-2016>
- Erikstad, L., Bakkestuen, V., Bekkby, T., Halvorsen, R., 2013. Impact of Scale and Quality of Digital Terrain Models on Predictability of Seabed Terrain Types. *Mar. Geod.* 36, 2–21. <https://doi.org/10.1080/01490419.2012.747454>
- Estes, L., Elsen, P.R., Treuer, T., Ahmed, L., Caylor, K., Chang, J., Choi, J.J., Ellis, E.C., 2018. The spatial and temporal domains of modern ecology. *Nat. Ecol. Evol.* 2, 819–826. <https://doi.org/10.1038/s41559-018-0524-4>
- European Commission, 2013. Interpretation Manual of European Union Habitats. [https://doi.org/10.1016/S0021-9290\(99\)00083-4](https://doi.org/10.1016/S0021-9290(99)00083-4)
- Farr, T.G., Rosen, P.A., Caro, E., Crippen, R., Duren, R., Hensley, S., Kobrick, M., Paller, M., Rodriguez, E., Roth, L., Seal, D., Shaffer, S., Shimada, J., Umland, J., Werner, M., Oskin, M., Burbank, D., Alsdorf, D., 2007. The Shuttle Radar Topography Mission. *Rev. Geophys.* 45, RG2004. <https://doi.org/10.1029/2005RG000183>
- Feliciano, E.A., Wdowinski, S., Potts, M.D., 2014. Assessing Mangrove Above-Ground Biomass and Structure using Terrestrial Laser Scanning: A Case Study in the Everglades National Park. *Wetlands* 34, 955–968. <https://doi.org/10.1007/s13157-014-0558-6>
- Fiorentino, D., Lecours, V., Brey, T., 2018. On the Art of Classification in Spatial Ecology: Fuzziness as an Alternative for Mapping Uncertainty. *Front. Ecol. Evol.* 6, 231. <https://doi.org/10.3389/fevo.2018.00231>
- Firth, L.B., Mieszkowska, N., Grant, L.M., Bush, L.E., Davies, A.J., Frost, M.T., Moschella, P.S., Burrows, M.T., Cunningham, P.N., Dye, S.R., Hawkins, S.J., 2015. Historical comparisons reveal multiple drivers of decadal change of an ecosystem engineer at the range edge. *Ecol. Evol.* 5, 3210–3222. <https://doi.org/10.1002/ece3.1556>
- Foody, G.M., 2020. Explaining the unsuitability of the kappa coefficient in the assessment and comparison of the accuracy of thematic maps obtained by image classification. *Remote Sens. Environ.* 239, 111630. <https://doi.org/10.1016/j.rse.2019.111630>
- Foody, G.M., 2002. Status of land cover classification accuracy assessment. *Remote Sens.*

- Environ. 80, 185–201. [https://doi.org/10.1016/S0034-4257\(01\)00295-4](https://doi.org/10.1016/S0034-4257(01)00295-4)
- Ford, H. V., Gove, J.M., Davies, A.J., Graham, N.A.J., Healey, J.R., Conklin, E.J., Williams, G.J., 2020. Spatial scaling properties of coral reef benthic communities. *Ecography* *ecog.05331*. <https://doi.org/10.1111/ecog.05331>
- Forlani, G., Dall'Asta, E., Diotri, F., Cella, U.M. di, Roncella, R., Santise, M., Forlani, G., Dall'Asta, E., Diotri, F., Cella, U.M. di, Roncella, R., Santise, M., 2018. Quality Assessment of DSMs Produced from UAV Flights Georeferenced with On-Board RTK Positioning. *Remote Sens.* 10, 311. <https://doi.org/10.3390/rs10020311>
- Fréchette, M., Butman, C.A., Geyer, W.R., 1989. The importance of boundary-layer flows in supplying phytoplankton to the benthic suspension feeder, *Mytilus edulis* L. *Limnol. Oceanogr.* 34, 19–36. <https://doi.org/10.4319/lo.1989.34.1.0019>
- Frost, N.J., Burrows, M.T., Johnson, M.P., Hanley, M.E., Hawkins, S.J., 2005. Measuring surface complexity in ecological studies. *Limnol. Oceanogr. Methods* 3, 203–210. <https://doi.org/10.4319/lom.2005.3.203>
- Godet, L., Fournier, J., Jaffré, M., Desroy, N., 2011. Influence of stability and fragmentation of a worm-reef on benthic macrofauna. *Estuar. Coast. Shelf Sci.* 92, 472–479. <https://doi.org/10.1016/j.ecss.2011.02.003>
- Gonzalez-Aguilera, D., Rodriguez-Gonzalvez, P., 2017. Drones—an open access journal. *Drones* 1, 1–5. <https://doi.org/10.3390/drones1010001>
- Gove, J.M., Williams, G.J., McManus, M.A., Clark, S.J., Ehses, J.S., Wedding, L.M., 2015. Coral reef benthic regimes exhibit non-linear threshold responses to natural physical drivers. *Mar. Ecol. Prog. Ser.* 522, 33–48. <https://doi.org/10.3354/MEPS11118>
- Graham, N.A.J., Jennings, S., MacNeil, M.A., Mouillot, D., Wilson, S.K., 2015. Predicting climate-driven regime shifts versus rebound potential in coral reefs. *Nature* 518, 94–97. <https://doi.org/10.1038/nature14140>
- Graham, N.A.J., Nash, K.L., 2013. The importance of structural complexity in coral reef ecosystems. *Coral Reefs* 32, 315–326. <https://doi.org/10.1007/s00338-012-0984-y>
- Graler, B., Pebesma, E., Heuvelink, G., 2016. Spatio-Temporal Interpolation using gstat [WWW Document]. URL <https://cran.r->

project.org/web/packages/gstat/vignettes/spatio-temporal-kriging.pdf

- Gratwicke, B., Speight, M.R., 2005. The relationship between fish species richness, abundance and habitat complexity in a range of shallow tropical marine habitats. *J. Fish Biol.* 66, 650–667. <https://doi.org/10.1111/j.0022-1112.2005.00629.x>
- Gringarten, E., Deutsch, C. V., 2001. Teacher's aide: Variogram interpretation and modeling. *Math. Geol.* 33, 507–534. <https://doi.org/10.1023/A:1011093014141>
- Groffman, P.M., Stylinski, C., Nisbet, M.C., Duarte, C.M., Jordan, R., Burgin, A., Previtali, M.A., Coloso, J., 2010. Restarting the conversation: challenges at the interface between ecology and society. *Front. Ecol. Environ.* 8, 284–291. <https://doi.org/10.1890/090160>
- Gruet, Y., 1986. Spatio-temporal Changes of Sabellarian Reefs Built by the Sedentary Polychaete *Sabellaria alveolata* (Linné). *Mar. Ecol.* 7, 303–319. <https://doi.org/10.1111/j.1439-0485.1986.tb00166.x>
- Gruszczyński, W., Matwijn, W., Ćwiąkała, P., 2017. Comparison of low-altitude UAV photogrammetry with terrestrial laser scanning as data-source methods for terrain covered in low vegetation. *ISPRS J. Photogramm. Remote Sens.* 126, 168–179. <https://doi.org/10.1016/j.isprsjprs.2017.02.015>
- Guan, H., Yu, Y., Ji, Z., Li, J., Zhang, Q., 2015. Deep learning-based tree classification using mobile LiDAR data. *Remote Sens. Lett.* 6, 864–873. <https://doi.org/10.1080/2150704X.2015.1088668>
- Guichard, F., Bourget, E., 1998. Topographic heterogeneity, hydrodynamics, and benthic community structure: A scale-dependent cascade. *Mar. Ecol. Prog. Ser.* 171, 59–70. <https://doi.org/10.3354/meps171059>
- Guichard, F., Halpin, P.M., Allison, G.W., Lubchenco, J., Menge, B.A., 2003. Mussel Disturbance Dynamics: Signatures of Oceanographic Forcing from Local Interactions. *Am. Nat.* 161, 889–904. <https://doi.org/10.1086/375300>
- Gutiérrez, D., Enríquez, E., Purca, S., Quipúzcoa, L., Marquina, R., Flores, G., Graco, M., 2008. Oxygenation episodes on the continental shelf of central Peru: Remote forcing and benthic ecosystem response. *Prog. Oceanogr.* 79, 177–189.

<https://doi.org/10.1016/j.pocean.2008.10.025>

- Haggarty, D., Yamanaka, L., 2018. Evaluating Rockfish Conservation Areas in southern British Columbia, Canada using a Random Forest model of rocky reef habitat. *Estuar. Coast. Shelf Sci.* 208, 191–204. <https://doi.org/10.1016/j.ecss.2018.05.011>
- Hannam, M., Moskal, L.M., 2015. Terrestrial laser scanning reveals seagrass microhabitat structure on a tideflat. *Remote Sens.* 7, 3037–3055. <https://doi.org/10.3390/rs70303037>
- Haralick, R.M., Shanmugam, K., Dinstein, I., 1973. Textural Features for Image Classification. *IEEE Trans. Syst. Man Cybern.* SMC-3, 610–621. <https://doi.org/10.1109/TSMC.1973.4309314>
- Helmuth, B., Denny, M.W., 2003. Predicting wave exposure in the rocky intertidal zone: Do bigger waves always lead to larger forces? *Limnol. Oceanogr.* 48, 1338–1345. <https://doi.org/10.4319/lo.2003.48.3.1338>
- Hendrick, V.J., Foster-Smith, R.L., 2006. *Sabellaria spinulosa* reef: A scoring system for evaluating “reefiness” in the context of the Habitats Directive. *J. Mar. Biol. Assoc. United Kingdom* 86, 665–677. <https://doi.org/10.1017/S0025315406013555>
- Hendrick, V.J., Hutchison, Z.L., Last, K.S., 2016. Sediment burial intolerance of marine macroinvertebrates. *PLoS One* 11, 149114. <https://doi.org/10.1371/journal.pone.0149114>
- Heritage, G.L., Large, A.R.G., 2009. Laser scanning for the environmental sciences. Wiley-Blackwell.
- Hesselbarth, M.H.K., Nowosad, J., Signer, J., Graham, L.J., 2021. Open-source Tools in R for Landscape Ecology. *Curr. Landsc. Ecol. Reports* 1–15. <https://doi.org/10.1007/s40823-021-00067-y>
- Hillman, S., Wallace, L., Reinke, K., Hally, B., Jones, S., Saldias, D.S., 2019. A Method for Validating the Structural Completeness of Understory Vegetation Models Captured with 3D Remote Sensing. *Remote Sens.* 11, 2118. <https://doi.org/10.3390/rs11182118>
- Holbrook, S.J., Schmitt, R.J., Ambrose, R.F., 1990. Biogenic habitat structure and

- characteristics of temperate reef fish assemblages. *Aust. J. Ecol.* 15, 489–503.
<https://doi.org/10.1111/j.1442-9993.1990.tb01473.x>
- Hollenbeck, J.P., Olsen, M.J., Haig, S.M., 2014. Using terrestrial laser scanning to support ecological research in the rocky intertidal zone. *J. Coast. Conserv.* 18, 701–714.
<https://doi.org/10.1007/s11852-014-0346-8>
- Holt, T., Rees, E., Hawkins, S., Seed, R., 1998. Biogenic Reefs (volume IX). An overview of dynamic and sensitivity characteristics for conservation management of marine SACs. Scottish Association for Marine Science (UK Marine SACs Project).
- Honkavaara, E., Litkey, P., Nurminen, K., Honkavaara, E., Litkey, P., Nurminen, K., 2013. Automatic Storm Damage Detection in Forests Using High-Altitude Photogrammetric Imagery. *Remote Sens.* 5, 1405–1424.
<https://doi.org/10.3390/rs5031405>
- Hooidonk, R. van, Maynard, J., Tamelander, J., Gove, J., Ahmadi, G., Raymundo, L., Williams, G., Heron, S.F., Planes, S., 2016. Local-scale projections of coral reef futures and implications of the Paris Agreement. *Sci. Reports* 2016 61 6, 1–8.
<https://doi.org/10.1038/srep39666>
- Hopkinson, B.M., King, A.C., Owen, D.P., Johnson-Roberson, M., Long, M.H., Bhandarkar, S.M., 2020. Automated classification of three-dimensional reconstructions of coral reefs using convolutional neural networks. *PLoS One* 15, e0230671.
<https://doi.org/10.1371/journal.pone.0230671>
- Horne, J.K., Schneider, D.C., 1995. Spatial Variance in Ecology. *Oikos* 74, 18.
<https://doi.org/10.2307/3545670>
- Huang, Z., Brooke, B.P., Harris, P.T., 2011. A new approach to mapping marine benthic habitats using physical environmental data. *Cont. Shelf Res.* 31, S4–S16.
<https://doi.org/10.1016/j.csr.2010.03.012>
- Ierodiaconou, D., Schimel, A.C.G., Kennedy, D., Monk, J., Gaylard, G., Young, M., Diesing, M., Rattray, A., 2018. Combining pixel and object based image analysis of ultra-high resolution multibeam bathymetry and backscatter for habitat mapping in shallow marine waters. *Mar. Geophys. Res.* 39, 271–288. <https://doi.org/10.1007/s11001-017-9338-z>

- Iglhaut, J., Cabo, C., Puliti, S., Piermattei, L., O'Connor, J., Rosette, J., 2019. Structure from Motion Photogrammetry in Forestry: a Review. Curr. For. Reports. <https://doi.org/10.1007/s40725-019-00094-3>
- Irving, R., 2009. The identification of the main characteristics of stony reef habitats under the Habitats Directive. JNCC Rep. No. 432 44.
- Jackson-Bué, T., Williams, G.J., Walker-Springett, G., Rowlands, S.J., Davies, A.J., 2021. Three-dimensional mapping reveals scale-dependent dynamics in biogenic reef habitat structure. Remote Sens. Ecol. Conserv. <https://doi.org/10.1002/RSE2.213>
- Jackson, E.L., Santos-Corujo, R.O., Pittman, S.J., 2018. Seascape patch dynamics. Seascape Ecol. 153–188.
- James, M.R., Robson, S., 2012. Straightforward reconstruction of 3D surfaces and topography with a camera: Accuracy and geoscience application. J. Geophys. Res. Earth Surf. 117, n/a-n/a. <https://doi.org/10.1029/2011JF002289>
- James, M.R., Robson, S., d'Oleire-Oltmanns, S., Niethammer, U., 2017a. Optimising UAV topographic surveys processed with structure-from-motion: Ground control quality, quantity and bundle adjustment. Geomorphology 280, 51–66. <https://doi.org/10.1016/j.geomorph.2016.11.021>
- James, M.R., Robson, S., Smith, M.W., 2017b. 3-D uncertainty-based topographic change detection with structure-from-motion photogrammetry: precision maps for ground control and directly georeferenced surveys. Earth Surf. Process. Landforms 42, 1769–1788. <https://doi.org/10.1002/esp.4125>
- James, P.M.A., Sturtevant, B.R., Townsend, P., Wolter, P., Fortin, M.J., 2011. Two-dimensional wavelet analysis of spruce budworm host basal area in the Border Lakes landscape. Ecol. Appl. 21, 2197–2209. <https://doi.org/10.1890/09-1876.1>
- Jaubet, M.L., Garaffo, G. V, Sánchez, M.A., Elías, R., 2013. Reef-forming polychaetes outcompetes ecosystem engineering mussels. Mar. Pollut. Bull. 71, 216–221. <https://doi.org/10.1016/j.marpolbul.2013.03.011>
- Jenkins, C., Eggleton, J., Barry, J., O'Connor, J., 2018. Advances in assessing *Sabellaria spinulosa* reefs for ongoing monitoring. Ecol. Evol. 8, 7673–7687.

<https://doi.org/10.1002/ece3.4292>

Jones, A.G., Dubois, S.F., Desroy, N., Fournier, J., 2018. Interplay between abiotic factors and species assemblages mediated by the ecosystem engineer *Sabellaria alveolata* (Annelida: Polychaeta). *Estuar. Coast. Shelf Sci.* 200, 1–18.

<https://doi.org/10.1016/j.ecss.2017.10.001>

Jones, C.G., Lawton, J.H., Shachak, M., 1994. Organisms as Ecosystem Engineers. *Oikos* 69, 373. <https://doi.org/10.2307/3545850>

Jouffray, J.B., Blasiak, R., Norström, A. V., Österblom, H., Nyström, M., 2020. The Blue Acceleration: The Trajectory of Human Expansion into the Ocean. *One Earth* 2, 43–54. <https://doi.org/10.1016/j.ONEEAR.2019.12.016>

Kaiser, M.S., Speckman, P.L., Jones, J.R., 1994. Statistical models for limiting nutrient relations in inland waters. *J. Am. Stat. Assoc.* 89, 410–423.

<https://doi.org/10.1080/01621459.1994.10476763>

Kalacska, M., Chmura, G.L., Lucanus, O., Bérubé, D., Arroyo-Mora, J.P., 2017. Structure from motion will revolutionize analyses of tidal wetland landscapes. *Remote Sens. Environ.* 199, 14–24. <https://doi.org/10.1016/j.RSE.2017.06.023>

Kalacska, M., Lucanus, O., Sousa, L., Vieira, T., Arroyo-Mora, J., 2018. Freshwater Fish Habitat Complexity Mapping Using Above and Underwater Structure-From-Motion Photogrammetry. *Remote Sens.* 10, 1912. <https://doi.org/10.3390/rs10121912>

Kaufman, L., Rousseeuw, P.J., 1990. Finding Groups in Data, Wiley Series in Probability and Statistics. John Wiley & Sons, Inc., Hoboken, NJ, USA.

<https://doi.org/10.1002/9780470316801>

Kedron, P.J., Frazier, A.E., 2019. Gradient Analysis and Surface Metrics for Landscape Ecology, in: *Current Trends in Landscape Research*. Springer, Cham, pp. 497–517.

https://doi.org/10.1007/978-3-030-30069-2_22

Kedron, P.J., Zhao, Y., Frazier, A.E., 2019. Three dimensional (3D) spatial metrics for objects. *Landsc. Ecol.* 34, 2123–2132. [https://doi.org/10.1007/s10980-019-00861-](https://doi.org/10.1007/s10980-019-00861-4)

4

Kerr, J.T., Ostrovsky, M., 2003. From space to species: Ecological applications for remote

sensing. Trends Ecol. Evol. 18, 299–305. [https://doi.org/10.1016/S0169-5347\(03\)00071-5](https://doi.org/10.1016/S0169-5347(03)00071-5)

Klausmeier, C.A., 1999. Regular and irregular patterns in semiarid vegetation. Science 284, 1826–1828. <https://doi.org/10.1126/science.284.5421.1826>

Koehl, M.A.R., 1999. Ecological biomechanics of benthic organisms. J. Exp. Biol. 202, 3469–3476.

Koenker, R., 2020. quantreg: Quantile Regression. R package version 5.83. <https://CRAN.R-project.org/package=quantreg>.

Koh, L.P., Wich, S.A., 2012. Dawn of drone ecology: low-cost autonomous aerial vehicles for conservation. Trop. Conserv. Sci. 5, 121–132. <https://doi.org/WOS:000310846600002>

Kostylev, V.E., Erlandsson, J., Mak, Y.M., Williams, G.A., Ming, M.Y., Williams, G.A., Mak, Y.M., Williams, G.A., Ming, M.Y., Williams, G.A., 2005. The relative importance of habitat complexity and surface area in assessing biodiversity: Fractal application on rocky shores. Ecol. Complex. 2, 272–286. <https://doi.org/10.1016/j.ecocom.2005.04.002>

Kovalenko, K.E., Thomaz, S.M., Warfe, D.M., 2012. Habitat complexity: Approaches and future directions. Hydrobiologia 685, 1–17. <https://doi.org/10.1007/s10750-011-0974-z>

Kuhn, M., 2008. Building Predictive Models in R Using the caret Package. J. Stat. Softw. 28, 1–26. <https://doi.org/10.18637/JSS.V028.I05>

Kuhn, M., Johnson, K., 2013. Applied predictive modeling, Applied Predictive Modeling. Springer New York. <https://doi.org/10.1007/978-1-4614-6849-3>

La Porta, B., Nicoletti, L., 2009. *Sabellaria alveolata* (Linnaeus) reefs in the central Tyrrhenian Sea (Italy) and associated polychaete fauna. Zoosymposia 2, 527–536. <https://doi.org/10.11646/zoosymposia.2.1.36>

Lacharité, M., Brown, C.J., Gazzola, V., 2018. Multisource multibeam backscatter data: developing a strategy for the production of benthic habitat maps using semi-automated seafloor classification methods. Mar. Geophys. Res. 39, 307–322.

<https://doi.org/10.1007/s11001-017-9331-6>

Lague, D., Brodu, N., Leroux, J., 2013. Accurate 3D comparison of complex topography with terrestrial laser scanner: Application to the Rangitikei canyon (N-Z). ISPRS J. Photogramm. Remote Sens. 82, 10–26.

<https://doi.org/10.1016/j.isprsjprs.2013.04.009>

Lamarche, G., Lurton, X., 2018. Recommendations for improved and coherent acquisition and processing of backscatter data from seafloor-mapping sonars. Mar. Geophys. Res. 39, 5–22. <https://doi.org/10.1007/s11001-017-9315-6>

Landres, P.B., Morgan, P., Swanson, F.J., 1999. Overview of the use of natural variability concepts in managing ecological systems. Ecol. Appl. 9, 1179–1188.

[https://doi.org/10.1890/1051-0761\(1999\)009\[1179:OOTUON\]2.0.CO;2](https://doi.org/10.1890/1051-0761(1999)009[1179:OOTUON]2.0.CO;2)

Langlois, E., Bonis, A., Bouzillé, J., 2003. Sediment and plant dynamics in saltmarshes pioneer zone: *Puccinellia maritima* as a key species? Estuar. Coast. Shelf Sci. 56, 239–249. [https://doi.org/10.1016/S0272-7714\(02\)00185-3](https://doi.org/10.1016/S0272-7714(02)00185-3)

Lausch, A., Blaschke, T., Haase, D., Herzog, F., Syrbe, R.U., Tischendorf, L., Walz, U., 2015. Understanding and quantifying landscape structure - A review on relevant process characteristics, data models and landscape metrics. Ecol. Modell. 295, 31–41.

<https://doi.org/10.1016/j.ecolmodel.2014.08.018>

Lawrence, R., Bunn, A., Powell, S., Zambon, M., 2004. Classification of remotely sensed imagery using stochastic gradient boosting as a refinement of classification tree analysis. Remote Sens. Environ. 90, 331–336.

<https://doi.org/10.1016/J.RSE.2004.01.007>

Lazarus, M., Belmaker, J., 2021. A review of seascape complexity indices and their performance in coral and rocky reefs. Methods Ecol. Evol. 12, 681–695.

<https://doi.org/10.1111/2041-210X.13557>

Le Cam, J.-B., Fournier, J., Etienne, S., Couden, J., 2011. The strength of biogenic sand reefs: Visco-elastic behaviour of cement secreted by the tube building polychaete *Sabellaria alveolata*, Linnaeus, 1767. Estuar. Coast. Shelf Sci. 91, 333–339.

<https://doi.org/10.1016/j.ecss.2010.10.036>

- Lecornu, B., Schlund, E., Basuyaux, O., Cantat, O., Dauvin, J.-C.C., 2016. Dynamics (from 2010-2011 to 2014) of *Sabellaria alveolata* reefs on the western coast of Cotentin (English Channel, France). *Reg. Stud. Mar. Sci.* 8, 157–169.
<https://doi.org/10.1016/j.rsma.2016.07.004>
- Lecours, V., Devillers, R., Edinger, E.N., Brown, C.J., Lucieer, V.L., 2017a. Influence of artefacts in marine digital terrain models on habitat maps and species distribution models: a multiscale assessment. *Remote Sens. Ecol. Conserv.* 3, 232–246.
<https://doi.org/10.1002/rse2.49>
- Lecours, V., Devillers, R., Schneider, D.C., Lucieer, V.L., Brown, C.J., Edinger, E.N., 2015. Spatial scale and geographic context in benthic habitat mapping: Review and future directions. *Mar. Ecol. Prog. Ser.* 535, 259–284. <https://doi.org/10.3354/meps11378>
- Lecours, V., Devillers, R., Simms, A.E., Lucieer, V.L., Brown, C.J., 2017b. Towards a framework for terrain attribute selection in environmental studies. *Environ. Model. Softw.* 89, 19–30. <https://doi.org/10.1016/j.envsoft.2016.11.027>
- Legendre, P., Fortin, M.J., 1989. Spatial pattern and ecological analysis. *Vegetatio* 80, 107–138. <https://doi.org/10.1007/BF00048036>
- Leon, J.X., Phinn, S.R., Hamylton, S., Saunders, M.I., 2013. Filling the “white ribbon” - a multisource seamless digital elevation model for Lizard Island, northern Great Barrier Reef. *Int. J. Remote Sens.* 34, 6337–6354.
<https://doi.org/10.1080/01431161.2013.800659>
- Leon, J.X., Roelfsema, C.M., Saunders, M.I., Phinn, S.R., 2015. Measuring coral reef terrain roughness using “Structure-from-Motion” close-range photogrammetry. *Geomorphology* 242, 21–28. <https://doi.org/10.1016/j.geomorph.2015.01.030>
- Lepczyk, C.A., Wedding, L.M., Asner, G.P., Pittman, S.J., Goulden, T., Linderman, M.A., Gang, J., Wright, R., 2021. Advancing Landscape and Seascape Ecology from a 2D to a 3D Science. *Bioscience* 71, 596–608. <https://doi.org/10.1093/biosci/biab001>
- Levin, S.A., 1992. The Problem of Pattern and Scale in Ecology: The Robert H. MacArthur Award Lecture Author(s): Simon A. Levin Source: *Ecology* 73, 1943–1967.
<https://doi.org/doi:10.2307/1941447>

- Levin, S.A., Paine, R.T., 1974. Disturbance, patch formation, and community structure. *Proc. Natl. Acad. Sci. U. S. A.* 71, 2744–2747.
<https://doi.org/10.1073/PNAS.71.7.2744>
- Li, J., Knapp, D.E., Fabina, N.S., Kennedy, E. V., Larsen, K., Lyons, M.B., Murray, N.J., Phinn, S.R., Roelfsema, C.M., Asner, G.P., 2020. A global coral reef probability map generated using convolutional neural networks. *Coral Reefs* 1–11.
<https://doi.org/10.1007/s00338-020-02005-6>
- Liaw, A., Wiener, M., 2002. Classification and Regression by randomForest. *R News* 2, 18–22.
- Limpenny, D.S., Foster-Smith, R.L., Edwards, T.M., Hendrick, V.J., Diesing, M., Eggleton, J.D., Meadows, W.J., Crutchfield, Z., Pfeifer, S., Reach, I.S., 2010. Best methods for identifying and evaluating *Sabellaria spinulosa* and cobble reef. Aggregate Levy Sustainability Fund Project MAL0008 134.
- Lin, Y.-C., Cheng, Y.-T., Zhou, T., Ravi, R., Hasheminasab, S.M., Flatt, J.E., Troy, C., Habib, A., 2019. Evaluation of UAV LiDAR for Mapping Coastal Environments. *Remote Sens.* 2019, Vol. 11, Page 2893 11, 2893. <https://doi.org/10.3390/RS11242893>
- Lindgarth, M., Gamfeldt, L., 2005. Comparing categorical and continuous ecological analyses: Effects of “wave exposure” on rocky shores. *Ecology* 86, 1346–1357.
<https://doi.org/10.1890/04-1168>
- Lindenbaum, C., Bennell, J.D., Rees, E.I.S., Mcclean, D., Cook, W., Wheeler, A.J., Sanderson, W.G., 2008. Small-scale variation within a *Modiolus modiolus* (Mollusca: Bivalvia) reef in the Irish Sea: I. Seabed mapping and reef morphology. *J. Mar. Biol. Assoc. United Kingdom* 88, 133–141. <https://doi.org/10.1017/S0025315408000374>
- Liu, Q.-X., Herman, P.M.J., Mooij, W.M., Huisman, J., Scheffer, M., Olff, H., van de Koppel, J., 2014. Pattern formation at multiple spatial scales drives the resilience of mussel bed ecosystems. *Nat. Commun.* 5, 5234. <https://doi.org/10.1038/ncomms6234>
- Liu, Q.X., Herman, P.M.J., Mooij, W.M., Huisman, J., Scheffer, M., Olff, H., Van De Koppel, J., 2014. Pattern formation at multiple spatial scales drives the resilience of mussel bed ecosystems. *Nat. Commun.* 5, 1–7. <https://doi.org/10.1038/ncomms6234>

- Lowe, R.J., Falter, J.L., Bandet, M.D., Pawlak, G., Atkinson, M.J., Monismith, S.G., Koseff, J.R., 2005. Spectral wave dissipation over a barrier reef. *J. Geophys. Res. C Ocean.* 110, 1–16. <https://doi.org/10.1029/2004JC002711>
- Lucieer, V., Hill, N.A., Barrett, N.S., Nichol, S., 2013. Do marine substrates “look” and “sound” the same? Supervised classification of multibeam acoustic data using autonomous underwater vehicle images. *Estuar. Coast. Shelf Sci.* 117, 94–106. <https://doi.org/10.1016/j.ecss.2012.11.001>
- Lucieer, V., Lecours, V., Dolan, M.F.J., 2018a. Charting the Course for Future Developments in Marine Geomorphometry: An Introduction to the Special Issue. *Geosci.* 2018, Vol. 8, Page 477 8, 477. <https://doi.org/10.3390/GEOSCIENCES8120477>
- Lucieer, V., Roche, M., Degrendele, K., Malik, M., Dolan, M., Lamarche, G., 2018b. User expectations for multibeam echo sounders backscatter strength data-looking back into the future. *Mar. Geophys. Res.* 39, 23–40. <https://doi.org/10.1007/s11001-017-9316-5>
- Maas, H. -G., Bienert, A., Scheller, S., Keane, E., 2008. Automatic forest inventory parameter determination from terrestrial laser scanner data. *Int. J. Remote Sens.* 29, 1579–1593. <https://doi.org/10.1080/01431160701736406>
- MacArthur, R.H., MacArthur, J.W., 1961. On Bird Species Diversity Author (s): Robert H . MacArthur and John W . MacArthur Published by : Wiley on behalf of the Ecological Society of America Stable URL : <https://www.jstor.org/stable/1932254> REFERENCES Linked references are available on JSTOR f. *Ecol. Soc. Am.* 42, 594–598.
- Maechler, M., Rousseeuw, P.J., Struyf, A., Hubert, M., Hornik, K., 2019. cluster: Cluster Analysis Basics and Extensions. R package version 2.1.0.
- Mancini, F., Dubbini, M., Gattelli, M., Stecchi, F., Fabbri, S., Gabbianelli, G., 2013. Using unmanned aerial vehicles (UAV) for high-resolution reconstruction of topography: The structure from motion approach on coastal environments. *Remote Sens.* 5, 6880–6898. <https://doi.org/10.3390/rs5126880>
- MarineSpace, 2019. Morlais Project Environmental Statement Chapter 9 : Benthic and

Intertidal Ecology Volume I.

- Marvin, D.C., Koh, L.P., Lynam, A.J., Wich, S., Davies, A.B., Krishnamurthy, R., Stokes, E., Starkey, R., Asner, G.P., 2016. Integrating technologies for scalable ecology and conservation. *Glob. Ecol. Conserv.* 7, 262–275.
<https://doi.org/10.1016/J.GECCO.2016.07.002>
- Mayer, L., Jakobsson, M., Allen, G., Dorschel, B., Falconer, R., Ferrini, V., Lamarche, G., Snaith, H., Weatherall, P., 2018. The Nippon Foundation—GEBCO Seabed 2030 Project: The Quest to See the World’s Oceans Completely Mapped by 2030. *Geosciences* 8, 63. <https://doi.org/10.3390/geosciences8020063>
- McCormick, M., 1994. Comparison of field methods for measuring surface topography and their associations with a tropical reef fish assemblage. *Mar. Ecol. Prog. Ser.* 112, 87–96.
- McDermid, G.J., Franklin, S.E., LeDrew, E.F., 2005. Remote sensing for large-area habitat mapping. *Prog. Phys. Geogr. Earth Environ.* 29, 449–474.
<https://doi.org/10.1191/0309133305pp455ra>
- McFarlane, D.A., Roberts, W., Buchroithner, M., Van Rentergem, G., Lundberg, J., Hautz, S., 2015. Terrestrial liDAR-based automated counting of swiftlet nests in the caves of gomantong, Sabah, Borneo. *Int. J. Speleol.* 44. <https://doi.org/10.5038/1827-806X.44.2.8>
- McGarigal, K., Marks, B.J., 1995. FRAGSTATS: spatial pattern analysis program for quantifying landscape structure, General Technical Report - US Department of Agriculture, Forest Service. <https://doi.org/10.2737/PNW-GTR-351>
- McGarigal, K., Tagil, S., Cushman, S.A., 2009. Surface metrics: An alternative to patch metrics for the quantification of landscape structure. *Landsc. Ecol.* 24, 433–450.
<https://doi.org/10.1007/s10980-009-9327-y>
- Meager, J.J., Schlacher, T.A., 2013. New metric of microhabitat complexity predicts species richness on a rocky shore. *Mar. Ecol.* 34, 484–491.
<https://doi.org/10.1111/maec.12049>
- Meager, J.J., Schlacher, T.A., Green, M., 2011. Topographic complexity and landscape

temperature patterns create a dynamic habitat structure on a rocky intertidal shore. *Mar. Ecol. Prog. Ser.* 428, 1–12. <https://doi.org/10.3354/meps09124>

Meentemeyer, V., 1989. Geographical perspectives of space, time, and scale. *Landsc. Ecol.* 3, 163–173. <https://doi.org/10.1007/BF00131535>

MESH project, 2008. MESH Guide to Habitat Mapping. *Jt. Nat. Conserv. Comm.* 86.

Meyer, H., Pebesma, E., 2022. Machine learning-based global maps of ecological variables and the challenge of assessing them. *Nat. Commun.* 2022 131 13, 1–4. <https://doi.org/10.1038/s41467-022-29838-9>

Meyer, H., Pebesma, E., 2021. Predicting into unknown space? Estimating the area of applicability of spatial prediction models. *Methods Ecol. Evol.* 12, 1620–1633. <https://doi.org/10.1111/2041-210X.13650>

Milan, D.J., Heritage, G.L., Large, A.R.G., Entwistle, N.S., 2010. Mapping hydraulic biotopes using terrestrial laser scan data of water surface properties. *Earth Surf. Process. Landforms* 35, 918–931. <https://doi.org/10.1002/esp.1948>

Millard, K., Richardson, M., 2015. On the Importance of Training Data Sample Selection in Random Forest Image Classification: A Case Study in Peatland Ecosystem Mapping. *Remote Sens.* 2015, Vol. 7, Pages 8489–8515 7, 8489–8515. <https://doi.org/10.3390/RS70708489>

Milling, C.R., Rachlow, J.L., Olsoy, P.J., Chappell, M.A., Johnson, T.R., Forbey, J.S., Shipley, L.A., Thornton, D.H., 2018. Habitat structure modifies microclimate: An approach for mapping fine-scale thermal refuge. *Methods Ecol. Evol.* 9, 1648–1657. <https://doi.org/10.1111/2041-210X.13008>

Misiuk, B., Brown, C.J., Robert, K., Lacharité, M., 2020. Harmonizing multi-source sonar backscatter datasets for seabed mapping using bulk shift approaches. *Remote Sens.* 12, 601. <https://doi.org/10.3390/rs12040601>

Mitchell, P.J., Downie, A.L., Diesing, M., 2018. How good is my map? A tool for semi-automated thematic mapping and spatially explicit confidence assessment. *Environ. Model. Softw.* 108, 111–122. <https://doi.org/10.1016/j.envsoft.2018.07.014>

Muir, J., Goodwin, N., Armston, J., Phinn, S., Scarth, P., 2017. An accuracy assessment of

- derived digital elevation models from terrestrial laser scanning in a sub-tropical forested environment. *Remote Sens.* 9, 843. <https://doi.org/10.3390/rs9080843>
- Murfitt, S.L., Allan, B.M., Bellgrove, A., Rattray, A., Young, M.A., Ierodionou, D., 2017. Applications of unmanned aerial vehicles in intertidal reef monitoring. *Sci. Rep.* 7, 1–11. <https://doi.org/10.1038/s41598-017-10818-9>
- Naimi, B., Hamm, N.A.S., Groen, T.A., Skidmore, A.K., Toxopeus, A.G., 2014. Where is positional uncertainty a problem for species distribution modelling? *Ecography* 37, 191–203. <https://doi.org/10.1111/j.1600-0587.2013.00205.x>
- Nash, K.L., Graham, N.A.J., Wilson, S.K., Bellwood, D.R., 2013. Cross-scale Habitat Structure Drives Fish Body Size Distributions on Coral Reefs. *Ecosystems* 16, 478–490. <https://doi.org/10.1007/s10021-012-9625-0>
- Navarrete, S.A., Wieters, E.A., Broitman, B.R., Castilla, J.C., 2005. Scales of benthic-pelagic coupling and the intensity of species interactions: From recruitment limitation to top-down control. *Proc. Natl. Acad. Sci. U. S. A.* 102, 18046–18051. <https://doi.org/10.1073/pnas.0509119102>
- Nex, F., Remondino, F., 2014. UAV for 3D mapping applications: A review. *Appl. Geomatics* 6, 1–15. <https://doi.org/10.1007/s12518-013-0120-x>
- Odum, E.P., 1969. The Strategy of Ecosystem Development. *Science* 164, 262–270.
- Olofsson, P., Foody, G.M., Herold, M., Stehman, S. V., Woodcock, C.E., Wulder, M.A., 2014. Good practices for estimating area and assessing accuracy of land change. *Remote Sens. Environ.* 148, 42–57. <https://doi.org/10.1016/j.rse.2014.02.015>
- Olsoy, P.J., Shipley, L.A., Rachlow, J.L., Forbey, J.S., Glenn, N.F., Burgess, M.A., Thornton, D.H., 2018. Unmanned aerial systems measure structural habitat features for wildlife across multiple scales. *Methods Ecol. Evol.* 9, 594–604. <https://doi.org/10.1111/2041-210X.12919>
- Orwig, D.A., Boucher, P., Paynter, I., Saenz, E., Li, Z., Schaaf, C., 2018. The potential to characterize ecological data with terrestrial laser scanning in Harvard Forest, MA. *Interface Focus*. <https://doi.org/10.1098/rsfs.2017.0044>
- Paine, R.T., Levin, S.A., 1981. Intertidal Landscapes: Disturbance and the Dynamics of

- Pattern. Ecol. Monogr. 51, 145–178. <https://doi.org/10.2307/2937261>
- Parrish, C.E., Magruder, L.A., Neuenschwander, A.L., Forfinski-Sarkozi, N., Alonzo, M., Jasinski, M., 2019. Validation of ICESat-2 ATLAS Bathymetry and Analysis of ATLAS's Bathymetric Mapping Performance. Remote Sens. 11, 1634. <https://doi.org/10.3390/rs11141634>
- Pasquarella, V.J., Holden, C.E., Kaufman, L., Woodcock, C.E., 2016. From imagery to ecology: leveraging time series of all available Landsat observations to map and monitor ecosystem state and dynamics. Remote Sens. Ecol. Conserv. 2, 152–170. <https://doi.org/10.1002/RSE2.24>
- Pearce, B., 2017. The ecology of *Sabellaria spinulosa* reefs. Plymouth University.
- Pearce, B., Fariñas-Franco, J.M., Wilson, C., Pitts, J., DeBurgh, A., Somerfield, P.J., 2014. Repeated mapping of reefs constructed by *Sabellaria spinulosa* Leuckart 1849 at an offshore wind farm site. Cont. Shelf Res. 83, 3–13. <https://doi.org/10.1016/j.csr.2014.02.003>
- Pearman, T.R.R., Robert, K., Callaway, A., Hall, R., Lo Iacono, C., Huvenne, V.A.I., 2020. Improving the predictive capability of benthic species distribution models by incorporating oceanographic data – Towards holistic ecological modelling of a submarine canyon. Prog. Oceanogr. 184. <https://doi.org/10.1016/j.pocean.2020.102338>
- Pebesma, E.J., 2004. Multivariable geostatistics in {S}: the gstat package. Comput. Geosci. 30, 683–691.
- Pennings, S.C., Callaway, R.M., 1992. Salt marsh plant zonation: the relative importance of competition and physical factors. Ecology 73, 681–690. <https://doi.org/10.2307/1940774>
- Perry, C.T., Alvarez-Filip, L., 2019. Changing geo-ecological functions of coral reefs in the Anthropocene. Funct. Ecol. 33, 976–988. <https://doi.org/10.1111/1365-2435.13247>
- Perry, G.L.W., 2002. Landscapes, space and equilibrium: Shifting viewpoints. Prog. Phys. Geogr. 26, 339–359. <https://doi.org/10.1191/0309133302pp341ra>

- Perry, J.N., Liebhold, A.M., Rosenberg, M.S., Dungan, J., Miriti, M., Jakomulska, A., Citron-Pousty, S., 2002. Illustrations and guidelines for selecting statistical methods for quantifying spatial pattern in ecological data. *Ecography* 25, 578–600.
<https://doi.org/10.1034/j.1600-0587.2002.250507.x>
- Peterson, R.A., Cavanaugh, J.E., 2020. Ordered quantile normalization: a semiparametric transformation built for the cross-validation era. *J. Appl. Stat.* 47, 2312–2327.
<https://doi.org/10.1080/02664763.2019.1630372>
- Pickett, S.T.A., Kolasa, J., Armesto, J.J., Collins, S.L., 1989. The Ecological Concept of Disturbance and Its Expression at Various Hierarchical Levels. *Oikos* 54, 129.
<https://doi.org/10.2307/3565258>
- Pimm, S.L., Alibhai, S., Bergl, R., Dehgan, A., Giri, C., Jewell, Z., Joppa, L., Kays, R., Loarie, S., 2015. Emerging Technologies to Conserve Biodiversity. *Trends Ecol. Evol.*
<https://doi.org/10.1016/j.tree.2015.08.008>
- Pittman, S.J., Brown, K.A., 2011. Multi-Scale Approach for Predicting Fish Species Distributions across Coral Reef Seascapes. *PLoS One* 6, e20583.
<https://doi.org/10.1371/JOURNAL.PONE.0020583>
- Pittman, S.J., Christensen, J.D., Caldow, C., Menza, C., Monaco, M.E., 2007. Predictive mapping of fish species richness across shallow-water seascapes in the Caribbean. *Ecol. Modell.* 204, 9–21. <https://doi.org/10.1016/J.ECOLMODEL.2006.12.017>
- Pittman, S.J., Costa, B.M., Battista, T.A., 2009. Using lidar bathymetry and boosted regression trees to predict the diversity and abundance of fish and corals. *J. Coast. Res.* 27–38. <https://doi.org/10.2112/SI53-004.1/28400/USING-LIDAR-BATHYMETRY-AND-BOOSTED-REGRESSION>
- Platt, T., Fuentes-Yaco, C., Frank, K.T., 2003. Spring algal bloom and larval fish survival. *Nature* 423, 398–399. <https://doi.org/10.1038/423398b>
- Plets, R., Clements, A., Quinn, R., Strong, J., Breen, J., Edwards, H., 2012. Marine substratum map of the Causeway Coast, Northern Ireland. *J. Maps* 8, 1–13.
<https://doi.org/10.1080/17445647.2012.661957>
- Plicanti, A., Domínguez, R., Dubois, S.F., Bertocci, I., Domínguez, R., Dubois, S.F., Bertocci,

I., 2016. Human impacts on biogenic habitats: Effects of experimental trampling on *Sabellaria alveolata* (Linnaeus, 1767) reefs. J. Exp. Mar. Bio. Ecol. 478, 34–44.
<https://doi.org/10.1016/j.jembe.2016.02.001>

Plotnick, R.E., Gardner, R.H., O’neill, R. V, 1993. Lacunarity indices as measures of landscape texture, Landscape Ecology. SPB Academic Publishing bv.

Ploton, P., Mortier, F., Réjou-Méchain, M., Barbier, N., Picard, N., Rossi, V., Dormann, C., Cornu, G., Viennois, G., Bayol, N., Lyapustin, A., Gourlet-Fleury, S., Pélissier, R., 2020. Spatial validation reveals poor predictive performance of large-scale ecological mapping models. Nat. Commun. 11, 1–11. <https://doi.org/10.1038/s41467-020-18321-y>

Pontius, R.G., Millones, M., 2011. Death to Kappa: birth of quantity disagreement and allocation disagreement for accuracy assessment.
<http://dx.doi.org/10.1080/01431161.2011.552923> 32, 4407–4429.
<https://doi.org/10.1080/01431161.2011.552923>

Porskamp, P., Rattray, A., Young, M., Ierodiaconou, D., 2018. Multiscale and hierarchical classification for benthic habitat mapping. Geosci. 8.
<https://doi.org/10.3390/geosciences8040119>

Prado, E., Rodríguez-Basalo, A., Cobo, A., Ríos, P., Sánchez, F., 2020. 3D fine-scale terrain variables from underwater photogrammetry: A new approach to benthic microhabitat modeling in a circalittoral Rocky shelf. Remote Sens. 12, 2466.
<https://doi.org/10.3390/RS12152466>

R Core Team, 2021. R: A Language and Environment for Statistical Computing.

R Core Team, 2020. R: A language and environment for statistical computing. R Foundation for Statistical Computing, Vienna, Austria. URL <https://www.R-project.org/>.

Ramirez-Reyes, C., Brauman, K.A., Chaplin-Kramer, R., Galford, G.L., Adamo, S.B., Anderson, C.B., Anderson, C., Allington, G.R.H., Bagstad, K.J., Coe, M.T., Cord, A.F., Dee, L.E., Gould, R.K., Jain, M., Kowal, V.A., Muller-Karger, F.E., Norriss, J., Potapov, P., Qiu, J., Rieb, J.T., Robinson, B.E., Samberg, L.H., Singh, N., Szeto, S.H., Voigt, B., Watson, K., Wright, T.M., 2019. Reimagining the potential of Earth observations for

- ecosystem service assessments. *Sci. Total Environ.* 665, 1053–1063.
<https://doi.org/10.1016/J.SCITOTENV.2019.02.150>
- Rattray, A., Ierodiaconou, D., Womersley, T., 2015. Wave exposure as a predictor of benthic habitat distribution on high energy temperate reefs. *Front. Mar. Sci.* 2, 8.
<https://doi.org/10.3389/fmars.2015.00008>
- Reichert, J., Backes, A.R., Schubert, P., Wilke, T., 2017. The power of 3D fractal dimensions for comparative shape and structural complexity analyses of irregularly shaped organisms. *Methods Ecol. Evol.* 8, 1650–1658.
<https://doi.org/10.1111/2041-210X.12829>
- Rhodes, C.J., Henrys, P., Siriwardena, G.M., Whittingham, M.J., Norton, L.R., 2015. The relative value of field survey and remote sensing for biodiversity assessment. *Methods Ecol. Evol.* 6, 772–781. <https://doi.org/10.1111/2041-210X.12385>
- Richardson, J.J., Monika Moskal, L., Bakker, J.D., 2014. Terrestrial laser scanning for vegetation sampling. *Sensors* 14, 20304–20319.
<https://doi.org/10.3390/s141120304>
- Risk, M.J., 1972. Fish Diversity on a Coral Reef in the Virgin Islands. *Atoll Res. Bull.* 153, 1–4. <https://doi.org/10.5479/si.00775630.153.1>
- Robins, P.E., Neill, S.P., Giménez, L., Jenkins, S.R., Malham, S.K., 2013. Physical and biological controls on larval dispersal and connectivity in a highly energetic shelf sea. *Limnol. Oceanogr.* 58, 505–524. <https://doi.org/10.4319/lo.2013.58.2.0505>
- Robinson, K.A., Ramsay, K., Lindenbaum, C., Frost, N., Moore, J., Wright, A.P., Petrey, D., 2011. Predicting the distribution of seabed biotopes in the southern Irish Sea. *Cont. Shelf Res.* 31, S120–S131. <https://doi.org/10.1016/j.csr.2010.01.010>
- Roche, R.C., Walker-Springett, K., Robins, P.E., Jones, J., Veneruso, G., Whitton, T.A., Piano, M., Ward, S.L., Duce, C.E., Waggitt, J.J., Walker-Springett, G.R., Neill, S.P., Lewis, M.J., King, J.W., 2016. Research priorities for assessing potential impacts of emerging marine renewable energy technologies: Insights from developments in Wales (UK). *Renew. Energy* 99, 1327–1341. <https://doi.org/10.1016/j.renene.2016.08.035>
- Rodriguez, A.B., Fodrie, F.J., Ridge, J.T., Lindquist, N.L., Theuerkauf, E.J., Coleman, S.E.,

- Grabowski, J.H., Brodeur, M.C., Gittman, R.K., Keller, D. a., Kenworthy, M.D., 2014. Oyster reefs can outpace sea-level rise. *Nat. Clim. Chang.* 4, 493–497.
<https://doi.org/10.1038/nclimate2216>
- Rogers, A., Blanchard, J.L., Mumby, P.J., 2014. Vulnerability of coral reef fisheries to a loss of structural complexity. *Curr. Biol.* 24, 1000–1005.
<https://doi.org/10.1016/j.cub.2014.03.026>
- Rosenberg, R., 1995. Benthic marine fauna structured by hydrodynamic processes and food availability. *Netherlands J. Sea Res.* 34, 303–317.
[https://doi.org/10.1016/0077-7579\(95\)90040-3](https://doi.org/10.1016/0077-7579(95)90040-3)
- Rossi, R.E., Mulla, D.J., Journel, A.G., Franz, E.H., 1992. Geostatistical tools for modeling and interpreting ecological spatial dependence. *Ecol. Monogr.* 62, 277–314.
<https://doi.org/10.2307/2937096>
- Rowland, C., Morton, D., Carrascao Tornero, L., McShane, G., O’Neil, A., Wood, C., 2017. Land Cover Map 2015 (25 m raster, GB).
- Royal Haskoning DHV, 2019. Morlais Project Environmental Statement Chapter 7 :
Metocean Conditions and Coastal Processes Volume I.
- Safriel, U.N., Ben-Eliahu, M.N., 1991. The influence of habitat structure and environmental stability on the species diversity of polychaetes in vermetid reefs, in: Bell, S.S., McCoy, E.D., Mushinsky, H.R. (Eds.), *Habitat Structure*. Chapman & Hall/CRC, London, pp. 349–368. <https://doi.org/10.1007/978-94-011-3076-9>
- Sagarin, R., Pauchard, A., 2010. Observational approaches in ecology open new ground in a changing world. *Front. Ecol. Environ.* 8, 379–386.
<https://doi.org/10.1890/090001>
- Sanz-Ablanedo, E., Chandler, J.H., Rodríguez-Pérez, J.R., Ordóñez, C., 2018. Accuracy of Unmanned Aerial Vehicle (UAV) and SfM photogrammetry survey as a function of the number and location of ground control points used. *Remote Sens.* 10.
<https://doi.org/10.3390/rs10101606>
- Sappington, J.M., Longshore, K.M., Thompson, D.B., 2007. Quantifying Landscape Ruggedness for Animal Habitat Analysis: A Case Study Using Bighorn Sheep in the

- Mojave Desert. *J. Wildl. Manage.* 71, 1419–1426. <https://doi.org/10.2193/2005-723>
- Saunders, S.C., Chen, J., Drummer, T.D., Gustafson, E.J., Brosnoks, K.D., 2005. Identifying scales of pattern in ecological data: A comparison of lacunarity, spectral and wavelet analyses. *Ecol. Complex.* 2, 87–105.
<https://doi.org/10.1016/j.ecocom.2004.11.002>
- Scheffers, B.R., Edwards, D.P., Diesmos, A., Williams, S.E., Evans, T.A., 2014. Microhabitats reduce animal's exposure to climate extremes. *Glob. Chang. Biol.* 20, 495–503.
<https://doi.org/10.1111/gcb.12439>
- Schiel, D.R., Wood, S.A., Dunmore, R.A., Taylor, D.I., 2006. Sediment on rocky intertidal reefs: Effects on early post-settlement stages of habitat-forming seaweeds. *J. Exp. Mar. Biol. Ecol.* 331, 158–172. <https://doi.org/10.1016/j.jembe.2005.10.015>
- Schneider, D.C., 2001. The rise of the concept of scale in ecology. *Bioscience* 51, 545–553.
[https://doi.org/10.1641/0006-3568\(2001\)051\[0545:TROTCO\]2.0.CO;2](https://doi.org/10.1641/0006-3568(2001)051[0545:TROTCO]2.0.CO;2)
- Sebens, K.P., Grace, S.P., Helmuth, B., Maney, E.J., Miles, J.S., 1998. Water flow and prey capture by three scleractinian corals, *Madracis mirabilis*, *Montastrea cavernosa* and *Porites porites* in a field enclosure. *Mar. Biol.* 131, 347–360.
<https://doi.org/10.1007/s002270050328>
- Seidleck, M., 2018. The ice, cloud, and land elevation satellite-2 - Overview, science, and applications, in: *IEEE Aerospace Conference Proceedings*. IEEE Computer Society, pp. 1–8. <https://doi.org/10.1109/AERO.2018.8396364>
- Shields, A., 1936. Anwendung der Aehnlichkeitsmechanik und der Turbulenzforschung auf die Geschiebebewegung. Technical University Berlin.
- Shields, M.A., Woolf, D.K., Grist, E.P.M., Kerr, S.A., Jackson, A.C., Harris, R.E., Bell, M.C., Beharie, R., Want, A., Osalusi, E., Gibb, S.W., Side, J., 2011. Marine renewable energy: The ecological implications of altering the hydrodynamics of the marine environment. *Ocean Coast. Manag.* 54, 2–9.
<https://doi.org/10.1016/j.OCECOAMAN.2010.10.036>
- Shiklomanov, A.N., Bradley, B.A., Dahlin, K.M., M Fox, A., Gough, C.M., Hoffman, F.M., M

Middleton, E., Serbin, S.P., Smallman, L., Smith, W.K., 2019. Enhancing global change experiments through integration of remote-sensing techniques. *Front. Ecol. Environ.* 17, 215–224. <https://doi.org/10.1002/fee.2031>

Skarlatos, D., Agrafiotis, P., 2018. A Novel Iterative Water Refraction Correction Algorithm for Use in Structure from Motion Photogrammetric Pipeline. *J. Mar. Sci. Eng.* 2018, Vol. 6, Page 77 6, 77. <https://doi.org/10.3390/JMSE6030077>

Smith, J., O'Brien, P.E., Stark, J.S., Johnstone, G.J., Riddle, M.J., 2015. Integrating multibeam sonar and underwater video data to map benthic habitats in an East Antarctic nearshore environment. *Estuar. Coast. Shelf Sci.* 164, 520–536. <https://doi.org/10.1016/j.ecss.2015.07.036>

Smith, M., Vericat, D., Gibbins, C., 2012. Through-water terrestrial laser scanning of gravel beds at the patch scale. *Earth Surf. Process. Landforms* 37, 411–421. <https://doi.org/10.1002/esp.2254>

Smith, W.H.F., Sandwell, D.T., 1997. Global sea floor topography from satellite altimetry and ship depth soundings. *Science* 277, 1956–1962. <https://doi.org/10.1126/science.277.5334.1956>

Sousa, W.P., 1984. Intertidal Mosaics: Patch Size, Propagule Availability, and Spatially Variable Patterns of Succession. *Ecology* 65, 1918–1935. <https://doi.org/10.2307/1937789>

Southward, A.J., Langmead, O., Hardman-Mountford, N.J., Aiken, J., Boalch, G.T., Dando, P.R., Genner, M.J., Joint, I., Kendall, M.A., Halliday, N.C., Harris, R.P., Leaper, R., Mieszkowska, N., Pingree, R.D., Richardson, A.J., Sims, D.W., Smith, T., Walne, A.W., Hawkins, S.J., 2004. Long-Term Oceanographic and Ecological Research in the Western English Channel. *Adv. Mar. Biol.* 47, 1–105. [https://doi.org/10.1016/S0065-2881\(04\)47001-1](https://doi.org/10.1016/S0065-2881(04)47001-1)

Stehman, S. V., Czaplewski, R.L., 1998. Design and analysis for thematic map accuracy assessment: Fundamental principles. *Remote Sens. Environ.* 64, 331–344. [https://doi.org/10.1016/S0034-4257\(98\)00010-8](https://doi.org/10.1016/S0034-4257(98)00010-8)

Stevenson, A., Mitchell, F.J.G., Davies, J.S., 2015. Predation has no competition: factors influencing space and resource use by echinoids in deep-sea coral habitats, as

- evidenced by continuous video transects. *Mar. Ecol.* 36, 1454–1467.
<https://doi.org/10.1111/maec.12245>
- Stone, R., Callaway, R., Bull, J.C., 2019. Are biodiversity offsetting targets of ecological equivalence feasible for biogenic reef habitats? *Ocean Coast. Manag.* 177, 97–111.
<https://doi.org/10.1016/j.ocecoaman.2019.04.003>
- Storlazzi, C.D., Dartnell, P., Hatcher, G.A., Gibbs, A.E., 2016. End of the chain? Rugosity and fine-scale bathymetry from existing underwater digital imagery using structure-from-motion (SfM) technology. *Coral Reefs* 35, 889–894.
<https://doi.org/10.1007/s00338-016-1462-8>
- Strong, J.A., 2020. An error analysis of marine habitat mapping methods and prioritised work packages required to reduce errors and improve consistency. *Estuar. Coast. Shelf Sci.* 240, 106684. <https://doi.org/10.1016/j.ecss.2020.106684>
- Taylor, R., 1998. Density, biomass and productivity of animals in four subtidal rocky reef habitats: the importance of small mobile invertebrates. *Mar. Ecol. Prog. Ser.* 172, 37–51. <https://doi.org/10.3354/meps172037>
- Torres-Pulliza, D., Dornelas, M.A., Pizarro, O., Bewley, M., Blowes, S.A., Boutros, N., Brambilla, V., Chase, T.J., Frank, G., Friedman, A., Hoogenboom, M.O., Williams, S., Zawada, K.J.A., Madin, J.S., 2020. A geometric basis for surface habitat complexity and biodiversity. *Nat. Ecol. Evol.* 1–7. <https://doi.org/10.1038/s41559-020-1281-8>
- Turner, M.G., 2010. Disturbance and landscape dynamics in a changing world 1. *Ecology* 91, 2833–2849. <https://doi.org/10.1890/10-0097.1>
- Turner, M.G., 1989. Landscape ecology: the effect of pattern on process. *Annu. Rev. Ecol. Syst.* 20, 171–197. <https://doi.org/10.1146/annurev.es.20.110189.001131>
- Turner, M.G., Romme, W.H., Gardner, R.H., O'Neill, R. V., Kratz, T.K., 1993. A revised concept of landscape equilibrium: Disturbance and stability on scaled landscapes. *Landsc. Ecol.* 8, 213–227. <https://doi.org/10.1007/BF00125352>
- Turner, W., Spector, S., Gardiner, N., Fladeland, M., Sterling, E., Steininger, M., 2003. Remote sensing for biodiversity science and conservation. *Trends Ecol. Evol.* [https://doi.org/10.1016/S0169-5347\(03\)00070-3](https://doi.org/10.1016/S0169-5347(03)00070-3)

- Underwood, A.J., Chapman, M.G., Connell, S.D., 2000. Observations in ecology: You can't make progress on processes without understanding the patterns. *J. Exp. Mar. Bio. Ecol.* 250, 97–115. [https://doi.org/10.1016/S0022-0981\(00\)00181-7](https://doi.org/10.1016/S0022-0981(00)00181-7)
- Urbina-Barreto, I., Chiroleu, F., Pinel, R., Fréchon, L., Mahamadaly, V., Elise, S., Kulbicki, M., Quod, J.P., Dutrieux, E., Garnier, R., Henrich Bruggemann, J., Penin, L., Adjeroud, M., 2021. Quantifying the shelter capacity of coral reefs using photogrammetric 3D modeling: From colonies to reefscapes. *Ecol. Indic.* 121, 107151. <https://doi.org/10.1016/j.ecolind.2020.107151>
- USGS, 2017. Agisoft Photoscan Workflow [WWW Document]. URL <https://uas.usgs.gov/nupo/pdf/USGSAgisoftPhotoScanWorkflow.pdf>
- Van De Koppel, J., Gascoigne, J.C., Theraulaz, G., Rietkerk, M., Mooij, W.M., Herman, P.M.J., 2008. Experimental evidence for spatial self-organization and its emergent effects in mussel bed ecosystems. *Science* 322, 739–742. <https://doi.org/10.1126/science.1163952>
- van Rein, H.B., Brown, C., Quinn, R., Breen, J., 2009. A review of sublittoral monitoring methods in temperate waters: A focus on scale. *Underw. Technol.* 28, 99–113. <https://doi.org/10.3723/ut.28.099>
- Vanden Borre, J., Paelinckx, D., Mûcher, C.A., Kooistra, L., Haest, B., De Blust, G., Schmidt, A.M., 2011. Integrating remote sensing in Natura 2000 habitat monitoring: Prospects on the way forward. *J. Nat. Conserv.* 19, 116–125. <https://doi.org/10.1016/J.JNC.2010.07.003>
- Vanstaen, K., Eggleton, J., 2011. Mapping Annex 1 reef habitat present in specific areas within the Lyme Bay and Torbay cSAC. Cefas report C5291B.
- Ventura, D., Dubois, S.F., Bonifazi, A., Jona Lasinio, G., Seminara, M., Gravina, M.F., Ardizzone, G., 2020. Integration of close-range underwater photogrammetry with inspection and mesh processing software: a novel approach for quantifying ecological dynamics of temperate biogenic reefs. *Remote Sens. Ecol. Conserv.* rse2.178. <https://doi.org/10.1002/rse2.178>
- Vierling, K.T., Vierling, L.A., Gould, W.A., Martinuzzi, S., Clawges, R.M., 2008. Lidar: Shedding new light on habitat characterization and modeling. *Front. Ecol. Environ.*

- 6, 90–98. <https://doi.org/10.1890/070001>
- Wadoux, A.M.J.C., Heuvelink, G.B.M., de Bruin, S., Brus, D.J., 2021. Spatial cross-validation is not the right way to evaluate map accuracy. *Ecol. Modell.* 457, 109692. <https://doi.org/10.1016/j.ecolmodel.2021.109692>
- Walbridge, S., Slocum, N., Pobuda, M., Wright, D.J., 2018. Unified Geomorphological Analysis Workflows with Benthic Terrain Modeler. *Geosciences* 8, 94. <https://doi.org/10.3390/geosciences8030094>
- Wallace, L., Lucieer, A., Malenovský, Z., Turner, D., Vopěnka, P., Wallace, L., Lucieer, A., Malenovský, Z., Turner, D., Vopěnka, P., 2016. Assessment of Forest Structure Using Two UAV Techniques: A Comparison of Airborne Laser Scanning and Structure from Motion (SfM) Point Clouds. *Forests* 7, 62. <https://doi.org/10.3390/f7030062>
- Wang, F., 1990. Fuzzy Supervised Classification of Remote Sensing Images. *IEEE Trans. Geosci. Remote Sens.* 28, 194–201. <https://doi.org/10.1109/36.46698>
- Ward, S.L., Neill, S.P., Van Landeghem, K.J.J., Scourse, J.D., 2015. Classifying seabed sediment type using simulated tidal-induced bed shear stress. *Mar. Geol.* 367, 94–104. <https://doi.org/10.1016/j.margeo.2015.05.010>
- Warfe, D.M., Barmuta, L.A., Wotherspoon, S., 2008. Quantifying habitat structure: surface convolution and living space for species in complex environments. *Oikos* 117, 1764–1773. <https://doi.org/10.1111/j.1600-0706.2008.16836.x>
- Warwick, R., Uncles, R., 1980. Distribution of Benthic Macrofauna Associations in the Bristol Channel in Relation to Tidal Stress. *Mar. Ecol. Prog. Ser.* 3, 97–103. <https://doi.org/10.3354/meps003097>
- Watt, P.J., Donoghue, D.N.M., 2005. Measuring forest structure with terrestrial laser scanning. *Int. J. Remote Sens.* 26, 1437–1446. <https://doi.org/10.1080/01431160512331337961>
- Wedding, L., Lepczyk, C., Pittman, S., Friedlander, A., Jorgensen, S., 2011. Quantifying seascape structure: extending terrestrial spatial pattern metrics to the marine realm. *Mar. Ecol. Prog. Ser.* 427, 219–232. <https://doi.org/10.3354/meps09119>
- Wedding, L.M., Friedlander, A.M., McGranaghan, M., Yost, R.S., Monaco, M.E., 2008. Using

bathymetric lidar to define nearshore benthic habitat complexity: Implications for management of reef fish assemblages in Hawaii. *Remote Sens. Environ.* 112, 4159–4165. <https://doi.org/10.1016/J.RSE.2008.01.025>

Wedding, L.M., Jorgensen, S., Lepczyk, C.A., Friedlander, A.M., 2019. Remote sensing of three-dimensional coral reef structure enhances predictive modeling of fish assemblages. *Remote Sens. Ecol. Conserv.* 5, 150–159. <https://doi.org/10.1002/rse2.115>

Weiner, J., 1995. On the Practice of Ecology. *Source J. Ecol.* 83, 153–158.

Weiss, A., 2001. Topographic position and landforms analysis. Poster Present. ESRI User Conf. San Diego, CA 64, 227–245.

Westhead, K., Smith, K., Campbell, E., Colenutt, A., McVey, S., 2015. Pushing the boundaries: Integration of multi-source digital elevation model data for seamless geological mapping of the UK's coastal zone. *Earth Environ. Sci. Trans. R. Soc. Edinburgh* 105, 263–271. <https://doi.org/10.1017/S1755691015000134>

Westoby, M.J., Brasington, J., Glasser, N.F., Hambrey, M.J., Reynolds, J.M., 2012. “Structure-from-Motion” photogrammetry: A low-cost, effective tool for geoscience applications. *Geomorphology* 179, 300–314. <https://doi.org/10.1016/j.geomorph.2012.08.021>

Wheatley, M., Johnson, C., 2009. Factors limiting our understanding of ecological scale. *Ecol. Complex.* 6, 150–159. <https://doi.org/10.1016/J.ECOCOM.2008.10.011>

Whitman, E.R., Reidenbach, M.A., 2012. Benthic flow environments affect recruitment of *Crassostrea virginica* larvae to an intertidal oyster reef. *Mar. Ecol. Prog. Ser.* 463, 177–191. <https://doi.org/10.3354/meps09882>

Whittaker, R.H., Levin, S.A., Root, R.B., 1973. Niche , Habitat , and Ecotope. *Am. Nat.* 107, 321–338.

Whitton, T., 2014. Characterization of the benthic habitats in the West Anglesey Demonstration Zone. SEACAMS report SC-RD-116.

Wicaksono, P., Aryaguna, P.A., Lazuardi, W., 2019. Benthic Habitat Mapping Model and Cross Validation Using Machine-Learning Classification Algorithms. *Remote Sens.*

- 11, 1279. <https://doi.org/10.3390/rs11111279>
- Wiens, J.A., 1989. Spatial Scaling in Ecology. *Funct. Ecol.* 3, 385–397.
<https://doi.org/10.2307/2389612>
- Wilding, T.A., Gill, A.B., Boon, A., Sheehan, E., Dauvin, J., Pezy, J.-P., O’Beirn, F., Janas, U., Rostin, L., De Mesel, I., 2017. Turning off the DRIP (‘Data-rich, information-poor’) – rationalising monitoring with a focus on marine renewable energy developments and the benthos. *Renew. Sustain. Energy Rev.* 74, 848–859.
<https://doi.org/10.1016/j.rser.2017.03.013>
- Wilkinson, M.W., Jones, R.R., Woods, C.E., Gilment, S.R., McCaffrey, K.J.W., Kokkalas, S., Long, J.J., 2016. A comparison of terrestrial laser scanning and structure-from-motion photogrammetry as methods for digital outcrop acquisition. *Geosphere* 12, 1865–1880. <https://doi.org/10.1130/GES01342.1>
- Williams, G.J., Graham, N.A.J., Jouffray, J.B., Norström, A. V., Nyström, M., Gove, J.M., Heenan, A., Wedding, L.M., 2019. Coral reef ecology in the Anthropocene. *Funct. Ecol.* 33, 1014–1022. <https://doi.org/10.1111/1365-2435.13290>
- Wilson, D.P., 1971. *Sabellaria* Colonies at Duckpool, North Cornwall. *J. Mar. Biol. Assoc. UK* 51, 509–580.
- Wilson, M.F.J., O’Connell, B., Brown, C., Guinan, J.C., Grehan, A.J., 2007. Multiscale Terrain Analysis of Multibeam Bathymetry Data for Habitat Mapping on the Continental Slope. *Mar. Geod.* 30, 3–35. <https://doi.org/10.1080/01490410701295962>
- Woodget, A.S., Carbonneau, P.E., Visser, F., Maddock, I.P., 2015. Quantifying submerged fluvial topography using hyperspatial resolution UAS imagery and structure from motion photogrammetry. *Earth Surf. Process. Landforms* 40, 47–64.
<https://doi.org/10.1002/esp.3613>
- Woodhead, A.J., Hicks, C.C., Norström, A. V., Williams, G.J., Graham, N.A.J., 2019. Coral reef ecosystem services in the Anthropocene. *Funct. Ecol.* 33, 1023–1034.
<https://doi.org/10.1111/1365-2435.13331>
- Wright, D.J., Lundblad, E.R., Larkin, E.M., Rinehart, R.W., Murphy, J., Cary-Kothera, L., Draganov, K., 2005. ArcGIS Benthic Terrain Modeler.

- Young, G.C., Dey, S., Rogers, A.D., Exton, D., 2017. Cost and time-effective method for multiscale measures of rugosity, fractal dimension, and vector dispersion from coral reef 3D models. *PLoS One* 12, e0175341.
<https://doi.org/10.1371/journal.pone.0175341>
- Zhang, W., Qi, J., Wan, P., Wang, H., Xie, D., Wang, X., Yan, G., 2016. An Easy-to-Use Airborne LiDAR Data Filtering Method Based on Cloth Simulation. *Remote Sens.* 8, 501. <https://doi.org/10.3390/rs8060501>
- Zvoleff, A., 2020. glcm: Calculate Textures from Grey-Level Co-Occurrence Matrices (GLCMs). R package version 1.6.5.
- Zwolak, K., Wigley, R., Bohan, A., Zarayskaya, Y., Bazhenova, E., Dorshow, W., Sumiyoshi, M., Sattiabaruth, S., Roperez, J., Proctor, A., Wallace, C., Sade, H., Ketter, T., Simpson, B., Tinmouth, N., Falconer, R., Ryzhov, I., Abou-Mahmoud, M.E., 2020. The Autonomous Underwater Vehicle Integrated with the Unmanned Surface Vessel Mapping the Southern Ionian Sea. The Winning Technology Solution of the Shell Ocean Discovery XPRIZE. *Remote Sens.* 2020, Vol. 12, Page 1344 12, 1344.
<https://doi.org/10.3390/RS12081344>